# Chapter 8
# Computational Nuclear Physics and Post Hartree-Fock Methods

**Justin G. Lietz, Samuel Novario, Gustav R. Jansen, Gaute Hagen, and Morten Hjorth-Jensen**

## 8.1 Introduction

Studies of dense baryonic matter are of central importance to our basic understanding of the stability of nuclear matter, spanning from matter at high densities and temperatures to matter as found within dense astronomical objects like neutron stars. An object like a neutron star offers an intriguing interplay between nuclear processes and astrophysical observables, spanning many orders of magnitude in density and several possible compositions of matter, from the crust of the star to a possible quark matter phase in its interior, see for example [1–8] for discussions. A central issue in studies of infinite nuclear matter is the determination of the equation of state (EoS), which can in turn be used to determine properties like the mass range, the

J.G. Lietz (✉) • S. Novario
Department of Physics and Astronomy and National Superconducting Cyclotron Laboratory, Michigan State University, East Lansing, MI, USA
e-mail: lietz@nscl.msu.edu; novarios@nscl.msu.edu

G.R. Jansen
National Center for Computational Sciences and Physics Division, Oak Ridge National Laboratory, Oak Ridge, TN, USA
e-mail: jansengr@ornl.gov

G. Hagen
Physics Division, Oak Ridge National Laboratory, Oak Ridge, TN, USA

Department of Physics and Astronomy, University of Tennessee, Knoxville, TN, USA
e-mail: hageng@ornl.gov

M. Hjorth-Jensen
National Superconducting Cyclotron Laboratory and Department of Physics and Astronomy, Michigan State University, East Lansing, Michigan, USA

Department of Physics, University of Oslo, Oslo, Norway
e-mail: hjensen@msu.edu



M. Hjorth-Jensen et al. (eds.), *An Advanced Course in Computational Nuclear Physics*, Lecture Notes in Physics 936, DOI 10.1007/978-3-319-53336-0_8

mass-radius relationship, the thickness of the crust and the rate by which a neutron star cools down over time. The EoS is also an important ingredient in studies of the energy release in supernova explosions.

The determination and our understanding of the EoS for dense nuclear matter is intimately linked with our capability to solve the nuclear many-body problem. In particular, to be able to provide precise constraints on the role of correlations beyond the mean field is crucial for improved and controlled calculations of the EoS. In recent years, there has been a considerable algorithmic development of first principle (or ab initio) methods for solving the nuclear many-body problem. Linked with a similar progress in the derivation of nuclear forces based on effective field theory (EFT), see Chaps. 4, 5 and 6 of the present text and [9–16], we are now in a situation where reliable results can be provided at different levels of approximation. The nuclear Hamiltonians which are now used routinely in nuclear structure and nuclear matter calculations, include both nucleon-nucleon (*NN*) and three-nucleon forces (3NFs) derived from EFT, see for example [5, 5, 17–26]. Parallel to the development of nuclear forces from EFT, which employ symmetries of quantum chromodynamics, there are recent and promising approaches to derive the EoS using forces constrained from lattice quantum chromodynamics calculations [27], see Chaps. 2 and 3 of the present text.

Theoretical studies of nuclear matter and the pertinent EoS span back to the very early days of nuclear many-body physics. These early developments are nicely summarized in for example the review of Day [28] from 1967. These early state-of-the-art calculations were performed using what is known as Brueckner-Bethe-Goldstone theory [29, 30], see for example [8, 20, 21, 31–33] for recent reviews and developments. In these calculations, mainly particle-particle correlations were summed to infinite order. Other correlations were often included in a perturbative way. A systematic inclusion of other correlations in a non-perturbative way are nowadays accounted for in many-body methods like coupled cluster theory [17, 19, 23, 34–38] (this chapter), various Monte Carlo methods [39–46] (Chap. 9), Green's function approaches [26, 32, 47, 48] (Chap. 11) and similarity renormalization group methods [24, 49] (Chap. 10), just to mention a few of the actual many-body methods which are used for nuclear matter studies. Many of these methods are discussed in detail in this and the following chapters.

The aim of this part of the present lecture notes (comprising this chapter and the three subsequent ones) is to provide the necessary ingredients for performing studies of neutron star matter (or matter in $\beta$-equilibrium) and symmetric nuclear matter. We will mainly focus on pure neutron matter, but the framework and formalism can easily be extended to other dense and homogeneous fermionic systems such as the electron gas in two and three dimensions. The introductory material we present here forms also the basis for the next three chapters, starting with the definition of the single-particle basis and our Hamiltonians as well as Hartree-Fock theory. For infinite matter, due to the translational invariance of the Hamiltonian, the single-particle basis, in terms of plane waves, is unchanged under Hartree-Fock calculations.

Neutron star matter at densities of $0.1\,\mathrm{fm}^{-3}$ and greater, is often assumed to consist mainly of neutrons, protons, electrons and muons in beta equilibrium. However, other baryons like various hyperons may exist, as well as possible mesonic condensates and transitions to quark degrees of freedom at higher densities [3, 4, 8, 50]. In this chapter we limit ourselves to matter composed of neutrons only. Furthermore, we will also consider matter at temperatures much lower than the typical Fermi energies.

In the next section we present some of the basic quantities that enter the different many-body methods discussed in this and the three subsequent chapters. All these methods start with some single-particle basis states, normally obtained via the solution of mean-field approaches like Hartree-Fock theory. Contributions from correlations beyond such a mean-field basis to selected observables, are then obtained via a plethora of many-body methods. These methods represent different mathematical algorithms used to solve either Schrödinger's or Dirac's equations for many interacting fermions. After the definitions of our basis states, we derive the Hartree-Fock equations in the subsequent section and move on with many-body perturbation theory, full configuration interaction theory and coupled cluster theory. Monte Carlo methods, Green's function theory approaches and Similarity Renormalization group approaches are discussed in the subsequent three chapters.

The strengths and weaknesses of these methods are discussed throughout these chapters, with applications to either a simple pairing model and/or pure neutron matter. Our focus will be on pure neutron matter, starting with a simple model for the interaction between nucleons. This allows us to focus on pedagogical and algorithmic aspects of the various many-body methods, avoiding thereby the full complexity of nuclear forces. If properly written however, the codes can easily be extended to include models of the nuclear interactions based on effective field theory (see Chaps. 4, 5 and 6 of the present text) and other baryon species than just neutrons. In our conclusions we point back to models for nuclear forces and their links to the underlying theory of the strong interaction discussed in the first chapters of this book, bridging thereby the gap between the theory of nuclear Hamiltonians and many-body methods.

## 8.2 Single-Particle Basis, Hamiltonians and Models for the Nuclear Force

### *8.2.1 Introduction to Nuclear Matter and Hamiltonians*

Although our focus here and in the coming chapters is on neutron matter only, our formalism lends itself easily to studies of nuclear matter with a given proton fraction and electrons. In this section we outline some of the background details, with a focus on the calculational basis and the representation of a nuclear Hamiltonian.

Neutron star matter is not composed of only neutrons. Rather, matter is composed of various baryons and leptons in chemical and charge equilibrium. The equilibrium conditions are governed by the weak processes (normally referred to as the processes for $\beta$-equilibrium)

$$b_1 \rightarrow b_2 + l + \bar{\nu}_l \qquad b_2 + l \rightarrow b_1 + \nu_l,$$

where $b_1$ and $b_2$ refer to different types of baryons, for example a neutron and a proton. The symbol $l$ is either an electron or a muon and $\bar{\nu}_l$ and $\nu_l$ their respective anti-neutrinos and neutrinos. Leptons like muons appear at a density close to nuclear matter saturation density $\rho_0$, the latter being

$$\rho_0 \approx 0.16 \pm 0.02 \text{ fm}^{-3},$$

with a corresponding energy per baryon $\mathscr{E}_0$ for symmetric nuclear matter at saturation density of

$$\mathscr{E}_0 = B/A = -15.6 \pm 0.2 \text{ MeV}.$$

The energy per baryon is the central quantity in the present studies. From the energy per baryon, we can define the pressure $P$ which counteracts the gravitational forces and hinders the gravitational collapse of a neutron star. The pressure is defined through the relation

$$P = \rho^2 \frac{\partial \mathscr{E}}{\partial \rho} = \rho \frac{\partial \varepsilon}{\partial \rho} - \varepsilon,$$

where $\varepsilon$ is the energy density and $\rho$ the density. Similarly, the chemical potential for particle species $i$ is given by

$$\mu_i = \left( \frac{\partial \varepsilon}{\partial \rho_i} \right).$$

In calculations of properties of neutron star matter in $\beta$-equilibrium, we need to calculate the energy per baryon $\mathscr{E}$ for several proton fractions $x_p$. The proton fraction corresponds to the ratio of protons as compared to the total nucleon number ($Z/A$). It is defined as

$$x_p = \frac{\rho_p}{\rho},$$

where $\rho = \rho_p + \rho_n$ is the total baryonic density if neutrons and protons are the only baryons present (the subscripts used here, $n, p, e, \mu$, refer to neutrons, protons, electrons and muons, respectively). If this is the case, the total Fermi momentum $k_F$ and the Fermi momenta $k_{Fp}$, $k_{Fn}$ for protons and neutrons, respectively, are related

to the total nucleon density $n$ by

$$\rho = \frac{2}{3\pi^2}k_F^3 = x_p\rho + (1-x_p)\rho = \frac{1}{3\pi^2}k_{Fp}^3 + \frac{1}{3\pi^2}k_{Fn}^3.$$

The energy per baryon will thus be labelled as $\mathscr{E}(\rho, x_p)$. The quantity $\mathscr{E}(\rho, 0)$ refers then to the energy per baryon for pure neutron matter while $\mathscr{E}(\rho, \frac{1}{2})$ is the corresponding value for symmetric nuclear matter.

An important ingredient in the discussion of the EoS and the criteria for matter in $\beta$-equilibrium is the so-called symmetry energy $\mathscr{S}(\rho)$, defined as the difference in energy for symmetric nuclear matter and pure neutron matter

$$\mathscr{S}(\rho) = \mathscr{E}(\rho, x_p = 0) - \mathscr{E}(\rho, x_p = 1/2).$$

If we expand the energy per baryon in the case of nucleonic degrees of freedom only in the proton concentration $x_p$ about the value of the energy for SNM ($x_p = \frac{1}{2}$), we obtain,

$$\mathscr{E}(\rho, x_p) = \mathscr{E}(n, x_p = \frac{1}{2}) + \frac{1}{2}\frac{d^2\mathscr{E}}{dx_p^2}(\rho)\left(x_p - 1/2\right)^2 + \ldots,$$

where the term $d^2\mathscr{E}/dx_p^2$ is to be associated with the symmetry energy $\mathscr{S}(\rho)$ in the empirical mass formula. If we assume that higher order derivatives in the above expansion are small, then through the conditions for $\beta$-equilibrium (see for example [8]) we can define the proton fraction by the symmetry energy as

$$\hbar c\left(3\pi^2\rho x_p\right)^{1/3} = 4\mathscr{S}(\rho)\left(1-2x_p\right),$$

where the electron chemical potential is given by $\mu_e = \hbar c k_F$, i.e. ultrarelativistic electrons are assumed. Thus, the symmetry energy is of paramount importance for studies of neutron star matter in $\beta$-equilibrium. One can extract information about the value of the symmetry energy at saturation density $\rho_0$ from systematic studies of the masses of atomic nuclei. However, these results are limited to densities around $\rho_0$ and for proton fractions close to $\frac{1}{2}$. Typical values for $\mathscr{S}(\rho)$ at $\rho_0$ are in the range 27–38 MeV [51]. For densities greater than $\rho_0$ it is more difficult to get a reliable information on the symmetry energy, and thereby the related proton fraction.

With this background, we are now ready to define our basic inputs and approximations to the various many-body theories discussed in this chapter and the three subsequent ones. We will assume that the interacting part of the Hamiltonian can be approximated by a two-body interaction. This means that our Hamiltonian is written as the sum of a one-body part and a two-body part

$$\hat{H} = \hat{H}_0 + \hat{H}_I = \sum_{i=1}^{A}\hat{h}_0(x_i) + \sum_{i<j}^{A}\hat{v}(r_{ij}),$$

with

$$\hat{H}_0 = \sum_{i=1}^{A} \hat{h}_0(x_i),$$

being the so-called unperturbed part of the Hamiltonian defined by the one-body operator

$$\hat{h}_0(x_i) = \hat{t}(x_i) + \hat{u}_{\text{ext}}(x_i),$$

where $\hat{t}$ represents the kinetic energy and $x_i$ represents both spatial and spin degrees of freedom. For many-body calculations of finite nuclei, the external potential $u_{\text{ext}}(x_i)$ is normally approximated by a harmonic oscillator or Woods-Saxon potential. For atoms, the external potential is defined by the Coulomb interaction an electron feels from the atomic nucleus. However, other potentials are fully possible, such as one derived from the self-consistent solution of the Hartree-Fock equations to be discussed below. Since we will work with infinite matter and plane wave basis states, the one-body operator is simply given by the kinetic energy operator. Finally, the term $\hat{H}_I$ represents the residual two-body interaction

$$\hat{H}_I = \sum_{i<j}^{A} \hat{v}(r_{ij}).$$

Our Hamiltonian is invariant under the permutation (interchange) of two particles. Since we deal with fermions however, the total wave function is anti-symmetric and we assume that we can approximate the exact eigenfunction for say the ground state with a Slater determinant

$$\Phi_0(x_1, x_2, \ldots, x_A, \alpha, \beta, \ldots, \sigma) = \frac{1}{\sqrt{A!}} \begin{vmatrix} \psi_\alpha(x_1) & \psi_\alpha(x_2) & \ldots\ldots & \psi_\alpha(x_A) \\ \psi_\beta(x_1) & \psi_\beta(x_2) & \ldots\ldots & \psi_\beta(x_A) \\ \ldots & \ldots & \ldots\ldots & \ldots \\ \ldots & \ldots & \ldots\ldots & \ldots \\ \psi_\sigma(x_1) & \psi_\sigma(x_2) & \ldots\ldots & \psi_\sigma(x_A) \end{vmatrix},$$

where $x_i$ stand for the coordinates and spin values of particle $i$ and $\alpha, \beta, \ldots, \gamma$ are quantum numbers needed to describe remaining quantum numbers.

The single-particle function $\psi_\alpha(x_i)$ are eigenfunctions of the one-body Hamiltonian $h_0$, that is

$$\hat{h}_0(x_i)\psi_\alpha(x_i) = \left(\hat{t}(x_i) + \hat{u}_{\text{ext}}(x_i)\right)\psi_\alpha(x_i) = \varepsilon_\alpha \psi_\alpha(x_i).$$

The energies $\varepsilon_\alpha$ are the so-called non-interacting single-particle energies, or unperturbed energies. The total energy is in this case the sum over all single-particle energies, if no two-body or more complicated many-body interactions are present.

The properties of the determinant lead to a straightforward implementation of the Pauli principle since no two particles can be at the same place (two columns being the same in the above determinant) and no two particles can be in the same state (two rows being the same). As a practical matter, however, Slater determinants beyond $N = 4$ quickly become unwieldy. Thus we turn to the occupation representation or second quantization to simplify calculations. For a good introduction to second quantization see for example [35, 52–54].

We start with a set of orthonormal single-particle states $\{\psi_\alpha(x)\}$. To each single-particle state $\psi_\alpha(x)$ we associate a creation operator $a_\alpha^\dagger$ and an annihilation operator $a_\alpha$. When acting on the vacuum state $|0\rangle$, the creation operator $a_\alpha^\dagger$ causes a particle to occupy the single-particle state $\psi_\alpha(x)$

$$\psi_\alpha(x) \rightarrow a_\alpha^\dagger|0\rangle.$$

But with multiple creation operators we can occupy multiple states

$$\psi_\alpha(x)\psi_\beta(x')\psi_\delta(x'') \rightarrow a_\alpha^\dagger a_\beta^\dagger a_\delta^\dagger|0\rangle.$$

Now we impose anti-symmetry by having the fermion operators satisfy the anti-commutation relations

$$a_\alpha^\dagger a_\beta^\dagger + a_\beta^\dagger a_\alpha^\dagger = \left\{a_\alpha^\dagger, a_\beta^\dagger\right\} = 0,$$

with the consequence that

$$a_\alpha^\dagger a_\beta^\dagger = -a_\beta^\dagger a_\alpha^\dagger.$$

Because of this property, we obtain $a_\alpha^\dagger a_\alpha^\dagger = 0$, enforcing the Pauli exclusion principle. Thus we can represent a Slater determinant using creation operators as

$$a_\alpha^\dagger a_\beta^\dagger a_\delta^\dagger \ldots |0\rangle,$$

where each index $\alpha, \beta, \delta, \ldots$ has to be unique.

We will now find it convenient to define a Fermi (F) level and introduce a new reference vacuum. The Fermi level is normally defined in terms of all occupied single-particle states below a certain single-particle energy. With the definition of a Fermi level we define our ansatz for the ground state, represented by a Slater determinant $\Phi_0$. We will throughout the rest of this text use creation and annihilation operators to represent quantum mechanical operators and states. It means that our

compact representation for a given Slater determinant in Fock space is

$$\Phi_0 = |i_1 \dots i_A\rangle = a^\dagger_{i_1} \dots a^\dagger_{i_A}|0\rangle$$

where $|0\rangle$ is the true vacuum and we have defined the creation and annihilation operators as

$$a^\dagger_p|0\rangle = |p\rangle, \quad a_p|q\rangle = \delta_{pq}|0\rangle$$

with the anti-commutation relations

$$\delta_{pq} = \left\{a_p, a^\dagger_q\right\},$$

and

$$\left\{a^\dagger_p, a_q\right\} = \left\{a_p, a_q\right\} = \left\{a^\dagger_p, a^\dagger_q\right\} = 0.$$

We can rewrite the ansatz for the ground state as

$$|\Phi_0\rangle = \prod_{i \le F} a^\dagger_i|0\rangle,$$

where we have introduced the shorthand labels for states below the Fermi level $F$ as $i, j, \dots \le F$. For single-particle states above the Fermi level we reserve the labels $a, b, \dots > F$, while the labels $p, q, \dots$ represent any possible single-particle state.

Since our focus is on infinite systems, the one-body part of the Hamiltonian is given by the kinetic energy operator only. In second quantization it is defined as

$$\hat{H}_0 = \hat{T} = \sum_{pq} \langle p|\hat{t}|q\rangle a^\dagger_p a_q,$$

where the matrix elements $\langle p|\hat{t}|q\rangle$ represent the expectation value of the kinetic energy operator (see the discussion below as well). The two-body interaction reads

$$\hat{H}_I = \hat{V} = \frac{1}{4} \sum_{pqrs} \langle pq|\hat{v}|rs\rangle_{AS} a^\dagger_p a^\dagger_q a_s a_r,$$

where we have defined the anti-symmetrized matrix elements

$$\langle pq|\hat{v}|rs\rangle_{AS} = \langle pq|\hat{v}|rs\rangle - \langle pq|\hat{v}|sr\rangle.$$

We can also define a three-body operator

$$\hat{V}_3 = \frac{1}{36}\sum_{pqrstu} \langle pqr|\hat{v}_3|stu\rangle_{AS} a_p^\dagger a_q^\dagger a_r^\dagger a_u a_t a_s,$$

with the anti-symmetrized matrix element

$$\begin{aligned}\langle pqr|\hat{v}_3|stu\rangle_{AS} = &\langle pqr|\hat{v}_3|stu\rangle + \langle pqr|\hat{v}_3|tus\rangle + \langle pqr|\hat{v}_3|ust\rangle - \langle pqr|\hat{v}_3|sut\rangle \\ &- \langle pqr|\hat{v}_3|tsu\rangle - \langle pqr|\hat{v}_3|uts\rangle.\end{aligned}$$

In this and the forthcoming chapters we will limit ourselves to two-body interactions at most. Throughout this chapter and the subsequent three we will drop the subscript *AS* and use only anti-symmetrized matrix elements.

Using the ansatz for the ground state $|\Phi_0\rangle$ as new reference vacuum state, we need to redefine the anticommutation relations to

$$\left\{a_p^\dagger, a_q\right\} = \delta_{pq},\ p,q \leq F,$$

and

$$\left\{a_p, a_q^\dagger\right\} = \delta_{pq},\ p,q > F.$$

It is easy to see that

$$a_i|\Phi_0\rangle = |\Phi_i\rangle \neq 0, \qquad a_a^\dagger|\Phi_0\rangle = |\Phi^a\rangle \neq 0,$$

and

$$a_i^\dagger|\Phi_0\rangle = 0 \qquad a_a|\Phi_0\rangle = 0.$$

With the new reference vacuum state the Hamiltonian can be rewritten as, see Problem 8.1,

$$\hat{H} = E_{\text{Ref}} + \hat{H}_N,$$

with the reference energy defined as the expectation value of the Hamiltonian using the reference state $\Phi_0$

$$E_{\text{Ref}} = \langle\Phi_0|\hat{H}|\Phi_0\rangle = \sum_{i\leq F}\langle i|\hat{h}_0|i\rangle + \frac{1}{2}\sum_{ij\leq F}\langle ij|\hat{v}|ij\rangle,$$

and the new normal-ordered Hamiltonian (all creation operators to the left of the annihilation operators) is defined as

$$\hat{H}_N = \sum_{pq} \langle p|\hat{h}_0|q\rangle \left\{a_p^\dagger a_q\right\} + \frac{1}{4}\sum_{pqrs} \langle pq|\hat{v}|rs\rangle \left\{a_p^\dagger a_q^\dagger a_s a_r\right\} + \sum_{pq,i\leq F} \langle pi|\hat{v}|qi\rangle \left\{a_p^\dagger a_q\right\}, \tag{8.1}$$

where the curly brackets represent normal-ordering with respect to the new reference vacuum state. The normal-ordered Hamiltonian can be rewritten in terms of a new one-body operator and a two-body operator as

$$\hat{H}_N = \hat{F}_N + \hat{V}_N,$$

with

$$\hat{F}_N = \sum_{pq} \langle p|\hat{f}|q\rangle \left\{a_p^\dagger a_q\right\}, \tag{8.2}$$

where

$$\langle p|\hat{f}|q\rangle = \langle p|\hat{h}_0|q\rangle + \sum_{i\leq F} \langle pi|\hat{v}|qi\rangle.$$

The last term on the right hand side represents a medium modification to the single-particle Hamiltonian due to the two-body interaction. Finally, the two-body interaction is given by

$$\hat{V}_N = \frac{1}{4}\sum_{pqrs} \langle pq|\hat{v}|rs\rangle \left\{a_p^\dagger a_q^\dagger a_s a_r\right\}.$$

### *8.2.2 Single-Particle Basis for Infinite Matter*

Infinite nuclear or neutron matter is a homogeneous system and the one-particle wave functions are given by plane wave functions normalized to a volume $\Omega$ for a box with length $L$ (the limit $L \to \infty$ is to be taken after we have computed various expectation values)

$$\psi_{\mathbf{k}\sigma}(\mathbf{r}) = \frac{1}{\sqrt{\Omega}} \exp\left(i\mathbf{kr}\right)\xi_\sigma$$

where **k** is the wave number and $\xi_\sigma$ is the spin function for either spin up or down nucleons

$$\xi_{\sigma=+1/2} = \begin{pmatrix} 1 \\ 0 \end{pmatrix} \qquad \xi_{\sigma=-1/2} = \begin{pmatrix} 0 \\ 1 \end{pmatrix}.$$

As an interesting aside, the recent works of Binder et al. [55] and McElvain and Haxton [56] offer new perspectives on the construction of effective Hamiltonians and choices of basis functions.

We focus first on the kinetic energy operator. We assume that we have periodic boundary conditions which limit the allowed wave numbers to

$$k_i = \frac{2\pi n_i}{L} \qquad i = x, y, z \qquad n_i = 0, \pm 1, \pm 2, \ldots$$

The operator for the kinetic energy can be written as

$$\hat{T} = \sum_{\mathbf{p}\sigma_p} \frac{\hbar^2 k_P^2}{2m} a^\dagger_{\mathbf{p}\sigma_p} a_{\mathbf{p}\sigma_p}.$$

When using periodic boundary conditions, the discrete-momentum single-particle basis functions (excluding spin and/or isospin degrees of freedom) result in the following single-particle energy

$$\varepsilon_{n_x,n_y,n_z} = \frac{\hbar^2}{2m}\left(\frac{2\pi}{L}\right)^2 \left(n_x^2 + n_y^2 + n_z^2\right) = \frac{\hbar^2}{2m}\left(k_{n_x}^2 + k_{n_y}^2 + k_{n_z}^2\right),$$

for a three-dimensional system with

$$k_{n_i} = \frac{2\pi n_i}{L}, \quad n_i = 0, \pm 1, \pm 2, \ldots,$$

We will select the single-particle basis such that both the occupied and unoccupied single-particle states have a closed-shell structure. This means that all single-particle states corresponding to energies below a chosen cutoff are included in the basis. We study only the unpolarized spin phase, in which all orbitals are occupied with one spin-up and one spin-down fermion (neutrons and protons in our case). With the kinetic energy rewritten in terms of the discretized momenta we can set up a list (assuming identical particles one and including spin up and spin down solutions) of single-particle energies with momentum quantum numbers such that $n_x^2 + n_y^2 + n_z^2 \leq 3$, as shown in for example Table 8.1.

Continuing in this way we get for $n_x^2 + n_y^2 + n_z^2 = 4$ a total of 12 additional states, resulting in 66 as a new magic number. For the lowest six energy values the degeneracy in energy gives us 2, 14, 38, 54, 66 and 114 as magic numbers. These numbers will then define our Fermi level when we compute the energy in

**Table 8.1** Total number of particle filling $N_{\uparrow\downarrow}$ for various $n_x^2 + n_y^2 + n_z^2$ values for one spin-1/2 fermion species

| $n_x^2 + n_y^2 + n_z^2$ | $n_x$ | $n_y$ | $n_z$ | $N_{\uparrow\downarrow}$ |
|---|---|---|---|---|
| 0 | 0 | 0 | 0 | 2 |
| 1 | −1 | 0 | 0 | |
| 1 | 1 | 0 | 0 | |
| 1 | 0 | −1 | 0 | |
| 1 | 0 | 1 | 0 | |
| 1 | 0 | 0 | −1 | |
| 1 | 0 | 0 | 1 | 14 |
| 2 | −1 | −1 | 0 | |
| 2 | −1 | 1 | 0 | |
| 2 | 1 | −1 | 0 | |
| 2 | 1 | 1 | 0 | |
| 2 | −1 | 0 | −1 | |
| 2 | −1 | 0 | 1 | |
| 2 | 1 | 0 | −1 | |
| 2 | 1 | 0 | 1 | |
| 2 | 0 | −1 | −1 | |
| 2 | 0 | −1 | 1 | |
| 2 | 0 | 1 | −1 | |
| 2 | 0 | 1 | 1 | 38 |
| 3 | −1 | −1 | −1 | |
| 3 | −1 | −1 | 1 | |
| 3 | −1 | 1 | −1 | |
| 3 | −1 | 1 | 1 | |
| 3 | 1 | −1 | −1 | |
| 3 | 1 | −1 | 1 | |
| 3 | 1 | 1 | −1 | |
| 3 | 1 | 1 | 1 | 54 |

Borrowing from nuclear shell-model terminology, filled shells corresponds to all single-particle states for one $n_x^2+n_y^2+n_z^2$ value being occupied. For matter with both protons and neutrons, the filling degree increased with a factor of 2

a Cartesian basis. When performing calculations based on many-body perturbation theory, coupled cluster theory or other many-body methods, we need then to add states above the Fermi level in order to sum over single-particle states which are not occupied.

If we wish to study infinite nuclear matter with both protons and neutrons, the above magic numbers become $4, 28, 76, 108, 132, 228, \ldots$.

Every number of particles for filled shells defines also the number of particles to be used in a given calculation. The number of particles can in turn be used to define

the density $\rho$ (or the Fermi momentum) of the system via

$$\rho = g\frac{k_F^3}{6\pi^2},$$

where $k_F$ is the Fermi momentum and the degeneracy $g$, which is two for one type of spin-1/2 particles and four for symmetric nuclear matter. With the density defined and having fixed the number of particles $A$ and the Fermi momentum $k_F$, we can define the length $L$ of the box used with periodic boundary contributions via the relation

$$V = L^3 = \frac{A}{\rho}.$$

With $L$ we can to define the spacing between various $k$-values given by

$$\Delta k = \frac{2\pi}{L}.$$

Here, $A$ is the number of nucleons. If we deal with the electron gas only, this needs to be replaced by the number of electrons $N$. Exercise 8.4 deals with the set up of a program that establishes the single-particle basis for nuclear matter calculations with input a given number of nucleons and a user specified density or Fermi momentum.

### 8.2.3 Two-Body Interaction

As mentioned above, we will employ a plane wave basis for our calculations of infinite matter properties. With a cartesian basis we can calculate directly the various matrix elements. However, a cartesian basis represents an approximation to the thermodynamical limit. In order to compare the stability of our basis with results from the thermodynamical limit, it is convenient to rewrite the nucleon-nucleon interaction in terms of a partial wave expansion. This will allow us to compute the Hartree-Fock energy of the ground state in the thermodynamical limit (with the caveat that we need to limit the number of partial waves). In order to find the expressions for the Hartree-Fock energy in a partial wave basis, we will find it convenient to rewrite our two-body force in terms of the relative and center-of-mass motion momenta.

The direct matrix element, with single-particle three-dimensional momenta $\mathbf{k}_p$, spin $\sigma_p$ and isospin $\tau_p$, is defined as

$$\langle \mathbf{k}_p\sigma_p\tau_p\mathbf{k}_q\sigma_q\tau_q|\hat{v}|\mathbf{k}_r\sigma_r\tau_r\mathbf{k}_s\sigma_s\tau_s\rangle,$$

or in a more compact form as $\langle \mathbf{pq}|\hat{v}|\mathbf{rs}\rangle$ where the boldfaced letters $\mathbf{p}$ etc represent the relevant quantum numbers, here momentum, spin and isospin. Introducing the

relative momentum

$$\mathbf{k} = \frac{1}{2}\left(\mathbf{k}_p - \mathbf{k}_q\right),$$

and the center-of-mass momentum

$$\mathbf{K} = \mathbf{k}_p + \mathbf{k}_q,$$

we have

$$\langle \mathbf{k}_p \sigma_p \tau_p \mathbf{k}_q \sigma_q \tau_q | \hat{v} | \mathbf{k}_r \sigma_r \tau_r \mathbf{k}_s \sigma_s \tau_s \rangle = \langle \mathbf{k}\mathbf{K} \sigma_p \tau_p \sigma_q \tau_q | \hat{v} | \mathbf{k}'\mathbf{K}' \sigma_r \tau_r \sigma_s \tau_s \rangle.$$

The nucleon-nucleon interaction conserves the total momentum and charge, implying that the above uncoupled matrix element reads

$$\begin{aligned}\langle \mathbf{k}\mathbf{K} \sigma_p \tau_p \sigma_q \tau_q | \hat{v} | \mathbf{k}'\mathbf{K}' \sigma_r \tau_r \sigma_s \tau_s \rangle &= \delta_{T_z, T_z'} \delta(\mathbf{K} - \mathbf{K}') \langle \mathbf{k} T_z S_z = (\sigma_a + \sigma_b) | \hat{v} | \mathbf{k}' T_z S_z' \\ &= (\sigma_c + \sigma_d) \rangle,\end{aligned}$$

where we have defined the isospin projections $T_z = \tau_p + \tau_q$ and $T_z' = \tau_r + \tau_s$. Defining $\hat{v} = \hat{v}(\mathbf{k}, \mathbf{k}')$, we can rewrite the previous equation in a more compact form as

$$\begin{aligned}\delta_{T_z, T_z'} \delta(\mathbf{K} - \mathbf{K}') \langle \mathbf{k} T_z S_z = (\sigma_p + \sigma_q) | \hat{v} | \mathbf{k}' T_z S_z' = (\sigma_r + \sigma_s) \rangle \\ = \delta_{T_z, T_z'} \delta(\mathbf{K} - \mathbf{K}') \langle T_z S_z | \hat{v}(\mathbf{k}, \mathbf{k}') | T_z S_z' \rangle.\end{aligned}$$

These matrix elements can in turn be rewritten in terms of the total two-body quantum numbers for the spin $S$ of two spin-1/2 fermions as

$$\langle \mathbf{k} T_z S_z | \hat{v}(\mathbf{k}, \mathbf{k}') | \mathbf{k}' T_z S_z' \rangle = \sum_{SS'} \langle \frac{1}{2}\sigma_p \frac{1}{2}\sigma_q | S S_z \rangle \langle \frac{1}{2}\sigma_r \frac{1}{2}\sigma_s | S' S_z' \rangle \langle \mathbf{k} T_z S S_z | \hat{v}(\mathbf{k}, \mathbf{k}') | \mathbf{k} T_z S' S_z' \rangle$$

The coefficients $\langle \frac{1}{2}\sigma_p \frac{1}{2}\sigma_q | S S_z \rangle$ are so-called Clebsch-Gordan recoupling coefficients. We will assume that our interactions conserve charge. We will refer to $T_z = 0$ as the *pn* (proton-neutron) channel, $T_z = -1$ as the *pp* (proton-proton) channel and $T_z = 1$ as the *nn* (neutron-neutron) channel.

The nucleon-nucleon force is often derived and analyzed theoretically in terms of a partial wave expansion. A state with linear momentum $\mathbf{k}$ can be written in terms of spherical harmonics $Y_{lm}$ as

$$|\mathbf{k}\rangle = \sum_{l=0}^{\infty} \sum_{m=-l}^{l} \imath^l Y_{lm} \langle \hat{k} | k l m_l \rangle.$$

In terms of the relative and center-of-mass momenta $\mathbf{k}$ and $\mathbf{K}$, the potential in momentum space is related to the nonlocal operator $V(\mathbf{r}, \mathbf{r}')$ by

$$\langle \mathbf{k}'\mathbf{K}'|\hat{v}|\mathbf{k}'\mathbf{K}\rangle = \int d\mathbf{r}d\mathbf{r}' e^{-\imath\mathbf{k}'\mathbf{r}'} V(\mathbf{r}', \mathbf{r}) e^{\imath\mathbf{k}\mathbf{r}} \delta(\mathbf{K}, \mathbf{K}').$$

We will assume that the interaction is spherically symmetric and use the partial wave expansion of the plane waves in terms of spherical harmonics. This means that we can separate the radial part of the wave function from its angular dependence. The wave function of the relative motion is described in terms of plane waves as

$$e^{\imath\mathbf{k}\mathbf{r}} = \langle \mathbf{r}|\mathbf{k}\rangle = 4\pi \sum_{lm} \imath^l j_l(kr) Y^*_{lm}(\hat{\mathbf{k}}) Y_{lm}(\hat{\mathbf{r}}),$$

where $j_l$ is a spherical Bessel function and $Y_{lm}$ the spherical harmonic. This partial wave basis is useful for defining the operator for the nucleon-nucleon interaction, which is symmetric with respect to rotations, parity and isospin transformations. These symmetries imply that the interaction is diagonal with respect to the quantum numbers of total angular momentum $J$, spin $S$ and isospin $T$. Using the above plane wave expansion, and coupling to final $J$, $S$ and $T$ we get

$$\langle \mathbf{k}'|V|\mathbf{k}\rangle = (4\pi)^2 \sum_{JM} \sum_{lm} \sum_{l'm'} \imath^{l+l'} Y^*_{lm}(\hat{\mathbf{k}}) Y_{l'm'}(\hat{\mathbf{k}}') \mathscr{C}^{l'SJ}_{m'M_SM} \mathscr{C}^{lSJ}_{mM_SM} \langle k'l'STJM|V|klSTJM\rangle,$$

where we have defined

$$\langle k'l'STJM|V|klSTJM\rangle = \int j_{l'}(k'r') \langle l'STJM|V(r', r)|lSTJM\rangle j_l(kr) r'^2 dr' r^2 dr.$$

We have omitted the momentum of the center-of-mass motion $\mathbf{K}$ and the corresponding orbital momentum $L$, since the interaction is diagonal in these variables.

The interaction we will use for these calculations is a semirealistic nucleon-nucleon potential known as the Minnesota potential [57] which has the form, $V_\alpha(r) = V_\alpha \exp(-\alpha r^2)$. The spin and isospin dependence of the Minnesota potential is given by,

$$V(r) = \frac{1}{2}\left(V_R + \frac{1}{2}\left(1 + P^\sigma_{12}\right) V_T + \frac{1}{2}\left(1 - P^\sigma_{12}\right) V_S\right)\left(1 - P^\sigma_{12} P^\tau_{12}\right),$$

where $P^\sigma_{12} = \frac{1}{2}(1 + \sigma_1 \cdot \sigma_2)$ and $P^\tau_{12} = \frac{1}{2}(1 + \tau_1 \cdot \tau_2)$ are the spin and isospin exchange operators, respectively. A Fourier transform to momentum space of the radial part $V_\alpha(r)$ is rather simple, see Problem 8.5, since the radial depends only on the magnitude of the relative distance and thereby the relative momentum $\mathbf{q} = \frac{1}{2}\left(\mathbf{k}_p - \mathbf{k}_q - \mathbf{k}_r + \mathbf{k}_s\right)$. Omitting spin and isospin dependencies, the momentum

**Table 8.2** Parameters used to define the Minnesota interaction model [57]

| $\alpha$ | $V_\alpha$ in MeV | $\kappa_\alpha$ in fm$^{-2}$ |
|---|---|---|
| $R$ | 200 | 1.487 |
| $T$ | 178 | 0.639 |
| $S$ | 91.85 | 0.465 |

space version of the interaction reads

$$\langle \mathbf{k}_p \mathbf{k}_q | V_\alpha | \mathbf{k}_r \mathbf{k}_s \rangle = \frac{V_\alpha}{L^3} \left(\frac{\pi}{\alpha}\right)^{3/2} \exp\left(\frac{-q^2}{4\alpha}\right) \delta_{\mathbf{k}_p + \mathbf{k}_q, \mathbf{k}_r + \mathbf{k}_s}$$

The various parameters defining the interaction model used in this work are listed in Table 8.2.

### 8.2.4 *Models from Effective Field Theory for the Two- and Three-Nucleon Interactions*

During the past two decades it has been demonstrated that chiral effective field theory represents a powerful tool to deal with hadronic interactions at low energy in a systematic and model-independent way (see [14–16, 18, 58–62]). Effective field theories (EFTs) are defined in terms of effective Lagrangians which are given by an infinite series of terms with increasing number of derivatives and/or nucleon fields, with the dependence of each term on the pion field prescribed by the rules of broken chiral symmetry. Applying this Lagrangian to a particular process, an unlimited number of Feynman graphs can be drawn. Therefore, a scheme is needed that makes the theory manageable and calculable. This scheme which tells us how to distinguish between large (important) and small (unimportant) contributions is chiral perturbation theory (ChPT). Chiral perturbation theory allows for an expansion in terms of $(Q/\Lambda_\chi)^\nu$, where $Q$ is generic for an external momentum (nucleon three-momentum or pion four-momentum) or a pion mass, and $\Lambda_\chi \sim 1$ GeV is the chiral symmetry breaking scale. Determining the power $\nu$ has become known as power counting.

Nuclear potentials are defined as sets of irreducible graphs up to a given order. The power $\nu$ of a few-nucleon diagram involving $A$ nucleons is given in terms of naive dimensional analysis by:

$$\nu = -2 + 2A - 2C + 2L + \sum_i \Delta_i \,, \tag{8.3}$$

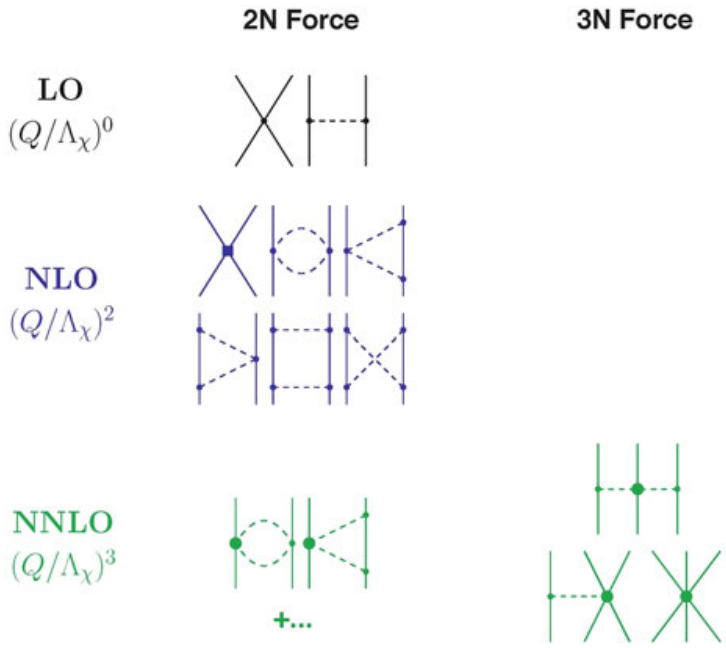


**Fig. 8.1** Nuclear forces in ChPT up to NNLO. *Solid lines* represent nucleons and *dashed lines* pions. *Small dots*, *large solid dots*, and *solid squares* denote vertices of index $\Delta_i = 0$, 1, and 2, respectively

with

$$\Delta_i \equiv d_i + \frac{n_i}{2} - 2\,,$$

where $A$ labels the number of nucleons, $C$ denotes the number of separately connected pieces and $L$ the number of loops in the diagram; $d_i$ is the number of derivatives or pion-mass insertions and $n_i$ the number of nucleon fields (nucleon legs) involved in vertex $i$; the sum runs over all vertices contained in the diagram under consideration. Note that $\Delta_i \geq 0$ for all interactions allowed by chiral symmetry. In this work we will focus on the simple Minnesota model discussed above. It is however possible, see also the exercises, to include two- and three-nucleon forces at order NNLO, as indicated in Fig. 8.1.

Below we revisit briefly the formalism and results presented in [62]. For further details on chiral effective field theory and nuclear interactions, see for example [15, 16, 18, 61, 62] For an irreducible *NN* diagram ("two-nucleon potential", $A = 2$, $C = 1$), Eq. (8.3) collapses to

$$\nu = 2L + \sum_i \Delta_i\,.$$

Thus, in terms of naive dimensional analysis or "Weinberg counting" [58], the various orders of the irreducible graphs which define the chiral *NN* potential are

given by (see Fig. 8.1)

$$V_{\rm LO} = V_{\rm ct}^{(0)} + V_{1\pi}^{(0)}$$
$$V_{\rm NLO} = V_{\rm LO} + V_{\rm ct}^{(2)} + V_{1\pi}^{(2)} + V_{2\pi}^{(2)}$$
$$V_{\rm NNLO} = V_{\rm NLO} + V_{1\pi}^{(3)} + V_{2\pi}^{(3)}$$

where the superscript denotes the order $\nu$ of the low-momentum expansion, LO stands for leading order, NLO for next-to-leading order and NNLO stands for next-to-next-to leading order. Contact potentials carry the subscript "ct" and pion-exchange potentials can be identified by an obvious subscript.

The charge-independent one-pion-exchange (1PE) potential reads

$$V_{1\pi}(\mathbf{k}\,',\mathbf{k}) = -\frac{g_A^2}{4f_\pi^2}\,\boldsymbol{\tau}_1\cdot\boldsymbol{\tau}_2\,\frac{\boldsymbol{\sigma}_1\cdot\mathbf{q}\;\boldsymbol{\sigma}_2\cdot\mathbf{q}}{q^2+m_\pi^2}\,, \tag{8.4}$$

where $\mathbf{k}\,'$ and $\mathbf{k}$ represent the final and initial nucleon momenta in the center-of-mass system (CMS) and $\mathbf{q} \equiv \mathbf{k}\,' - \mathbf{k}$ is the momentum transfer; $\boldsymbol{\sigma}_{1,2}$ and $\boldsymbol{\tau}_{1,2}$ are the spin and isospin operators of nucleon 1 and 2; $g_A$, $f_\pi$, and $m_\pi$ denote axial-vector coupling constant, the pion decay constant, and the pion mass, respectively. Since higher order corrections contribute only to mass and coupling constant renormalizations and since, on shell, there are no relativistic corrections, the on-shell 1PE has the form of Eq. (8.4) to all orders.

It is well known that for high-precision *NN* potentials, charge dependence is important. To take into account the charge dependence of the 1PE contribution we define a pion-mass dependent 1PE by

$$V_{1\pi}(m_\pi) \equiv -\frac{g_A^2}{4f_\pi^2}\,\frac{\boldsymbol{\sigma}_1\cdot\mathbf{q}\;\boldsymbol{\sigma}_2\cdot\mathbf{q}}{q^2+m_\pi^2}.$$

The 1PE for proton-proton (*pp*) and neutron-neutron (*nn*) terms are then given by

$$V_{1\pi}^{(pp)}(\mathbf{k}\,',\mathbf{k}) = V_{1\pi}^{(nn)}(\mathbf{k}\,',\mathbf{k}) = V_{1\pi}(m_{\pi^0})\,,$$

while for the neutron-proton (*np*) part we have

$$V_{1\pi}^{(np)}(\mathbf{k}\,',\mathbf{k}) = -V_{1\pi}(m_{\pi^0}) + (-1)^{T+1}\,2\,V_{1\pi}(m_{\pi^\pm})\,,$$

where $T$ denotes the isospin of the two-nucleon system. The pion masses are defined as $m_{\pi^0} = 134.9766\,\text{MeV}$ and $m_{\pi^\pm} = 139.5702\,\text{MeV}$. For the leading-order, next-to-leading order and NNLO, we refer the reader to [15, 62]. The final interaction at

order NNLO is multiplied with the following factors [15],

$$\widehat{V}(\mathbf{k}\,',\mathbf{k}) \equiv \frac{1}{(2\pi)^3}\sqrt{\frac{M_N}{E_{p'}}}\,V(\mathbf{p}\,',\mathbf{p})\,\sqrt{\frac{M_N}{E_p}}$$

with $E_p = \sqrt{M_N^2 + p^2}$ and where the factor $1/(2\pi)^3$ is just added for convenience. The potential $\widehat{V}$ satisfies the nonrelativistic Lippmann-Schwinger (LS) equation, see [15] for discussions,

$$\widehat{T}(\mathbf{k}\,',\mathbf{k}) = \widehat{V}(\mathbf{k}\,',\mathbf{k}) + \int d^3p''\,\widehat{V}(\mathbf{k}\,',\mathbf{k}\,'')\,\frac{M_N}{k^2 - k''^2 + i\epsilon}\,\widehat{T}(\mathbf{k}\,'',\mathbf{k})\,.$$

In *pp* scattering, we use $M_N = M_p = 938.2720\,\text{MeV}$, and in *nn* scattering, $M_N = M_n = 939.5653\,\text{MeV}$. Moreover, the on-shell momentum is simply

$$p^2 = \frac{1}{2}M_N T_{\text{lab}}\,,$$

where $T_{\text{lab}}$ denotes the kinetic energy of the incident nucleon in the laboratory system ("Lab. Energy"). For *np* scattering, we have the relations

$$M_N = \frac{2M_pM_n}{M_p + M_n} = 938.9182\,\text{MeV, and}$$

$$p^2 = \frac{M_p^2 T_{\text{lab}}(T_{\text{lab}} + 2M_n)}{(M_p + M_n)^2 + 2T_{\text{lab}}M_p}\,,$$

which are based upon relativistic kinematics.

Iteration of $\hat{V}$ in the Lippman-Schwinger equation discussed above, requires cutting $\hat{V}$ off for high momenta to avoid infinities. This is consistent with the fact that ChPT is a low-momentum expansion which is valid only for momenta $Q \ll \Lambda_\chi \approx 1\,\text{GeV}$. Therefore, the potential $\hat{V}$ is multiplied with the regulator function $f(k', k)$,

$$\hat{V}(\mathbf{k}\,',\mathbf{k}) \longmapsto \hat{V}(\mathbf{k}\,',\mathbf{k})\,f(k', k)$$

with

$$f(p', p) = \exp[-(p'/\Lambda)^{2n} - (p/\Lambda)^{2n}],$$

as a possible example.

Up to NNLO in chiral perturbation theory there are, in addition to the two-body interaction diagrams discussed above, also a few three-body interaction diagrams, see Fig. 8.1. In chiral perturbation theory, the orders are generated systematically, and at a given chiral order the number of Feynman diagrams is finite. Consistency

requires that a calculation includes all diagrams which are present at the chosen order. There are in total five contact terms that determine the strength of the NNLO three-nucleon force (3NF); $c_1, c_3$, and $c_4$ are associated with the three-body two-pion-exchange (2PE) diagram, $c_D$ and $c_E$ determine the strength of the one-pion-exchange plus contact (1PE) diagram and the pure contact (CNT) diagram, respectively. References [16, 63] give an extensive discussions of these terms.

## 8.3 Hartree-Fock Theory

Hartree-Fock (HF) theory is an algorithm for finding an approximative expression for the ground state of a given Hamiltonian. The basic ingredients contain a single-particle basis $\{\psi_\alpha\}$ defined by the solution of the following eigenvalue problem

$$\hat{h}^{\rm HF}\psi_\alpha = \varepsilon_\alpha\psi_\alpha,$$

with the Hartree-Fock Hamiltonian defined as

$$\hat{h}^{\rm HF} = \hat{t} + \hat{u}_{\rm ext} + \hat{u}^{\rm HF}.$$

The term $\hat{u}^{\rm HF}$ is a single-particle potential to be determined by the HF algorithm. The HF algorithm means to select $\hat{u}^{\rm HF}$ in order to have

$$\langle\hat{H}\rangle = E^{\rm HF} = \langle\Phi_0^{HF}|\hat{H}|\Phi_0^{HF}\rangle,$$

as a local minimum with a Slater determinant $\Phi_0^{HF}$ being the ansatz for the ground state. The variational principle ensures that $E^{\rm HF} \geq E_0$, with $E_0$ representing the exact ground state energy.

We will show that the Hartree-Fock Hamiltonian $\hat{h}^{\rm HF}$ equals our definition of the operator $\hat{f}$ discussed in connection with the new definition of the normal-ordered Hamiltonian, that is we have, for a specific matrix element

$$\langle p|\hat{h}^{\rm HF}|q\rangle = \langle p|\hat{f}|q\rangle = \langle p|\hat{t} + \hat{u}_{\rm ext}|q\rangle + \sum_{i\leq F}\langle pi|\hat{V}|qi\rangle,$$

meaning that

$$\langle p|\hat{u}^{\rm HF}|q\rangle = \sum_{i\leq F}\langle pi|\hat{V}|qi\rangle.$$

The so-called Hartree-Fock potential $\hat{u}^{\rm HF}$ adds an explicit medium dependence due to the summation over all single-particle states below the Fermi level $F$. It brings also in an explicit dependence on the two-body interaction (in nuclear physics we can also have complicated three- or higher-body forces). The two-body interaction,

with its contribution from the other bystanding fermions, creates an effective mean field in which a given fermion moves, in addition to the external potential $\hat{u}_{\text{ext}}$ which confines the motion of the fermion. For systems like nuclei or infinite nuclear matter, there is no external confining potential. Nuclei and nuclear matter are examples of self-bound systems, where the binding arises due to the intrinsic nature of the strong force. For nuclear systems thus, there would be no external one-body potential in the Hartree-Fock Hamiltonian.

Another possibility is to expand the single-particle functions in a known basis and vary the coefficients, that is, the new single-particle wave function is written as a linear expansion in terms of a fixed chosen orthogonal basis (for example the well-known harmonic oscillator functions or the hydrogen-like functions etc). We define our new Hartree-Fock single-particle basis by performing a unitary transformation on our previous basis (labelled with Greek indices) as

$$\psi_p^{HF} = \sum_{\lambda} C_{p\lambda}\phi_{\lambda}. \tag{8.5}$$

In this case we vary the coefficients $C_{p\lambda}$. If the basis has infinitely many solutions, we need to truncate the above sum. We assume that the basis $\phi_\lambda$ is orthogonal. A unitary transformation keeps the orthogonality, as discussed in Problem 8.6 below.

It is normal to choose a single-particle basis defined as the eigenfunctions of parts of the full Hamiltonian. The typical situation consists of the solutions of the one-body part of the Hamiltonian, that is we have

$$\hat{h}_0\phi_\lambda = \epsilon_\lambda\phi_\lambda.$$

For infinite nuclear matter $\hat{h}_0$ is given by the kinetic energy operator and the states are given by plane wave functions. Due to the translational invariance of the two-body interaction, the Hartree-Fock single-particle eigenstates are also given by the same functions. For infinite matter thus, it is only the single-particle energies that change when we solve the Hartree-Fock equations.

The single-particle wave functions $\phi_\lambda(\mathbf{r})$, defined by the quantum numbers $\lambda$ and $\mathbf{r}$ are defined as the overlap

$$\phi_\lambda(\mathbf{r}) = \langle \mathbf{r}|\lambda\rangle.$$

In our discussions we will use our definitions of single-particle states above and below the Fermi ($F$).

We use Greek letters to refer to our original single-particle basis. The expectation value for the energy with the ansatz $\Phi_0$ for the ground state reads (see Problem 8.7, with application to infinite nuclear matter)

$$E[\Phi_0] = \sum_{\mu\leq F}\langle\mu|h|\mu\rangle + \frac{1}{2}\sum_{\mu,\nu\leq F}\langle\mu\nu|\hat{v}|\mu\nu\rangle.$$

Now we are interested in defining a new basis defined in terms of a chosen basis as defined in Eq. (8.5). We define the energy functional as

$$E[\Phi^{HF}] = \sum_{i \leq F} \langle i|h|i\rangle + \frac{1}{2} \sum_{ij \leq F} \langle ij|\hat{v}|ij\rangle, \tag{8.6}$$

where $\Phi^{HF}$ is the new Slater determinant defined by the new basis of Eq. (8.5).

Using Eq. (8.5) we can rewrite Eq. (8.6) as

$$E[\Psi] = \sum_{i \leq F} \sum_{\alpha\beta} C^*_{i\alpha} C_{i\beta} \langle \alpha|h|\beta\rangle + \frac{1}{2} \sum_{ij \leq F} \sum_{\alpha\beta\gamma\delta} C^*_{i\alpha} C^*_{j\beta} C_{i\gamma} C_{j\delta} \langle \alpha\beta|\hat{v}|\gamma\delta\rangle. \tag{8.7}$$

In order to find the variational minimum of the above functional, we introduce a set of Lagrange multipliers, noting that since $\langle i|j\rangle = \delta_{i,j}$ and $\langle \alpha|\beta\rangle = \delta_{\alpha,\beta}$, the coefficients $C_{i\gamma}$ obey the relation

$$\langle i|j\rangle = \delta_{i,j} = \sum_{\alpha\beta} C^*_{i\alpha} C_{i\beta} \langle \alpha|\beta\rangle = \sum_{\alpha} C^*_{i\alpha} C_{i\alpha},$$

which allows us to define a functional to be minimized that reads

$$F[\Phi^{HF}] = E[\Phi^{HF}] - \sum_{i \leq F} \epsilon_i \sum_{\alpha} C^*_{i\alpha} C_{i\alpha}. \tag{8.8}$$

Minimizing with respect to $C^*_{i\alpha}$ (the equations for $C^*_{i\alpha}$ and $C_{i\alpha}$ can be written as two independent equations) we obtain

$$\frac{d}{dC^*_{i\alpha}} \left[ E[\Phi^{HF}] - \sum_{j} \epsilon_j \sum_{\alpha} C^*_{j\alpha} C_{j\alpha} \right] = 0,$$

which yields for every single-particle state $i$ and index $\alpha$ (recalling that the coefficients $C_{i\alpha}$ are matrix elements of a unitary matrix, or orthogonal for a real symmetric matrix) the following Hartree-Fock equations

$$\sum_{\beta} C_{i\beta} \langle \alpha|h|\beta\rangle + \sum_{j \leq F} \sum_{\beta\gamma\delta} C^*_{j\beta} C_{j\delta} C_{i\gamma} \langle \alpha\beta|\hat{v}|\gamma\delta\rangle = \epsilon^{HF}_i C_{i\alpha}.$$

We can rewrite this equation as (changing dummy variables)

$$\sum_{\beta} \left\{ \langle \alpha|h|\beta\rangle + \sum_{j \leq F} \sum_{\gamma\delta} C^*_{j\gamma} C_{j\delta} \langle \alpha\gamma|\hat{v}|\beta\delta\rangle \right\} C_{i\beta} = \epsilon^{HF}_i C_{i\alpha}.$$

Note that the sums over Greek indices run over the number of basis set functions (in principle an infinite number).

Defining

$$h_{\alpha\beta}^{HF} = \langle\alpha|h|\beta\rangle + \sum_{j\leq F}\sum_{\gamma\delta} C_{j\gamma}^{*}C_{j\delta}\langle\alpha\gamma|\hat{v}|\beta\delta\rangle,$$

we can rewrite the new equations as

$$\sum_{\beta} h_{\alpha\beta}^{HF}C_{i\beta} = \epsilon_i^{HF}C_{i\alpha}. \tag{8.9}$$

The latter is nothing but a standard eigenvalue problem. Our Hartree-Fock matrix is thus

$$\hat{h}_{\alpha\beta}^{HF} = \langle\alpha|\hat{h}_0|\beta\rangle + \sum_{j\leq F}\sum_{\gamma\delta} C_{j\gamma}^{*}C_{j\delta}\langle\alpha\gamma|\hat{v}|\beta\delta\rangle.$$

The Hartree-Fock equations are solved in an iterative way starting with a guess for the coefficients $C_{j\gamma} = \delta_{j,\gamma}$ and solving the equations by diagonalization till the new single-particle energies $\epsilon_i^{\mathrm{HF}}$ do not change anymore by a user defined small quantity.

Normally we assume that the single-particle basis $|\beta\rangle$ forms an eigenbasis for the operator $\hat{h}_0$, meaning that the Hartree-Fock matrix becomes

$$\hat{h}_{\alpha\beta}^{HF} = \epsilon_\alpha\delta_{\alpha,\beta} + \sum_{j\leq F}\sum_{\gamma\delta} C_{j\gamma}^{*}C_{j\delta}\langle\alpha\gamma|\hat{v}|\beta\delta\rangle.$$

### *8.3.1 Hartree-Fock Algorithm with Simple Python Code*

The equations are often rewritten in terms of a so-called density matrix, which is defined as

$$\rho_{\gamma\delta} = \sum_{i\leq F}\langle\gamma|i\rangle\langle i|\delta\rangle = \sum_{i=1}^{N} C_{i\gamma}C_{i\delta}^{*}. \tag{8.10}$$

It means that we can rewrite the Hartree-Fock Hamiltonian as

$$\hat{h}_{\alpha\beta}^{HF} = \epsilon_\alpha\delta_{\alpha,\beta} + \sum_{\gamma\delta}\rho_{\gamma\delta}\langle\alpha\gamma|V|\beta\delta\rangle.$$

It is convenient to use the density matrix since we can precalculate in every iteration the product of the eigenvector components $C$.

The Hartree-Fock equations are, in their simplest form, solved in an iterative way, starting with a guess for the coefficients $C_{i\alpha}$. We label the coefficients as $C_{i\alpha}^{(n)}$, where the superscript $n$ stands for iteration $n$. To set up the algorithm we can proceed as follows.

1. We start with a guess $C_{i\alpha}^{(0)} = \delta_{i,\alpha}$. Alternatively, we could have used random starting values as long as the vectors are normalized. Another possibility is to give states below the Fermi level a larger weight. We construct then the density matrix and the Hartree-Fock Hamiltonian.
2. The Hartree-Fock matrix simplifies then to

$$\hat{h}_{\alpha\beta}^{HF}(0) = \epsilon_\alpha \delta_{\alpha,\beta} + \sum_{\gamma\delta} \rho_{\gamma\delta}^{(0)} \langle \alpha\gamma | V | \beta\delta \rangle.$$

   Solving the Hartree-Fock eigenvalue problem yields then new eigenvectors $C_{i\alpha}^{(1)}$ and eigenvalues $\epsilon_i^{\mathrm{HF}}(1)$.
3. With the new eigenvectors we can set up a new Hartree-Fock potential

$$\sum_{\gamma\delta} \rho_{\gamma\delta}^{(1)} \langle \alpha\gamma | V | \beta\delta \rangle.$$

   The diagonalization with the new Hartree-Fock potential yields new eigenvectors and eigenvalues.
4. This process is continued till a user defined test is satisfied. As an example, we can require that

$$\frac{\sum_p |\epsilon_i^{(n)} - \epsilon_i^{(n-1)}|}{m} \leq \lambda,$$

   where $\lambda$ is a small number defined by the user ($\lambda \sim 10^{-8}$ or smaller) and $p$ runs over all calculated single-particle energies and $m$ is the number of single-particle states.

The following simple Python program implements the above algorithm using the density matrix formalism outlined above. We have omitted the functions that set up the single-particle basis and the anti-symmetrized two-body interaction matrix elements. These have to be provided, see https://github.com/ManyBodyPhysics/LectureNotesPhysics/tree/master/Programs/Chapter8-programs/python for full code and matrix elements.

```
# We skip here functions that set up the one- and two-body parts
     of the Hamiltonian
# These functions need to be defined by the user. The two-body
    interaction below is
# calculated by calling the function TwoBodyInteraction(alpha,
    gamma,beta,delta)
# Similarly, the one-body part is computed by the function
    singleparticleH(alpha)
# We have omitted specific quantum number tests as well (isospin
     conservation,
# momentum conservation etc)
import numpy as np
from decimal import Decimal

if __name__ == '__main__':

  """ Star HF-iterations, preparing variables and density matrix
       """

       """ Coefficients for setting up density matrix, assuming
           only one along the diagonals """
  C = np.eye(spOrbitals) # HF coefficients
       DensityMatrix = np.zeros([spOrbitals,spOrbitals])
       for gamma in range(spOrbitals):
          for delta in range(spOrbitals):
             sum = 0.0
             for i in range(Nparticles):
                sum += C[gamma][i]*C[delta][i]
             DensityMatrix[gamma][delta] = Decimal(sum)
       maxHFiter = 100
       epsilon = 1.0e-5
       difference = 1.0
  hf_count = 0
  oldenergies = np.zeros(spOrbitals)
  newenergies = np.zeros(spOrbitals)
  while hf_count < maxHFiter and difference > epsilon:
          HFmatrix = np.zeros([spOrbitals,spOrbitals])
    for alpha in range(spOrbitals):
      for beta in range(spOrbitals):
                     """ Setting up the Fock matrix using the
                         density matrix and antisymmetrized two-
                         body interaction """
                sumFockTerm = 0.0
                      for gamma in range(spOrbitals):
                         for delta in range(spOrbitals):
                            sumFockTerm += DensityMatrix[gamma][
                                delta]*
                                       TwoBodyInteraction(alpha,
                                           gamma,beta,delta)
                      HFmatrix[alpha][beta] = Decimal(sumFockTerm
                          )
                      """ Adding the one-body term """
```

```
                    if beta == alpha: HFmatrix[alpha][alpha] +=
                         singleparticleH(alpha)
spenergies, C = np.linalg.eigh(HFmatrix)
          """ Setting up new density matrix """
          DensityMatrix = np.zeros([spOrbitals,spOrbitals])
          for gamma in range(spOrbitals):
             for delta in range(spOrbitals):
                sum = 0.0
                for i in range(Nparticles):
                   sum += C[gamma][i]*C[delta][i]
                DensityMatrix[gamma][delta] = Decimal(sum)
newenergies = spenergies
          """ Brute force computation of difference between
              previous and new sp HF energies """
          sum =0.0
          for i in range(spOrbitals):
             sum += (abs(newenergies[i]-oldenergies[i]))/
                 spOrbitals
          difference = sum
          oldenergies = newenergies
          print "Single-particle energies, ordering may have
              changed "
          for i in range(spOrbitals):
             print('{0:4d} {1:.4f}'.format(i, Decimal(
                 oldenergies[i])))
hf_count += 1
```

We end this section by rewriting the ground state energy by adding and subtracting $\hat{u}^{HF}$. Using anti-symmetrized two-body matrix elements we have

$$E_0^{HF} = \langle \Phi_0 | \hat{H} | \Phi_0 \rangle = \sum_{i \leq F}^{A} \langle i | \hat{h}_0 + \hat{u}^{HF} | i \rangle + \frac{1}{2} \sum_{i \leq F}^{A} \sum_{j \leq F}^{A} \langle ij | \hat{v} | ij \rangle - \sum_{i \leq F}^{A} \langle i | \hat{u}^{HF} | i \rangle,$$

which results in

$$E_0^{HF} = \sum_{i \leq F}^{A} \varepsilon_i^{HF} + \frac{1}{2} \sum_{i \leq F}^{A} \sum_{j \leq F}^{A} \langle ij | \hat{v} | ij \rangle - \sum_{i \leq F}^{A} \langle i | \hat{u}^{HF} | i \rangle.$$

Our single-particle states $ijk\ldots$ are now single-particle states obtained from the solution of the Hartree-Fock equations.

Using our definition of the Hartree-Fock single-particle energies we obtain then the following expression for the total ground-state energy

$$E_0^{HF} = \sum_{i \leq F}^{A} \varepsilon_i - \frac{1}{2} \sum_{i \leq F}^{A} \sum_{j \leq F}^{A} \langle ij | \hat{v} | ij \rangle.$$

This equation demonstrates that the total energy is not given as the sum of the individual single-particle energies.

## 8.4 Full Configuration Interaction Theory

Full configuration theory (FCI), which represents a discretized variant of the continuous eigenvalue problem, allows for, in principle, an exact (to numerical precision) solution of Schrödinger's equation for many interacting fermions or bosons with a given basis set. This basis set defines an effective Hilbert space. For fermionic problems, the standard approach is to define an upper limit for the set of single-particle states. As an example, if we use the harmonic oscillator one-body Hamiltonian to generate an orthogonal single-particle basis, truncating the basis at some oscillator excitation energy provides thereby an upper limit. Similarly, truncating the maximum values of $n_{x,y,z}$ for plane wave states with periodic boundary conditions, yields a similar upper limit. Table 8.1 lists several possible truncations to the basis set in terms of the single-particle energies as functions of $n_{x,y,z}$. This single-particle basis is then used to define all possible Slater determinants which can be constructed with a given number of fermions $A$. The total number of Slater determinants determines thereafter the dimensionality of the Hamiltonian matrix and thereby an effective Hilbert space. If we are able to set up the Hamiltonian matrix and solve the pertinent eigenvalue problem within this basis set, FCI provides numerically exact solutions to all states of interest for a given many-body problem. The dimensionality of the problem explodes however quickly. To see this it suffices to consider the total number of Slater determinants which can be built with say $N$ neutrons distributed among $n$ single-particle states. The total number is

$$\binom{n}{N} = \frac{n!}{(n-N)!N!}.$$

As an example, for a model space which comprises the first four major harmonic oscillator shells only, that is the $0s$, $0p$, $1s0d$ and $1p0f$ shells we have 40 single particle states for neutrons and protons. For the eight neutrons of oxygen-16 we would then have

$$\binom{40}{8} = \frac{40!}{(32)!8!} \sim 8 \times 10^7,$$

possible Slater determinants. Multiplying this with the number of proton Slater determinants we end up with approximately $d \sim 10^{15}$ possible Slater determinants and a Hamiltonian matrix of dimension $10^{15} \times 10^{15}$, an intractable problem if we wish to diagonalize the Hamiltonian matrix. The dimensionality can be reduced if we look at specific symmetries, however these symmetries will never reduce the problem to dimensionalities which can be handled by standard eigenvalue solvers.

These are normally lumped into two main categories, direct solvers for matrices of dimensionalities which are smaller than $d \sim 10^5$, and iterative eigenvalue solvers (when only selected states are being sought after) for dimensionalities up to $10^{10} \times 10^{10}$.

Due to its discreteness thus, the effective Hilbert space will always represent an approximation to the full continuous problem. However, with a given Hamiltonian matrix and effective Hilbert space, FCI provides us with true benchmarks that can convey important information on correlations beyond Hartree-Fock theory and various approximative many-body methods like many-body perturbation theory, coupled cluster theory, Green's function theory and the Similarity Renormalization Group approach. These methods are all discussed in this text. Assuming that we can diagonalize the Hamiltonian matrix, and thereby obtain the exact solutions, this section serves the aim to link the exact solution obtained from FCI with various approximative methods, hoping thereby that eventual differences can shed light on which correlations play a major role and should be included in the above approximative methods. The simple pairing model discussed in Problem 8.10 is an example of a system that allows us to compare exact solutions with those defined by many-body perturbation theory to a given order in the interaction, coupled cluster theory, Green's function theory and the Similarity Renormalization Group (SRG).

In order to familiarize the reader with these approximative many-body methods, we start with the general definition of the full configuration interaction problem.

We have defined the ansatz for the ground state as

$$|\Phi_0\rangle = \left(\prod_{i \leq F} \hat{a}_i^\dagger\right)|0\rangle,$$

where the variable $i$ defines different single-particle states up to the Fermi level. We have assumed that we have $A$ nucleons and that the chosen single-particle states are eigenstates of the one-body Hamiltonian $\hat{h}_0$ (defining thereby an orthogonal basis set). A given one-particle-one-hole ($1p1h$) state can be written as

$$|\Phi_i^a\rangle = \hat{a}_a^\dagger \hat{a}_i |\Phi_0\rangle,$$

while a $2p2h$ state can be written as

$$|\Phi_{ij}^{ab}\rangle = \hat{a}_a^\dagger \hat{a}_b^\dagger \hat{a}_j \hat{a}_i |\Phi_0\rangle,$$

and a general $ApAh$ state as

$$|\Phi_{ijk\ldots}^{abc\ldots}\rangle = \hat{a}_a^\dagger \hat{a}_b^\dagger \hat{a}_c^\dagger \ldots \hat{a}_k \hat{a}_j \hat{a}_i |\Phi_0\rangle.$$

As before, we use letters $ijkl\ldots$ for states below the Fermi level and $abcd\ldots$ for states above the Fermi level. A general single-particle state is given by letters $pqrs\ldots$.

We can then expand our exact state function for the ground state as

$$|\Psi_0\rangle = C_0|\Phi_0\rangle + \sum_{ai} C_i^a|\Phi_i^a\rangle + \sum_{abij} C_{ij}^{ab}|\Phi_{ij}^{ab}\rangle + \cdots = (C_0 + \hat{C})|\Phi_0\rangle,$$

where we have introduced the so-called correlation operator

$$\hat{C} = \sum_{ai} C_i^a \hat{a}_a^\dagger \hat{a}_i + \sum_{abij} C_{ij}^{ab} \hat{a}_a^\dagger \hat{a}_b^\dagger \hat{a}_j \hat{a}_i + \dots$$

Since the normalization of $\Psi_0$ is at our disposal and since $C_0$ is by assumption not zero, we may arbitrarily set $C_0 = 1$ with corresponding proportional changes in all other coefficients. Using this so-called intermediate normalization we have

$$\langle\Psi_0|\Phi_0\rangle = \langle\Phi_0|\Phi_0\rangle = 1,$$

resulting in

$$|\Psi_0\rangle = (1 + \hat{C})|\Phi_0\rangle.$$

We rewrite

$$|\Psi_0\rangle = C_0|\Phi_0\rangle + \sum_{ai} C_i^a|\Phi_i^a\rangle + \sum_{abij} C_{ij}^{ab}|\Phi_{ij}^{ab}\rangle + \dots,$$

in a more compact form as

$$|\Psi_0\rangle = \sum_{PH} C_H^P \Phi_H^P = \left(\sum_{PH} C_H^P \hat{A}_H^P\right)|\Phi_0\rangle,$$

where $H$ stands for $0, 1, \dots, n$ hole states and $P$ for $0, 1, \dots, n$ particle states. The operator $\hat{A}_H^P$ represents a given set of particle-hole excitations. For a two-particle-to-hole excitation this operator is given by $\hat{A}_{2h}^{2p} = \hat{a}_a^\dagger \hat{a}_b^\dagger \hat{a}_j \hat{a}_i$. Our requirement of unit normalization gives

$$\langle\Psi_0|\Psi_0\rangle = \sum_{PH} |C_H^P|^2 = 1,$$

and the energy can be written as

$$E = \langle\Psi_0|\hat{H}|\Psi_0\rangle = \sum_{PP'HH'} C_H^{*P} \langle\Phi_H^P|\hat{H}|\Phi_{H'}^{P'}\rangle C_{H'}^{P'}.$$

The last equation is normally solved by diagonalization, with the Hamiltonian matrix defined by the basis of all possible Slater determinants. A diagonalization is equivalent to finding the variational minimum of

$$\langle \Psi_0 | \hat{H} | \Psi_0 \rangle - \lambda \langle \Psi_0 | \Psi_0 \rangle,$$

where $\lambda$ is a variational multiplier to be identified with the energy of the system.

The minimization process results in

$$0 = \delta \left[ \langle \Psi_0 | \hat{H} | \Psi_0 \rangle - \lambda \langle \Psi_0 | \Psi_0 \rangle \right] \tag{8.11}$$

$$= \sum_{P'H'} \left\{ \delta[C_H^{*P}] \langle \Phi_H^P | \hat{H} | \Phi_{H'}^{P'} \rangle C_{H'}^{P'} + C_H^{*P} \langle \Phi_H^P | \hat{H} | \Phi_{H'}^{P'} \rangle \delta[C_{H'}^{P'}] - \lambda (\delta[C_H^{*P}] C_{H'}^{P'} + C_H^{*P} \delta[C_{H'}^{P'}] \right\}. \tag{8.12}$$

Since the coefficients $\delta[C_H^{*P}]$ and $\delta[C_{H'}^{P'}]$ are complex conjugates it is necessary and sufficient to require the quantities that multiply with $\delta[C_H^{*P}]$ to vanish.

This leads to

$$\sum_{P'H'} \langle \Phi_H^P | \hat{H} | \Phi_{H'}^{P'} \rangle C_{H'}^{P'} - \lambda C_H^P = 0,$$

for all sets of $P$ and $H$.

If we then multiply by the corresponding $C_H^{*P}$ and sum over $PH$ we obtain

$$\sum_{PP'HH'} C_H^{*P} \langle \Phi_H^P | \hat{H} | \Phi_{H'}^{P'} \rangle C_{H'}^{P'} - \lambda \sum_{PH} |C_H^P|^2 = 0,$$

leading to the identification $\lambda = E$. This means that we have for all $PH$ sets

$$\sum_{P'H'} \langle \Phi_H^P | \hat{H} - E | \Phi_{H'}^{P'} \rangle = 0. \tag{8.13}$$

An alternative way to derive the last equation is to start from

$$(\hat{H} - E) | \Psi_0 \rangle = (\hat{H} - E) \sum_{P'H'} C_{H'}^{P'} | \Phi_{H'}^{P'} \rangle = 0,$$

and if this equation is successively projected against all $\Phi_H^P$ in the expansion of $\Psi$, we end up with Eq. (8.13).

If we are able to solve this equation by numerical diagonalization in a large Hilbert space (it will be truncated in terms of the number of single-particle states included in the definition of Slater determinants), it can then serve as a benchmark for other many-body methods which approximate the correlation operator $\hat{C}$. Our pairing model discussed in Problem 8.10 is an example of a system which can

be diagonalized exactly, providing thereby benchmarks for different approximative methods.

To better understand the meaning of possible configurations and the derivation of a Hamiltonian matrix, we consider here a simple example of six fermions. We assume we can make an ansatz for the ground state with all six fermions below the Fermi level. We label this state as a zero-particle-zero-hole state $0p-0h$. With six nucleons we can make at most $6p-6h$ excitations. If we have an infinity of single particle states above the Fermi level, we will obviously have an infinity of say $2p-2h$ excitations. Each specific way to distribute the particles represents a configuration. We will always have to truncate the basis of single-particle states. This gives us a finite number of possible Slater determinants. Our Hamiltonian matrix would then look like (where each block which is marked with an $x$ can contain a large quantity of non-zero matrix elements) as shown here if the Hamiltonian contains at most a two-

| | $0p-0h$ | $1p-1h$ | $2p-2h$ | $3p-3h$ | $4p-4h$ | $5p-5h$ | $6p-6h$ |
|---|---|---|---|---|---|---|---|
| $0p-0h$ | $x$ | $x$ | $x$ | 0 | 0 | 0 | 0 |
| $1p-1h$ | $x$ | $x$ | $x$ | $x$ | 0 | 0 | 0 |
| $2p-2h$ | $x$ | $x$ | $x$ | $x$ | $x$ | 0 | 0 |
| $3p-3h$ | 0 | $x$ | $x$ | $x$ | $x$ | $x$ | 0 |
| $4p-4h$ | 0 | 0 | $x$ | $x$ | $x$ | $x$ | $x$ |
| $5p-5h$ | 0 | 0 | 0 | $x$ | $x$ | $x$ | $x$ |
| $6p-6h$ | 0 | 0 | 0 | 0 | $x$ | $x$ | $x$ |

body interaction, as demonstrated in Problem 8.8. If we use a so-called canonical Hartree-Fock basis [35], this corresponds to a particular unitary transformation where matrix elements of the type $\langle 0p-0h|\hat{H}|1p-1h\rangle = \langle \Phi_0|\hat{H}|\Phi_i^a\rangle = 0$. With a canonical Hartree-Fock basis our Hamiltonian matrix reads

| | $0p-0h$ | $1p-1h$ | $2p-2h$ | $3p-3h$ | $4p-4h$ | $5p-5h$ | $6p-6h$ |
|---|---|---|---|---|---|---|---|
| $0p-0h$ | $\tilde{x}$ | 0 | $\tilde{x}$ | 0 | 0 | 0 | 0 |
| $1p-1h$ | 0 | $\tilde{x}$ | $\tilde{x}$ | $\tilde{x}$ | 0 | 0 | 0 |
| $2p-2h$ | $\tilde{x}$ | $\tilde{x}$ | $\tilde{x}$ | $\tilde{x}$ | $\tilde{x}$ | 0 | 0 |
| $3p-3h$ | 0 | $\tilde{x}$ | $\tilde{x}$ | $\tilde{x}$ | $\tilde{x}$ | $\tilde{x}$ | 0 |
| $4p-4h$ | 0 | 0 | $\tilde{x}$ | $\tilde{x}$ | $\tilde{x}$ | $\tilde{x}$ | $\tilde{x}$ |
| $5p-5h$ | 0 | 0 | 0 | $\tilde{x}$ | $\tilde{x}$ | $\tilde{x}$ | $\tilde{x}$ |
| $6p-6h$ | 0 | 0 | 0 | 0 | $\tilde{x}$ | $\tilde{x}$ | $\tilde{x}$ |

If we do not make any truncations in the possible sets of Slater determinants (many-body states) we can make by distributing $A$ nucleons among $n$ single-particle states, we call such a calculation for a full configuration interaction (FCI) approach. If we make truncations, we have several different possibilities to reduce the dimensionality of the problem. A well-known example is the standard nuclear

shell-model. For the nuclear shell model we define an effective Hilbert space with respect to a given core. The calculations are normally then performed for all many-body states that can be constructed from the effective Hilbert spaces. This approach requires a properly defined effective Hamiltonian. Another possibility to constrain the dimensionality of the problem is to truncate in the number of excitations. As an example, we can limit the possible Slater determinants to only $1p-1h$ and $2p-2h$ excitations. This is called a configuration interaction calculation at the level of singles and doubles excitations. If we truncate at the level of three-particle-three-hole excitations we end up with singles, doubles and triples excitations. Such truncations reduce considerably the size of the Hamiltonian matrices to be diagonalized, but can lead to so-called unlinked contributions, and thereby wrong results, for a given expectation value [34]. A third possibility is to constrain the number of excitations by an energy cutoff. This cutoff defines a maximum excitation energy. The maximum excitation energy is normally given by the sum of single-particle energies defined by the unperturbed one-body part of the Hamiltonian. A commonly used basis in nuclear physics is the harmonic oscillator. The cutoff in energy is then defined by the maximum number of harmonic oscillator excitations. If we do not define a core, this defines normally what is called the no-core shell-model approach, see for example [25, 64].

### 8.4.1 A Non-practical Way of Solving the Eigenvalue Problem

For reasons to come (links with coupled cluster theory and many-body perturbation theory), we will rewrite Eq. (8.13) as a set of coupled non-linear equations in terms of the unknown coefficients $C_H^P$. To obtain the eigenstates and eigenvalues in terms of non-linear equations is less efficient than using standard eigenvalue solvers [65]. However, this digression serves the scope of linking full configuration interaction theory with approximative solutions to the many-body problem.

To see this, we look at the contributions arising from

$$\langle \Phi_H^P| = \langle \Phi_0|$$

in Eq. (8.13), that is we multiply with $\langle \Phi_0|$ from the left in

$$(\hat{H}-E)\sum_{P'H'} C_{H'}^{P'}|\Phi_{H'}^{P'}\rangle = 0.$$

If we assume that we have a two-body operator at most, the Slater-Condon rule for a two-body interaction, see Problem 8.8, results in an expression for the correlation

energy in terms of $C_i^a$ and $C_{ij}^{ab}$ only, namely

$$\langle \Phi_0|\hat{H}-E|\Phi_0\rangle + \sum_{ai}\langle \Phi_0|\hat{H}-E|\Phi_i^a\rangle C_i^a + \sum_{abij}\langle \Phi_0|\hat{H}-E|\Phi_{ij}^{ab}\rangle C_{ij}^{ab} = 0,$$

or

$$E - E_{\mathrm{Ref}} = \Delta E = \sum_{ai}\langle \Phi_0|\hat{H}|\Phi_i^a\rangle C_i^a + \sum_{abij}\langle \Phi_0|\hat{H}|\Phi_{ij}^{ab}\rangle C_{ij}^{ab},$$

where the energy $E_{\mathrm{Ref}}$ is the reference energy and $\Delta E$ defines the so-called correlation energy. The single-particle basis functions could result from a Hartree-Fock calculation or they could be the eigenstates of the one-body operator that defined the non-interacting part of the Hamiltonian.

In our Hartree-Fock discussions, we have already computed the matrix $\langle \Phi_0|\hat{H}|\Phi_i^a\rangle$ and $\langle \Phi_0|\hat{H}|\Phi_{ij}^{ab}\rangle$. If we are using a Hartree-Fock basis we have $\langle \Phi_0|\hat{H}|\Phi_i^a\rangle = 0$ and we are left with a *correlation energy* given by

$$E - E_{\mathrm{Ref}} = \Delta E^{HF} = \sum_{abij}\langle \Phi_0|\hat{H}|\Phi_{ij}^{ab}\rangle C_{ij}^{ab}.$$

Inserting the various matrix elements we can rewrite the previous equation as

$$\Delta E = \sum_{ai}\langle i|\hat{f}|a\rangle C_i^a + \sum_{abij}\langle ij|\hat{v}|ab\rangle C_{ij}^{ab}. \tag{8.14}$$

This equation determines the correlation energy but not the coefficients $C$. We need more equations. Our next step is to set up

$$\langle \Phi_i^a|\hat{H}-E|\Phi_0\rangle + \sum_{bj}\langle \Phi_i^a|\hat{H}-E|\Phi_j^b\rangle C_j^b + \sum_{bcjk}\langle \Phi_i^a|\hat{H}-E|\Phi_{jk}^{bc}\rangle C_{jk}^{bc} + \sum_{bcdjkl}\langle \Phi_i^a|\hat{H}-E|\Phi_{jkl}^{bcd}\rangle C_{jkl}^{bcd} = 0,$$

as this equation will allow us to find an expression for the coefficients $C_i^a$ through

$$\langle i|\hat{f}|a\rangle + \langle \Phi_i^a|\hat{H}|\Phi_i^a\rangle C_i^a + \sum_{bj\neq ai}\langle \Phi_i^a|\hat{H}|\Phi_j^b\rangle C_j^b + \sum_{bcjk}\langle \Phi_i^a|\hat{H}|\Phi_{jk}^{bc}\rangle C_{jk}^{bc} + \sum_{bcdjkl}\langle \Phi_i^a|\hat{H}|\Phi_{jkl}^{bcd}\rangle C_{jkl}^{bcd} = EC_i^a. \tag{8.15}$$

We see that on the right-hand side we have the energy $E$. This leads to a non-linear equation in the unknown coefficients since the coefficients appear also in

the definition of the correlation energy of Eq. (8.14). These equations are normally solved iteratively, that is we start with a guess for the coefficients $C_i^a$. A common choice is to use perturbation theory as a starting point for the unknown coefficients. For the one-particle-one-hole coefficients, the wave operator (see Sect. 8.5) to first order in the interaction is given by

$$C_i^a = \frac{\langle i|\hat{f}|a\rangle}{\epsilon_i - \epsilon_a}.$$

The observant reader will however see that we need an equation for $C_{jk}^{bc}$ and $C_{jkl}^{bcd}$ and more complicated particle-hole excitations as well. To find the equations for these coefficients we need then to continue our multiplications from the left with the various $\Phi_H^P$ terms.

For $C_{jk}^{bc}$ we have

$$0 = \langle \Phi_{ij}^{ab}|\hat{H} - E|\Phi_0\rangle + \sum_{kc}\langle \Phi_{ij}^{ab}|\hat{H} - E|\Phi_k^c\rangle C_k^c \tag{8.16}$$

$$+ \sum_{cdkl}\langle \Phi_{ij}^{ab}|\hat{H} - E|\Phi_{kl}^{cd}\rangle C_{kl}^{cd} + \sum_{cdeklm}\langle \Phi_{ij}^{ab}|\hat{H} - E|\Phi_{klm}^{cde}\rangle C_{klm}^{cde}$$

$$+ \sum_{cdefklmn}\langle \Phi_{ij}^{ab}|\hat{H} - E|\Phi_{klmn}^{cdef}\rangle C_{klmn}^{cdef}. \tag{8.17}$$

We can isolate the coefficients $C_{kl}^{cd}$ in a similar way as we did for the coefficients $C_i^a$. A standard choice for the first iteration is to use again perturbation theory to first order in the interaction and set

$$C_{ij}^{ab} = \frac{\langle ij|\hat{v}|ab\rangle}{\epsilon_i + \epsilon_j - \epsilon_a - \epsilon_b}.$$

At the end we can rewrite our solution of the Schrödinger equation in terms of a series coupled equations for the coefficients $C_H^P$. This is a very cumbersome way of solving a many-body problem. However, by using this iterative scheme we can illustrate how we can compute the various terms in the wave operator or correlation operator $\hat{C}$. We will later identify the calculation of the various terms $C_H^P$ as parts of different many-body approximations to full configuration interaction theory.

### 8.4.2 Short Summary

If we can directly diagonalize large matrices, full configuration interaction theory is the method of choice since we obtain all eigenvectors and eigenvalues. The eigenvectors are obtained directly from the coefficients $C_H^P$ which result from the

diagonalization. We can then compute expectation values of other operators, as well as transition probabilities. Moreover, correlations are easy to understand in terms of contributions to a given operator beyond the Hartree-Fock contribution. For larger dimensionalities $d$, with $d > 10^5$, iterative methods [65] like Lanczos' [66] or Davidson's [67, 68] algorithms are frequently used. These methods yield, with a finite number of iteration, only a subset of all eigenvalues of interest. Lanczos' algorithm converges to the extreme values, yielding the lowest-lying and highest-lying eigenstates, see for example [65] for a proof.

With the eigenvectors we can compute the correlation energy, which is defined as (with a two-body Hamiltonian)

$$\Delta E = \sum_{ai} \langle i|\hat{f}|a\rangle C_i^a + \sum_{abij} \langle ij|\hat{v}|ab\rangle C_{ij}^{ab}.$$

The energy of the ground state is then

$$E = E_{\text{Ref}} + \Delta E.$$

However, as we have seen, even for a small case like the four first major shells and oxygen-16 with 16 active nucleons, the dimensionality becomes quickly intractable. If we wish to include single-particle states that reflect weakly bound systems, we need a much larger single-particle basis. We need thus approximative methods that sum specific correlations to infinite order. All these methods start normally with a Hartree-Fock basis as the calculational basis. In the next section we discuss one of these possible approximative methods, namely many-body perturbation theory.

## 8.5 Many-Body Perturbation Theory

We assume here that we are only interested in the non-degenerate ground state of a given system and expand the exact wave function in terms of a series of Slater determinants

$$|\Psi_0\rangle = |\Phi_0\rangle + \sum_{m=1}^{\infty} C_m |\Phi_m\rangle,$$

where we have assumed that the true ground state is dominated by the solution of the unperturbed problem, that is

$$\hat{H}_0|\Phi_0\rangle = W_0|\Phi_0\rangle.$$

The state $|\Psi_0\rangle$ is not normalized and we employ again intermediate normalization via $\langle\Phi_0|\Psi_0\rangle = 1$.

The Schrödinger equation is given by

$$\hat{H}|\Psi_0\rangle = E|\Psi_0\rangle,$$

and multiplying the latter from the left with $\langle\Phi_0|$ gives

$$\langle\Phi_0|\hat{H}|\Psi_0\rangle = E\langle\Phi_0|\Psi_0\rangle = E,$$

and subtracting from this equation

$$\langle\Psi_0|\hat{H}_0|\Phi_0\rangle = W_0\langle\Psi_0|\Phi_0\rangle = W_0,$$

and using the fact that the operators $\hat{H}$ and $\hat{H}_0$ are hermitian results in

$$\Delta E = E - W_0 = \langle\Phi_0|\hat{H}_I|\Psi_0\rangle, \tag{8.18}$$

which is an exact result. This resembles our previous definition of the correlation energy except that the reference energy is now defined by the unperturbed energy $W_0$. The reader should contrast this equation to our previous definition of the correlation energy

$$\Delta E = \sum_{ai}\langle i|\hat{f}|a\rangle C_i^a + \sum_{abij}\langle ij|\hat{v}|ab\rangle C_{ij}^{ab},$$

and the total energy

$$E = E_{\text{Ref}} + \Delta E,$$

where the reference energy is given by

$$E_{\text{Ref}} = \langle\Phi_0|\hat{H}|\Phi_0\rangle.$$

Equation (8.18) forms the starting point for all perturbative derivations. However, as it stands it represents nothing but a mere formal rewriting of Schrödinger's equation and is not of much practical use. The exact wave function $|\Psi_0\rangle$ is unknown. In order to obtain a perturbative expansion, we need to expand the exact wave function in terms of the interaction $\hat{H}_I$.

Here we have assumed that our model space defined by the operator $\hat{P}$ is one-dimensional, meaning that

$$\hat{P} = |\Phi_0\rangle\langle\Phi_0|,$$

and

$$\hat{Q} = \sum_{m=1}^{\infty} |\Phi_m\rangle\langle\Phi_m|.$$

We can thus rewrite the exact wave function as

$$|\Psi_0\rangle = (\hat{P} + \hat{Q})|\Psi_0\rangle = |\Phi_0\rangle + \hat{Q}|\Psi_0\rangle.$$

Going back to the Schrödinger equation, we can rewrite it as, adding and a subtracting a term $\omega|\Psi_0\rangle$ as

$$\left(\omega - \hat{H}_0\right)|\Psi_0\rangle = \left(\omega - E + \hat{H}_I\right)|\Psi_0\rangle,$$

where $\omega$ is an energy variable to be specified later.

We assume also that the resolvent of $\left(\omega - \hat{H}_0\right)$ exits, that is it has an inverse which defines the unperturbed Green's function as

$$\left(\omega - \hat{H}_0\right)^{-1} = \frac{1}{\left(\omega - \hat{H}_0\right)}.$$

We can rewrite Schrödinger's equation as

$$|\Psi_0\rangle = \frac{1}{\omega - \hat{H}_0}\left(\omega - E + \hat{H}_I\right)|\Psi_0\rangle,$$

and multiplying from the left with $\hat{Q}$ results in

$$\hat{Q}|\Psi_0\rangle = \frac{\hat{Q}}{\omega - \hat{H}_0}\left(\omega - E + \hat{H}_I\right)|\Psi_0\rangle,$$

which is possible since we have defined the operator $\hat{Q}$ in terms of the eigenfunctions of $\hat{H}_0$.

Since these operators commute we have

$$\hat{Q}\frac{1}{\left(\omega - \hat{H}_0\right)}\hat{Q} = \hat{Q}\frac{1}{\left(\omega - \hat{H}_0\right)} = \frac{\hat{Q}}{\left(\omega - \hat{H}_0\right)}.$$

With these definitions we can in turn define the wave function as

$$|\Psi_0\rangle = |\Phi_0\rangle + \frac{\hat{Q}}{\omega - \hat{H}_0}\left(\omega - E + \hat{H}_I\right)|\Psi_0\rangle.$$

This equation is again nothing but a formal rewrite of Schrödinger's equation and does not represent a practical calculational scheme. It is a non-linear equation in two unknown quantities, the energy $E$ and the exact wave function $|\Psi_0\rangle$. We can however start with a guess for $|\Psi_0\rangle$ on the right hand side of the last equation.

The most common choice is to start with the function which is expected to exhibit the largest overlap with the wave function we are searching after, namely $|\Phi_0\rangle$. This can again be inserted in the solution for $|\Psi_0\rangle$ in an iterative fashion and if we continue along these lines we end up with

$$|\Psi_0\rangle = \sum_{i=0}^{\infty} \left\{ \frac{\hat{Q}}{\omega - \hat{H}_0} \left(\omega - E + \hat{H}_I\right)\right\}^i |\Phi_0\rangle,$$

for the wave function and

$$\Delta E = \sum_{i=0}^{\infty} \langle \Phi_0 | \hat{H}_I \left\{ \frac{\hat{Q}}{\omega - \hat{H}_0} \left(\omega - E + \hat{H}_I\right)\right\}^i |\Phi_0\rangle,$$

which is now a perturbative expansion of the exact energy in terms of the interaction $\hat{H}_I$ and the unperturbed wave function $|\Psi_0\rangle$.

In our equations for $|\Psi_0\rangle$ and $\Delta E$ in terms of the unperturbed solutions $|\Phi_i\rangle$ we have still an undetermined parameter $\omega$ and a dependency on the exact energy $E$. Not much has been gained thus from a practical computational point of view.

In Brilluoin-Wigner perturbation theory [35] it is customary to set $\omega = E$. This results in the following perturbative expansion for the energy $\Delta E$

$$\Delta E = \sum_{i=0}^{\infty} \langle \Phi_0 | \hat{H}_I \left\{ \frac{\hat{Q}}{\omega - \hat{H}_0} \left(\omega - E + \hat{H}_I\right)\right\}^i |\Phi_0\rangle \tag{8.19}$$

$$= \langle \Phi_0 | \left( \hat{H}_I + \hat{H}_I \frac{\hat{Q}}{E - \hat{H}_0} \hat{H}_I + \hat{H}_I \frac{\hat{Q}}{E - \hat{H}_0} \hat{H}_I \frac{\hat{Q}}{E - \hat{H}_0} \hat{H}_I + \dots \right) |\Phi_0\rangle. \tag{8.20}$$

This expression depends however on the exact energy $E$ and is again not very convenient from a practical point of view. It can obviously be solved iteratively, by starting with a guess for $E$ and then solve till some kind of self-consistency criterion has been reached.

Defining $e = E - \hat{H}_0$ and recalling that $\hat{H}_0$ commutes with $\hat{Q}$ by construction and that $\hat{Q}$ is an idempotent operator $\hat{Q}^2 = \hat{Q}$, we can rewrite the denominator in the above expansion for $\Delta E$ as

$$\hat{Q} \frac{1}{\hat{e} - \hat{Q}\hat{H}_I\hat{Q}} = \hat{Q} \left[ \frac{1}{\hat{e}} + \frac{1}{\hat{e}} \hat{Q}\hat{H}_I\hat{Q} \frac{1}{\hat{e}} + \frac{1}{\hat{e}} \hat{Q}\hat{H}_I\hat{Q} \frac{1}{\hat{e}} \hat{Q}\hat{H}_I\hat{Q} \frac{1}{\hat{e}} + \dots \right] \hat{Q}.$$

Inserted in the expression for $\Delta E$ we obtain

$$\Delta E = \langle \Phi_0 | \hat{H}_I + \hat{H}_I \hat{Q} \frac{1}{E - \hat{H}_0 - \hat{Q}\hat{H}_I\hat{Q}} \hat{Q}\hat{H}_I | \Phi_0 \rangle.$$

In Rayleigh-Schrödinger (RS) perturbation theory [35] we set $\omega = W_0$ and obtain the following expression for the energy difference

$$\Delta E = \sum_{i=0}^{\infty} \langle \Phi_0 | \hat{H}_I \left\{ \frac{\hat{Q}}{W_0 - \hat{H}_0} \left( \hat{H}_I - \Delta E \right) \right\}^i | \Phi_0 \rangle \tag{8.21}$$

$$\langle \Phi_0 | \left( \hat{H}_I + \hat{H}_I \frac{\hat{Q}}{W_0 - \hat{H}_0} (\hat{H}_I - \Delta E) + \hat{H}_I \frac{\hat{Q}}{W_0 - \hat{H}_0} (\hat{H}_I - \Delta E) \frac{\hat{Q}}{W_0 - \hat{H}_0} (\hat{H}_I - \Delta E) + \dots \right) | \Phi_0 \rangle. \tag{8.22}$$

The operator $\hat{Q}$ commutes with $\hat{H}_0$ and since $\Delta E$ is a constant we obtain that

$$\hat{Q}\Delta E | \Phi_0 \rangle = \hat{Q}\Delta E | \hat{Q}\Phi_0 \rangle = 0.$$

Inserting this result in the expression for the energy gives us

$$\Delta E = \langle \Phi_0 | \left( \hat{H}_I + \hat{H}_I \frac{\hat{Q}}{W_0 - \hat{H}_0} \hat{H}_I + \hat{H}_I \frac{\hat{Q}}{W_0 - \hat{H}_0} (\hat{H}_I - \Delta E) \frac{\hat{Q}}{W_0 - \hat{H}_0} \hat{H}_I + \dots \right) | \Phi_0 \rangle.$$

We can now perturbatively expand this expression in terms of the interaction $\hat{H}_I$, which is assumed to be small. We obtain then

$$\Delta E = \sum_{i=1}^{\infty} \Delta E^{(i)},$$

with the following expression for $\Delta E^{(i)}$

$$\Delta E^{(1)} = \langle \Phi_0 | \hat{H}_I | \Phi_0 \rangle,$$

which is just the contribution to first order in perturbation theory,

$$\Delta E^{(2)} = \langle \Phi_0 | \hat{H}_I \frac{\hat{Q}}{W_0 - \hat{H}_0} \hat{H}_I | \Phi_0 \rangle,$$

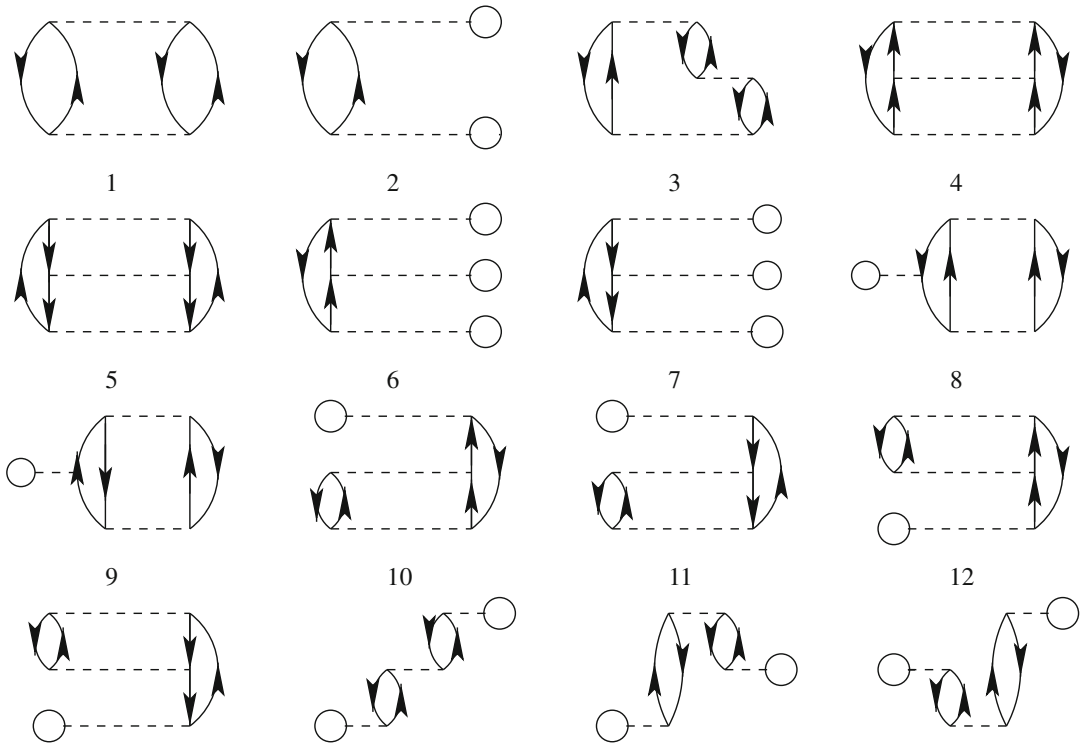


**Fig. 8.2** Linked anti-symmetrized Goldstone diagrams which enter the definition of the ground-state correlation energy $\Delta E_0$ to third order in the interaction. We have not included the first-order contribution

which is the contribution to second order and

$$\Delta E^{(3)} = \langle \Phi_0 | \hat{H}_I \frac{\hat{Q}}{W_0 - \hat{H}_0} \hat{H}_I \frac{\hat{Q}}{W_0 - \hat{H}_0} \hat{H}_I \Phi_0 \rangle - \langle \Phi_0 | \hat{H}_I \frac{\hat{Q}}{W_0 - \hat{H}_0} \langle \Phi_0 | \hat{H}_I | \Phi_0 \rangle \frac{\hat{Q}}{W_0 - \hat{H}_0} \hat{H}_I | \Phi_0 \rangle,$$

being the third-order contribution. There exists a formal theory for the calculation of $\Delta E_0$, see for example [35]. According to the well-known Goldstone linked-diagram theory, the energy shift $\Delta E_0$ is given exactly by the diagrammatic expansion shown in Fig. 8.2, where ground state diagrams to third order are listed. This theory is a linked-cluster perturbation expansion for the ground state energy of a many-body system, and applies equally well to both nuclear matter and closed-shell nuclei such as the doubly magic nucleus $^{40}$Ca. We assume the reader is familiar with the standard rules for deriving and setting up the analytical expressions for various Feymann-Goldstone diagrams [35]. In an infinite system like nuclear matter or the homogenous electron gas, all diagrams with so-called Hartree-Fock insertions like diagrams (2), (6), (7), (10–16) are zero due to lack of momentum conservation. They would also be zero in case a canonical [35] Hartree-Fock basis is employed.

Using the above standard diagram rules, the various diagrams contained in Fig. 8.2 can be readily calculated (in an uncoupled scheme). Diagram (1) results in

$$(1) = \frac{1}{2^2}\sum_{ij\leq F}\sum_{ab>F}\frac{\langle ij|\hat{v}|ab\rangle\langle ab|\hat{v}|ij\rangle}{\varepsilon_i+\varepsilon_j-\varepsilon_a-\varepsilon_b}, \tag{8.23}$$

while diagram (2) is zero due to lack of momentum conservation. We have two factors of $1/2$ since there are two equivalent pairs of fermions (two particle states and two hole states) starting at the same vertex and ending at the same vertex. The expression for diagram (3) is

$$(3) = \sum_{ijk\leq k_F}\sum_{abc>F}\frac{\langle ij|\hat{v}|ab\rangle\langle bk|\hat{v}|ic\rangle\langle ac|\hat{v}|ik\rangle}{(\varepsilon_i+\varepsilon_j-\varepsilon_a-\varepsilon_b)(\varepsilon_i+\varepsilon_k-\varepsilon_a-\varepsilon_c)}. \tag{8.24}$$

Diagrams (4) and (5) read

$$(4) = \frac{1}{2^3}\sum_{ij\leq F}\sum_{abcd>F}\frac{\langle ij|\hat{v}|cd\rangle\langle cd|\hat{v}|ab\rangle\langle ab|\hat{v}|ij\rangle}{(\varepsilon_i+\varepsilon_j-\varepsilon_c-\varepsilon_d)(\varepsilon_i+\varepsilon_j-\varepsilon_a-\varepsilon_b)}, \tag{8.25}$$

$$(5) = \frac{1}{2^3}\sum_{ijkl\leq F}\sum_{ab>F}\frac{\langle ab|\hat{v}|kl\rangle\langle kl|\hat{v}|ij\rangle\langle ij|\hat{v}|ab\rangle}{(\varepsilon_i+\varepsilon_j-\varepsilon_a-\varepsilon_b)(\varepsilon_k+\varepsilon_l-\varepsilon_a-\varepsilon_b)}, \tag{8.26}$$

where the factor $(1/2)^3$ arises due to three equivalent pairs of lines starting and ending at the same vertex. The last two contributions have an even number of hole lines and closed loops, resulting thus in a positive sign. In Problem 8.9, you are asked to calculate the expressions for diagrams like (8) and (9) in the above figure.

In the expressions for the various diagrams the quantity $\varepsilon$ denotes the single-particle energies defined by $H_0$. The steps leading to the above expressions for the various diagrams are rather straightforward. Though, if we wish to compute the matrix elements for the interaction $\hat{v}$, a serious problem arises. Typically, the matrix elements will contain a term $V(|\mathbf{r}|)$ which represents the interaction potential $V$ between two nucleons, where $\mathbf{r}$ is the internucleon distance. All modern models for $V$ have a strong short-range repulsive core. Hence, matrix elements involving $V(|\mathbf{r}|)$, will result in large (or infinitely large for a potential with a hard core) and repulsive contributions to the ground-state energy. A perturbative expansion in terms of such interaction matrix elements may thus lead to a slowly converging expansion. A standard recipe to circumvent such problems has been to sum up a selected class of correlations. We discuss such possibilities in Sect. 8.6.

### 8.5.1 Interpreting the Correlation Energy and the Wave Operator

In Sect. 8.4 we showed that we could rewrite the exact state function for the ground state as a linear expansion in terms of all possible Slater determinants. We expanded our exact state function for the ground state as

$$|\Psi_0\rangle = C_0|\Phi_0\rangle + \sum_{ai} C_i^a|\Phi_i^a\rangle + \sum_{abij} C_{ij}^{ab}|\Phi_{ij}^{ab}\rangle + \cdots = (C_0 + \hat{C})|\Phi_0\rangle,$$

where we introduced the so-called correlation operator

$$\hat{C} = \sum_{ai} C_i^a \hat{a}_a^\dagger \hat{a}_i + \sum_{abij} C_{ij}^{ab} \hat{a}_a^\dagger \hat{a}_b^\dagger \hat{a}_j \hat{a}_i + \ldots$$

In a shell-model calculation, the unknown coefficients in $\hat{C}$ are the eigenvectors that result from the diagonalization of the Hamiltonian matrix.

How can we use perturbation theory to determine the same coefficients? Let us study the contributions to second order in the interaction, namely

$$\Delta E^{(2)} = \langle \Phi_0|\hat{H}_I \frac{\hat{Q}}{W_0 - \hat{H}_0} \hat{H}_I|\Phi_0\rangle.$$

This contribution will also be discussed in connection with the development of a many-body program for nuclear matter, as well as the simple pairing model of Problem 8.10. The intermediate states given by $\hat{Q}$ can at most be of a $2p-2h$ nature if we have a two-body Hamiltonian. This means that to second order in perturbation theory we can at most have $1p-1h$ and $2p-2h$ excitations as intermediate states. When we diagonalize, these contributions are included to infinite order. This means that in order to include such correlations to higher order in the interaction, we need to go to higher-orders in perturbation theory.

If we limit the attention to a Hartree-Fock basis, we have that $\langle \Phi_0|\hat{H}_I|2p-2h\rangle$ is the only contribution since matrix elements involving $\langle \Phi_0|\hat{H}_I|1p-1h\rangle$ are zero and the contribution to the energy from second order in Rayleigh-Schrödinger perturbation theory reduces to

$$\Delta E^{(2)} = \frac{1}{4} \sum_{abij} \langle ij|\hat{v}|ab\rangle \frac{\langle ab|\hat{v}|ij\rangle}{\epsilon_i + \epsilon_j - \epsilon_a - \epsilon_b}.$$

Here we have used the results from Problem 8.8. If we compare this to the correlation energy obtained from full configuration interaction theory with a Hartree-Fock basis, we found that

$$E - E_{\text{Ref}} = \Delta E = \sum_{abij} \langle ij|\hat{v}|ab\rangle C_{ij}^{ab},$$

where the energy $E_{\mathrm{Ref}}$ is the reference energy and $\Delta E$ defines the so-called correlation energy.

We see that if we set

$$C_{ij}^{ab} = \frac{1}{4}\frac{\langle ab|\hat{v}|ij\rangle}{\epsilon_i + \epsilon_j - \epsilon_a - \epsilon_b},$$

we have a perfect agreement between configuration interaction theory and many-body perturbation theory. However, configuration interaction theory includes $2p-2h$ (and more complicated ones as well) correlations to infinite order. In order to make a meaningful comparison we would at least need to sum such correlations to infinite order in perturbation theory. The last equation serves however as a very useful comparison between configuration interaction theory and many-body perturbation theory. Furthermore, for our nuclear matter studies, one-particle-one-hole intermediate excitations are zero due to the requirement of momentum conservation in infinite systems. These two-particle-two-hole correlations can also be summed to infinite order and a particular class of such excitations are given by two-particle excitations only. These represent in case of nuclear interactions, which are strongly repulsive at short interparticle distances, a physically intuitive way to understand the renormalization of nuclear forces. Such correlations are easily computed by simple matrix inversion techniques and have been widely employed in nuclear many-body theory. Summing up two-particle excitations to infinite order leads to an effective two-body interaction which renormalizes the short-range part of the nuclear interactions.

In summary, many-body perturbation theory introduces order-by-order specific correlations and we can make comparisons with exact calculations like those provided by configuration interaction theory. The advantage of for example Rayleigh-Schrödinger perturbation theory is that at every order in the interaction, we know how to calculate all contributions. The two-body matrix elements can for example be tabulated or computed on the fly. However, many-body perturbation theory suffers from not being variational and there is no guarantee that higher-order terms will improve the order-by-order convergence. It is also extremely tedious to compute terms beyond third order, in particular if one is interested in effective valence space interactions. There are however classes of correlations which can be summed up to infinite order in the interaction. The hope is that such correlations can mitigate specific convergence issues, although there is no a priori guarantee thereof. Examples are the so-called TDA and RPA classes of diagrams [52–54], as well as the resummation of two-particle-two-hole correlations discussed in Chap. 11. If we limit ourselves to the resummation of two-particle correlations only, these lead us to the so-called $G$-matrix resummation of diagrams, see for example [28]. There are however computationally inexpensive methods which sum larger classes of correlations to infinite order in the interaction. This leads us to Sect. 8.6 and the final many-body method of this chapter, coupled cluster theory.

## 8.6 Coupled Cluster Theory

Coester and Kümmel [69–71] developed the ideas that led to coupled cluster theory in the late 1950s. The correlated wave function of a many-body system $|\ \Psi\rangle$ can be formulated as an exponential of correlation operators $T$ acting on a reference state $|\ \Phi\rangle$,

$$|\ \Psi\rangle = \exp\left(\hat{T}\right)|\ \Phi\rangle.$$

We will discuss how to define the operators later in this work. This simple ansatz carries enormous power. It leads to a non-perturbative many-body theory that includes summation of ladder diagrams [30], ring diagrams [72], and an infinite-order generalization of many-body perturbation theory [73]. Developments and applications of coupled cluster theory took different routes in chemistry and nuclear physics. In quantum chemistry, coupled cluster developments and applications have proven to be extremely useful, see for example the review by Barrett and Musial as well as the recent textbook by Shavitt and Bartlett [35]. Many previous applications to nuclear physics struggled with the repulsive character of the nuclear forces and limited basis sets used in the computations [71]. Most of these problems have been overcome during the last decade and coupled cluster theory is one of the computational methods of preference for doing nuclear physics, with applications ranging from light nuclei to medium-heavy nuclei, see for example the recent reviews [17, 19, 23, 38].

### *8.6.1 A Quick Tour of Coupled Cluster Theory*

The ansatz for the ground state is given by

$$|\Psi_0\rangle = |\Psi_{CC}\rangle = e^{\hat{T}}|\Phi_0\rangle = \left(\sum_{n=1}^{A}\frac{1}{n!}\hat{T}^n\right)|\Phi_0\rangle,$$

where $A$ represents the maximum number of particle-hole excitations and $\hat{T}$ is the cluster operator defined as

$$\hat{T} = \hat{T}_1 + \hat{T}_2 + \ldots + \hat{T}_A$$

$$\hat{T}_n = \left(\frac{1}{n!}\right)^2 \sum_{\substack{i_1,i_2,\ldots i_n \\ a_1,a_2,\ldots a_n}} t_{i_1 i_2 \ldots i_n}^{a_1 a_2 \ldots a_n} a_{a_1}^\dagger a_{a_2}^\dagger \ldots a_{a_n}^\dagger a_{i_n} \ldots a_{i_2} a_{i_1}.$$

The energy is given by

$$E_{\mathrm{CC}} = \langle \Phi_0 | \overline{H} | \Phi_0 \rangle,$$

where $\overline{H}$ is a similarity transformed Hamiltonian

$$\overline{H} = e^{-\hat{T}} \hat{H}_N e^{\hat{T}}$$
$$\hat{H}_N = \hat{H} - \langle \Phi_0 | \hat{H} | \Phi_0 \rangle.$$

The coupled cluster energy is a function of the unknown cluster amplitudes $t_{i_1 i_2 \ldots i_n}^{a_1 a_2 \ldots a_n}$, given by the solutions to the amplitude equations

$$0 = \langle \Phi_{i_1 \ldots i_n}^{a_1 \ldots a_n} | \overline{H} | \Phi_0 \rangle. \tag{8.27}$$

In order to set up the above equations, the similarity transformed Hamiltonian $\overline{H}$ is expanded using the Baker-Campbell-Hausdorff expression,

$$\overline{H} = \hat{H}_N + \left[\hat{H}_N, \hat{T}\right] + \frac{1}{2}\left[\left[\hat{H}_N, \hat{T}\right], \hat{T}\right] + \ldots + \frac{1}{n!}\left[\ldots\left[\hat{H}_N, \hat{T}\right], \ldots \hat{T}\right] + \ldots \tag{8.28}$$

and simplified using the connected cluster theorem [35]

$$\overline{H} = \hat{H}_N + \left(\hat{H}_N \hat{T}\right)_c + \frac{1}{2}\left(\hat{H}_N \hat{T}^2\right)_c + \cdots + \frac{1}{n!}\left(\hat{H}_N \hat{T}^n\right)_c + \ldots$$

We will discuss parts of the derivation below. For the full derivation of these expressions, see for example [35].

A much used approximation is to truncate the cluster operator $\hat{T}$ at the $n = 2$ level. This defines the so-called singles and doubles approximation to the coupled cluster state function, normally shortened to CCSD. The coupled cluster wavefunction is now given by

$$|\Psi_{CC}\rangle = e^{\hat{T}_1 + \hat{T}_2} |\Phi_0\rangle$$

where

$$\hat{T}_1 = \sum_{ia} t_i^a a_a^\dagger a_i$$
$$\hat{T}_2 = \frac{1}{4} \sum_{ijab} t_{ij}^{ab} a_a^\dagger a_b^\dagger a_j a_i.$$

The amplitudes $t$ play a role similar to the coefficients $C$ in the shell-model calculations. They are obtained by solving a set of non-linear equations similar

to those discussed above in connection with the configuration interaction theory discussion, see Eqs. (8.15) and (8.16).

In our configuration interaction theory discussion the correlation energy is defined as (with a two-body Hamiltonian)

$$\Delta E = \sum_{ai} \langle i|\hat{f}|a\rangle C_i^a + \sum_{abij} \langle ij|\hat{v}|ab\rangle C_{ij}^{ab}.$$

We can obtain a similar expression for the correlation energy using coupled cluster theory. Using Eq. (8.28) we can write the expression for the coupled cluster ground state energy as an infinite sum over nested commutators

$$\begin{aligned} E_{CC} = \langle \Phi_0| \Big( \hat{H}_N + \left[\hat{H}_N, \hat{T}\right] + \frac{1}{2}\left[\left[\hat{H}_N, \hat{T}\right], \hat{T}\right] \\ + \frac{1}{3!}\left[\left[\left[\hat{H}_N, \hat{T}\right], \hat{T}\right], \hat{T}\right] \\ + \frac{1}{4!}\left[\left[\left[\left[\hat{H}_N, \hat{T}\right], \hat{T}\right], \hat{T}\right], \hat{T}\right] + \dots \Big) |\Phi_0\rangle \,. \end{aligned}$$

One can show that this infinite series truncates naturally at a given order of nested commutators [35]. Let us demonstrate briefly how we can construct the expressions for the correlation energy by approximating $\hat{T}$ at the CCSD level, that is $\hat{T} \approx \hat{T}_1 + \hat{T}_2$. The first term is zero by construction

$$\langle \Phi_0| \hat{H}_N |\Phi_0\rangle = 0.$$

The second term can be split into the following contributions

$$\langle \Phi_0| \left[\hat{H}_N, \hat{T}\right] |\Phi_0\rangle = \langle \Phi_0| \left( \left[\hat{F}_N, \hat{T}_1\right] + \left[\hat{F}_N, \hat{T}_2\right] + \left[\hat{V}_N, \hat{T}_1\right] + \left[\hat{V}_N, \hat{T}_2\right] \right) |\Phi_0\rangle \,.$$

Let us start with $\left[\hat{F}_N, \hat{T}_1\right]$, where the one-body operator $\hat{F}_N$ is defined in Eq. (8.2). In the equations below we employ the shorthand $f_q^p = \langle p|\hat{f}|q\rangle$. We write out the commutator as

$$\begin{aligned} \left[\hat{F}_N, \hat{T}_1\right] &= \sum_{pqia} \left( f_q^p \left\{a_p^\dagger a_q\right\} t_i^a \left\{a_a^\dagger a_i\right\} - t_i^a \left\{a_a^\dagger a_i\right\} f_q^p \left\{a_p^\dagger a_q\right\} \right) \\ &= \sum_{pqia} f_q^p t_i^a \left( \left\{a_p^\dagger a_q\right\} \left\{a_a^\dagger a_i\right\} - \left\{a_a^\dagger a_i\right\} \left\{a_p^\dagger a_q\right\} \right). \end{aligned}$$

We have kept here the curly brackets that indicate that the chains of operators are normal ordered with respect to the new reference state. If we consider the second set of operators and rewrite them with curly brackets (bringing back the normal ordering) we have

$$\begin{aligned}
\left\{a_a^\dagger a_i\right\}\left\{a_p^\dagger a_q\right\} &= \left\{a_a^\dagger a_i a_p^\dagger a_q\right\} = \left\{a_p^\dagger a_q a_a^\dagger a_i\right\} \\
\left\{a_p^\dagger a_q\right\}\left\{a_a^\dagger a_i\right\} &= \left\{a_p^\dagger a_q a_a^\dagger a_i\right\} \\
&\quad + \left\{\overbrace{a_p^\dagger a_q a_a^\dagger} a_i\right\} + \left\{a_p^\dagger \overbrace{a_q a_a^\dagger} a_i\right\} \\
&\quad + \left\{\overbrace{a_p^\dagger a_q a_a^\dagger} a_i\right\} \\
&= \left\{a_p^\dagger a_q a_a^\dagger a_i\right\} + \delta_{qa}\left\{a_p^\dagger a_i\right\} + \delta_{pi}\left\{a_q a_a^\dagger\right\} + \delta_{qa}\delta_{pi}.
\end{aligned}$$

We can then rewrite the two sets of operators as

$$\left\{a_p^\dagger a_q\right\}\left\{a_a^\dagger a_i\right\} - \left\{a_a^\dagger a_i\right\}\left\{a_p^\dagger a_q\right\} = \delta_{qa}\left\{a_p^\dagger a_i\right\} + \delta_{pi}\left\{a_q a_a^\dagger\right\} + \delta_{qa}\delta_{pi}.$$

Inserted into the original expression, we arrive at the explicit value of the commutator

$$\left[\hat{F}_N, \hat{T}_1\right] = \sum_{pai} f_a^p t_i^a \left\{a_p^\dagger a_i\right\} + \sum_{qai} f_q^i t_i^a \left\{a_q a_a^\dagger\right\} + \sum_{ai} f_a^i t_i^a.$$

We are now ready to compute the expectation value with respect to our reference state. Since the two first terms require the ground state linking to a one-particle-one-hole state, the first two terms are zero and we are left with

$$\langle \Phi_0 | \left[\hat{F}_N, \hat{T}_1\right] | \Phi_0 \rangle = \sum_{ai} f_a^i t_i^a. \tag{8.29}$$

The two first terms will however contribute to the calculation of the Hamiltonian matrix element which connects the ground state and a one-particle-one-hole excitation.

Let us next look at the term $\left[\hat{F}_N, \hat{T}_2\right]$. We have

$$\begin{aligned}
\left[\hat{F}_N, \hat{T}_2\right] &= \left[\sum_{pq} f_q^p \left\{a_p^\dagger a_q\right\}, \frac{1}{4}\sum_{ijab} t_{ij}^{ab}\left\{a_a^\dagger a_b^\dagger a_j a_i\right\}\right] \\
&= \frac{1}{4}\sum_{\substack{pq \\ ijab}} f_q^p t_{ij}^{ab}\left(\left\{a_p^\dagger a_q\right\}\left\{a_a^\dagger a_b^\dagger a_j a_i\right\} - \left\{a_a^\dagger a_b^\dagger a_j a_i\right\}\left\{a_p^\dagger a_q\right\}\right).
\end{aligned}$$

The last set of operators can be rewritten as

$$\left\{a_a^\dagger a_b^\dagger a_j a_i\right\}\left\{a_p^\dagger a_q\right\} = \left\{a_a^\dagger a_b^\dagger a_j a_i a_p^\dagger a_q\right\}$$

$$
\begin{aligned}
&= \left\{a_p^\dagger a_q a_a^\dagger a_b^\dagger a_j a_i\right\} \\
\{a_p^\dagger a_q\}\left\{a_a^\dagger a_b^\dagger a_j a_i\right\} &= \left\{a_p^\dagger a_q a_a^\dagger a_b^\dagger a_j a_i\right\} + \left\{\overbrace{a_p^\dagger a_q a_a^\dagger a_b^\dagger} a_j a_i\right\} + \left\{\overbrace{a_p^\dagger a_q a_a^\dagger a_b^\dagger a_j} a_i\right\} \\
&\quad + \left\{a_p^\dagger \overbrace{a_q a_a^\dagger} a_b^\dagger a_j a_i\right\} + \left\{a_p^\dagger \overbrace{a_q a_a^\dagger a_b^\dagger} a_j a_i\right\} + \left\{\overbrace{a_p^\dagger a_q a_a^\dagger} \overbrace{a_b^\dagger a_j} a_i\right\} \\
&\quad + \left\{\overbrace{a_p^\dagger a_q} \overbrace{a_a^\dagger a_b^\dagger} a_j a_i\right\} + \left\{\overbrace{a_p^\dagger a_q a_a^\dagger a_b^\dagger} a_j a_i\right\} + \left\{\overbrace{a_p^\dagger a_q a_a^\dagger a_b^\dagger a_j} a_i\right\} \\
&= \left\{a_p^\dagger a_q a_a^\dagger a_b^\dagger a_j a_i\right\} - \delta_{pj}\left\{a_q a_a^\dagger a_b^\dagger a_i\right\} + \delta_{pi}\left\{a_q a_a^\dagger a_b^\dagger a_j\right\} \\
&\quad + \delta_{qa}\left\{a_p^\dagger a_b^\dagger a_j a_i\right\} - \delta_{qb}\left\{a_p^\dagger a_a^\dagger a_j a_i\right\} - \delta_{pj}\delta_{qa}\left\{a_b^\dagger a_i\right\} \\
&\quad + \delta_{pi}\delta_{qa}\left\{a_b^\dagger a_j\right\} + \delta_{pj}\delta_{qb}\left\{a_a^\dagger a_i\right\} - \delta_{pi}\delta_{qb}\left\{a_a^\dagger a_j\right\}.
\end{aligned}
$$

We can then rewrite the two sets of operators as

$$
\begin{aligned}
&\Big(\left\{a_p^\dagger a_q\right\}\left\{a_a^\dagger a_b^\dagger a_j a_i\right\} - \left\{a_a^\dagger a_b^\dagger a_j a_i\right\}\left\{a_p^\dagger a_q\right\}\Big) \\
&= -\delta_{pj}\left\{a_q a_a^\dagger a_b^\dagger a_i\right\} + \delta_{pi}\left\{a_q a_a^\dagger a_b^\dagger a_j\right\} + \delta_{qa}\left\{a_p^\dagger a_b^\dagger a_j a_i\right\} \\
&\quad - \delta_{qb}\left\{a_p^\dagger a_a^\dagger a_j a_i\right\} - \delta_{pj}\delta_{qa}\left\{a_b^\dagger a_i\right\} + \delta_{pi}\delta_{qa}\left\{a_b^\dagger a_j\right\} + \delta_{pj}\delta_{qb}\left\{a_a^\dagger a_i\right\} \\
&\quad - \delta_{pi}\delta_{qb}\left\{a_a^\dagger a_j\right\},
\end{aligned}
$$

which, when inserted into the original expression gives us

$$
\begin{aligned}
\left[\hat{F}_N, \hat{T}_2\right] = \frac{1}{4}\sum_{\substack{pq\\abij}} f_q^p t_{ij}^{ab}\Big( &- \delta_{pj}\left\{a_q a_a^\dagger a_b^\dagger a_i\right\} + \delta_{pi}\left\{a_q a_a^\dagger a_b^\dagger a_j\right\} \\
&+ \delta_{qa}\left\{a_p^\dagger a_b^\dagger a_j a_i\right\} - \delta_{qb}\left\{a_p^\dagger a_a^\dagger a_j a_i\right\} - \delta_{pj}\delta_{qa}\left\{a_b^\dagger a_i\right\} \\
&+ \delta_{pi}\delta_{qa}\left\{a_b^\dagger a_j\right\} + \delta_{pj}\delta_{qb}\left\{a_a^\dagger a_i\right\} - \delta_{pi}\delta_{qb}\left\{a_a^\dagger a_j\right\}\Big).
\end{aligned}
$$

After renaming indices and changing the order of operators, we arrive at the explicit expression

$$\left[\hat{F}_N, \hat{T}_2\right] = \frac{1}{2}\sum_{qijab} f_q^i t_{ij}^{ab} \left\{a_q a_a^\dagger a_b^\dagger a_j\right\} + \frac{1}{2}\sum_{pijab} f_a^p t_{ij}^{ab} \left\{a_p^\dagger a_b^\dagger a_j a_i\right\} + \sum_{ijab} f_a^i t_{ij}^{ab} \left\{a_b^\dagger a_j\right\}.$$

In this case we have two sets of two-particle-two-hole operators and one-particle-one-hole operators and all these terms result in zero expectation values. However, these terms are important for the amplitude equations. In a similar way we can compute the terms involving the interaction $\hat{V}_N$. We obtain then

$$\begin{aligned}
\langle\Phi_0|\left[\hat{V}_N, \hat{T}_1\right]|\Phi_0\rangle &= \langle\Phi_0|\left[\frac{1}{4}\sum_{pqrs}\langle pq|\,\hat{v}\,|rs\rangle\left\{a_p^\dagger a_q^\dagger a_s a_r\right\}, \sum_{ia} t_i^a\left\{a_a^\dagger a_i\right\}\right]|\Phi_0\rangle \\
&= \frac{1}{4}\sum_{\substack{pqr\\sia}}\langle pq|\,|rs\rangle\, t_i^a\,\langle\Phi_0|\left[\left\{a_p^\dagger a_q^\dagger a_s a_r\right\}, \left\{a_a^\dagger a_i\right\}\right]|\Phi_0\rangle \\
&= 0,
\end{aligned}$$

and

$$\begin{aligned}
&\langle\Phi_0|\left[\hat{V}_N, \hat{T}_2\right]|\Phi_0\rangle \\
&= \langle\Phi_0|\left[\frac{1}{4}\sum_{pqrs}\langle pq|\,\hat{v}\,|rs\rangle\left\{a_p^\dagger a_q^\dagger a_s a_r\right\}, \frac{1}{4}\sum_{ijab} t_{ij}^{ab}\left\{a_a^\dagger a_b^\dagger a_j a_i\right\}\right]|\Phi_0\rangle \\
&= \frac{1}{16}\sum_{\substack{pqr\\sijab}}\langle pq|\,\hat{v}\,|rs\rangle\, t_{ij}^{ab}\,\langle\Phi_0|\left[\left\{a_p^\dagger a_q^\dagger a_s a_r\right\}, \left\{a_a^\dagger a_b^\dagger a_j a_i\right\}\right]|\Phi_0\rangle \\
&= \frac{1}{16}\sum_{\substack{pqr\\sijab}}\langle pq|\,\hat{v}\,|rs\rangle\, t_{ij}^{ab}\,\langle\Phi_0|\Big(\left\{\overbrace{a_p^\dagger a_q^\dagger a_s a_r a_a^\dagger a_b^\dagger a_j a_i}\right\} + \left\{\overbrace{a_p^\dagger a_q^\dagger a_s a_r a_a^\dagger a_b^\dagger a_j a_i}\right\} \\
&\quad \left\{\overbrace{a_p^\dagger a_q^\dagger a_s a_r a_a^\dagger a_b^\dagger a_j a_i}\right\} + \left\{\overbrace{a_p^\dagger a_q^\dagger a_s a_r a_a^\dagger a_b^\dagger a_j a_i}\right\}\Big)|\Phi_0\rangle \\
&= \frac{1}{4}\sum_{ijab}\langle ij|\,\hat{v}\,|ab\rangle\, t_{ij}^{ab}.
\end{aligned}$$

The final contribution to the correlation energy comes from the non-linear terms with the amplitudes squared. The contribution from $\hat{T}^2$ is given by

$$
\begin{aligned}
&\langle \Phi_0| \frac{1}{2}\left(\hat{V}_N \hat{T}_1^2\right) |\Phi_0\rangle \\
&= \frac{1}{8}\sum_{pqrs}\sum_{ijab} \langle pq|\,\hat{v}\,|rs\rangle\, t_i^a t_j^b\, \langle \Phi_0| \left(\left\{a_p^\dagger a_q^\dagger a_s a_r\right\}\left\{a_a^\dagger a_i\right\}\left\{a_b^\dagger a_j\right\}\right)_c |\Phi_0\rangle \\
&= \frac{1}{8}\sum_{pqrs}\sum_{ijab} \langle pq|\,\hat{v}\,|rs\rangle\, t_i^a t_j^b\, \langle \Phi_0| \\
&\Big(\Big\{\overbrace{a_p^\dagger a_q^\dagger a_s a_r a_a^\dagger a_i a_b^\dagger a_j}\Big\} + \Big\{\overbrace{a_p^\dagger a_q^\dagger a_s a_r a_a^\dagger a_i a_b^\dagger a_j}\Big\} + \Big\{\overbrace{a_p^\dagger a_q^\dagger a_s a_r a_a^\dagger a_i a_b^\dagger a_j}\Big\} \\
&+ \Big\{\overbrace{a_p^\dagger a_q^\dagger a_s a_r a_a^\dagger a_i a_b^\dagger a_j}\Big\}\Big) |\Phi_0\rangle \\
&= \frac{1}{2}\sum_{ijab} \langle ij|\,\hat{v}\,|ab\rangle\, t_i^a t_j^b .
\end{aligned}
$$

Collecting all terms we have the final expression for the correlation energy with a two-body interaction given by

$$
\Delta E = \sum_{ai}\langle i|\hat{f}|a\rangle t_i^a + \frac{1}{2}\sum_{ijab}\langle ij|\,\hat{v}\,|ab\rangle\, t_i^a t_j^b + \frac{1}{4}\sum_{ijab}\langle ij|\hat{v}|ab\rangle t_{ij}^{ab}. \tag{8.30}
$$

We leave it as a challenge to the reader to derive the corresponding equations for the Hamiltonian matrix elements of Eq. (8.27).

There are several interesting features with the coupled cluster equations. With a truncation like CCSD or even with the inclusion of triples (CCSDT), we can include to infinite order correlations based on one-particle-one-hole and two-particle-two-hole contributions. We can include a large basis of single-particle states, normally not possible in standard FCI calculations. Typical FCI calculations for light nuclei $A \leq 16$ can be performed in at most some few harmonic oscillator shells. For heavier nuclei, at most two major shells can be included due to too large dimensionalities. However, coupled cluster theory is non-variational and if we want to find properties of excited states, additional calculations via for example equation of motion methods are needed [17, 35]. If correlations are strong, a single-reference ansatz may not be the best starting point and a multi-reference approximation is needed [74]. Furthermore, we cannot quantify properly the error we make when truncations are made in the cluster operator.

### 8.6.2 The CCD Approximation

We will now approximate the cluster operator $\hat{T}$ to include only $2p-2h$ correlations. This leads to the so-called CCD approximation, that is

$$\hat{T} \approx \hat{T}_2 = \frac{1}{4}\sum_{abij} t_{ij}^{ab} a_a^\dagger a_b^\dagger a_j a_i,$$

meaning that we have

$$|\Psi_0\rangle \approx |\Psi_{CCD}\rangle = \exp\left(\hat{T}_2\right)|\Phi_0\rangle.$$

Inserting these equations in the expression for the computation of the energy we have, with a Hamiltonian defined with respect to a general reference vacuum

$$\hat{H} = \hat{H}_N + E_{\text{ref}},$$

with

$$\hat{H}_N = \sum_{pq}\langle p|\hat{f}|q\rangle a_p^\dagger a_q + \frac{1}{4}\sum_{pqrs}\langle pq|\hat{v}|rs\rangle a_p^\dagger a_q^\dagger a_s a_r,$$

we obtain that the energy can be written as

$$\langle\Phi_0|\exp\left(-\hat{T}_2\right)\hat{H}_N\exp\left(\hat{T}_2\right)|\Phi_0\rangle = \langle\Phi_0|\hat{H}_N(1+\hat{T}_2)|\Phi_0\rangle = E_{CCD}.$$

This quantity becomes

$$E_{CCD} = E_{\text{ref}} + \frac{1}{4}\sum_{abij}\langle ij|\hat{v}|ab\rangle t_{ij}^{ab},$$

where the latter is the correlation energy from this level of approximation of coupled cluster theory. Similarly, the expression for the amplitudes reads (see Problem 8.13)

$$\langle\Phi_{ij}^{ab}|\exp\left(-\hat{T}_2\right)\hat{H}_N\exp\left(\hat{T}_2\right)|\Phi_0\rangle = 0.$$

These equations can be reduced to (after several applications of Wick's theorem), for all $i > j$ and all $a > b$,

$$0 = \langle ab|\hat{v}|ij\rangle + \left(\epsilon_a + \epsilon_b - \epsilon_i - \epsilon_j\right) t_{ij}^{ab} + \frac{1}{2}\sum_{cd}\langle ab|\hat{v}|cd\rangle t_{ij}^{cd} + \frac{1}{2}\sum_{kl}\langle kl|\hat{v}|ij\rangle t_{kl}^{ab}$$
$$+ \hat{P}(ij|ab)\sum_{kc}\langle kb|\hat{v}|cj\rangle t_{ik}^{ac} + \frac{1}{4}\sum_{klcd}\langle kl|\hat{v}|cd\rangle t_{ij}^{cd} t_{kl}^{ab} + \hat{P}(ij)\sum_{klcd}\langle kl|\hat{v}|cd\rangle t_{ik}^{ac} t_{jl}^{bd}$$
$$- \frac{1}{2}\hat{P}(ij)\sum_{klcd}\langle kl|\hat{v}|cd\rangle t_{ik}^{dc} t_{lj}^{ab} - \frac{1}{2}\hat{P}(ab)\sum_{klcd}\langle kl|\hat{v}|cd\rangle t_{lk}^{ac} t_{ij}^{db}, \tag{8.31}$$

where we have defined

$$\hat{P}\,(ab) = 1 - \hat{P}_{ab},$$

where $\hat{P}_{ab}$ interchanges two particles occupying the quantum numbers $a$ and $b$. The operator $\hat{P}(ij|ab)$ is defined as

$$\hat{P}(ij|ab) = (1 - \hat{P}_{ij})(1 - \hat{P}_{ab}).$$

The single-particle energies $\epsilon_p$ are normally taken to be Hartree-Fock single-particle energies. Recall also that the unknown amplitudes $t_{ij}^{ab}$ represent anti-symmetrized matrix elements, meaning that they obey the same symmetry relations as the two-body interaction, that is

$$t_{ij}^{ab} = -t_{ji}^{ab} = -t_{ij}^{ba} = t_{ji}^{ba}.$$

The two-body matrix elements are also anti-symmetrized, meaning that

$$\langle ab|\hat{v}|ij\rangle = -\langle ab|\hat{v}|ji\rangle = -\langle ba|\hat{v}|ij\rangle = \langle ba|\hat{v}|ji\rangle.$$

The non-linear equations for the unknown amplitudes $t_{ij}^{ab}$ are solved iteratively. We discuss the implementation of these equations below.

### 8.6.3 Approximations to the Full CCD Equations

It is useful to make approximations to the equations for the amplitudes. These serve as important benchmarks when we are to develop a many-body code. The standard method for solving these equations is to set up an iterative scheme where method's like Newton's method or similar root searching methods are used to find the amplitudes, see for example [75].

Iterative solvers need a guess for the amplitudes. A good starting point is to use the correlated wave operator from perturbation theory to first order in the interaction. This means that we define the zeroth approximation to the amplitudes as

$$(t_{ij}^{ab})^{(0)} = \frac{\langle ab|\hat{v}|ij\rangle}{\left(\epsilon_i + \epsilon_j - \epsilon_a - \epsilon_b\right)},$$

leading to our first approximation for the correlation energy at the CCD level to be equal to second-order perturbation theory without $1p-1h$ excitations, namely

$$\Delta E_{\mathrm{CCD}}^{(0)} = \frac{1}{4}\sum_{abij}\langle ij|\hat{v}|ab\rangle (t_{ij}^{ab})^{(0)} = \frac{1}{4}\sum_{abij}\frac{\langle ij|\hat{v}|ab\rangle\langle ab|\hat{v}|ij\rangle}{\left(\epsilon_i + \epsilon_j - \epsilon_a - \epsilon_b\right)}.$$

With this starting point, we are now ready to solve Eq. (8.31) iteratively. Before we attack the full equations, it is however instructive to study a truncated version of the equations. We will first study the following approximation where we take away all terms except the linear terms that involve the single-particle energies and the two-particle intermediate excitations, that is

$$0 = \langle ab|\hat{v}|ij\rangle + \left(\epsilon_a + \epsilon_b - \epsilon_i - \epsilon_j\right) t_{ij}^{ab} + \frac{1}{2}\sum_{cd}\langle ab|\hat{v}|cd\rangle t_{ij}^{cd}. \tag{8.32}$$

In the above and following equations we have dropped the subscript which indicates the number of iterations. Setting the single-particle energies for the hole states equal to an energy variable $\omega = \epsilon_i + \epsilon_j$, Eq. (8.32) reduces to the well-known equations for the so-called $G$-matrix, widely used in infinite matter and finite nuclei studies, see for example [8, 28]. The equation can then be reordered and solved by matrix inversion. To see this let us define the following quantity

$$\tau_{ij}^{ab} = \left(\omega - \epsilon_a - \epsilon_b\right) t_{ij}^{ab},$$

and inserting

$$1 = \frac{(\omega - \epsilon_c - \epsilon_d)}{(\omega - \epsilon_c - \epsilon_d)},$$

in the intermediate sums over $cd$ in Eq. (8.32), we can rewrite the latter equation as

$$\tau_{ij}^{ab}(\omega) = \langle ab|\hat{v}|ij\rangle + \frac{1}{2}\sum_{cd}\langle ab|\hat{v}|cd\rangle\frac{1}{\omega - \epsilon_c - \epsilon_d}\tau_{ij}^{cd}(\omega),$$

where we have inserted an explicit energy dependence via the parameter $\omega$. This equation, transforming a two-particle configuration into a single index, can be rewritten as a matrix inversion problem. Alternatively, the same equation can

be solved by iteration. Solving the equations for a fixed energy $\omega$ allows us to compare directly with results from Green's function theory when only two-particle intermediate states are included.

To solve Eq. (8.32), we start with a guess for the unknown amplitudes, normally using the wave operator defined by first order in perturbation theory, leading to a zeroth-order approximation for the correlation energy given by second-order perturbation theory. A simple approach to the solution of Eq. (8.32), is thus to

1. Start with a guess for the amplitudes and compute the zeroth approximation to the correlation energy.
2. Use the ansatz for the amplitudes to solve Eq. (8.32) via for example your root-finding method of choice (Newton's method or modifications thereof can be used) and continue these iterations till the correlation energy does not change more than a prefixed quantity $\lambda$; $\Delta E_{\mathrm{CCD}}^{(i)} - \Delta E_{\mathrm{CCD}}^{(i-1)} \leq \lambda$.
3. It is common during the iterations to scale the amplitudes with a parameter $\alpha$, with $\alpha \in (0, 1]$ as $t^{(i)} = \alpha t^{(i)} + (1-\alpha)t^{(i-1)}$.

The next approximation is to include the two-hole term in Eq. (8.31), a term which allows us to make a link with Green's function theory with two-particle and two-hole correlations discussed in Chap. 11. This means that we solve

$$0 = \langle ab|\hat{v}|ij\rangle + \left(\epsilon_a + \epsilon_b - \epsilon_i - \epsilon_j\right) t_{ij}^{ab} + \frac{1}{2}\sum_{cd}\langle ab|\hat{v}|cd\rangle t_{ij}^{cd} + \frac{1}{2}\sum_{kl}\langle kl|\hat{v}|ij\rangle t_{kl}^{ab}. \tag{8.33}$$

This equation is solved the same way as we would do for Eq. (8.32). The final step is then to include all terms in Eq. (8.31).

## 8.7 Developing a Numerical Project

A successful numerical project relies on us having expertise in several scientific and engineering disciplines. We need a thorough understanding of the relevant scientific domain to ask the right questions and interpret the results, but the tools we use require a proficiency in mathematics to develop models and work out analytical results, in numerics to choose the correct algorithms, in computer science to understand what can go wrong with our algorithms when the problem is discretized and solved on a digital computer, and in software engineering to develop and maintain a computer program that solves our problem.

Independent of your scientific background, you are probably also educated in mathematics and numerics. Unfortunately, the computer science and software engineering aspects of computing are often neglected and thought of as skills you pick up along the way. This is a problem for many reasons. First, running a numerical project is very similar to running a physical experiment. The codes

we develop are the blueprints the compiler uses to build the experiment from the components of the computer. It is unthinkable to publish results from a physical experiment without a thorough understanding of the experimental equipment. Second, the blueprints are not only used to tell the compiler what to build, but also by humans to understand what is being built, how to fix it if something goes wrong, and how to improve it. If the blueprints are not properly written and readable, human understanding is lost. Last, components of an experiment are always tested individually to establish tolerances and that they work according to specification. In software engineering, this corresponds to writing testable code where you can be confident of the quality of each piece. These are skills many writers of scientific software never learn and as a consequence many numerical experiments are not properly understood and are never independently verified.

In this section we will focus on some key tools and strategies that we feel are important for developing and running a numerical experiment. Our main concerns are that our results can be validated, independently verified, and run efficiently. In addition, we will discuss tools that make the whole process somewhat easier. We will cover testing, tracking changes with version control software, public code repositories, and touch upon simple profiling tools to guide the optimization process. Finally we will present a numerical project where we have developed a code to calculate properties of nuclear matter using coupled-cluster theory. Here, we will make extensive use of the simple pairing model of Problem 8.10. This model allows for benchmarks against exact results. In addition, it provides analytical answers to several approximations, from perturbation theory to specific terms in the solution of the coupled cluster equations, the in-medium similarity renormalization group approach of Chap. 10 and the Green's function approach of Chap. 11.

### *8.7.1 Validation and Verification*

The single most important thing in a numerical experiment is to get the correct answer. A close second is to be confident that the answer is correct and why. A lucky coincidence must be distinguishable from a consistently correct result. The only way to do this is to validate the code by writing and running tests—lots of tests. Ideally, every aspect of a code should be tested and it should be possible to run the tests automatically. As most of you have probably experienced, it's very easy to introduce errors into a project. And very often, symptoms of the errors are not visible where the errors have been introduced. By having a large set of automated tests and running them often, symptoms of errors can be discovered quickly and the errors tracked down while recent changes are fresh in memory.

As scientists we are trained to validate our methods and findings. By applying the same rigorous process to our software, we can achieve the same level of confidence in our code as we have for the rest of our work. We advocate testing at three distinct levels. Let's start with discussing validation tests, as this is the type of test you are probably most familiar with. In a validation test, your application is run as in

production mode and the test fails if it cannot reproduce a known result. The known result could be a published benchmark, a simplified model where analytical results are available, an approximate result from a different method, or even an earlier result from the same code. We will discuss this type of testing further in Sect. 8.7.4.

Analogous to testing individual components in a physical experiment, is a type of test called a unit test. This is a very fine-grained test that will typically only test a class or a procedure, or even a small part of your code at a time. This is where you test that a data structure has been correctly filled, that an algorithm works appropriately, that a file has been read correctly, and basically every other component test you can think of. It does take a little more work to setup as testing needs to be done outside of your normal program flow. Typically this involves writing different executables that create the necessary dependencies before testing a component. The advantages of writing unit tests are many. First, because you know that the individual pieces of your code work independently, you will achieve a higher degree of confidence in your results. Second, you will develop a programming style that favors highly decoupled units because such units are easier to test. This allows talking about the code at a higher level of abstraction, which helps understanding. Last, your tests become the documentation of how your code is supposed to be used. This might not seem important while your are actively working on a project, but it will be invaluable down the line when you want to add new features. Also, when you share your code as part of the scientific process, these tests will be the way your peers will start to understand your work. This means that your final production code will also include various tests.

While validation tests test your code at the coarsest level, and unit tests test your code at the finest level, integration tests test how your components work together. If, for example, your program solves differential equations as parts of a larger problem, the components that make up your differential-equation solver can be tested alone. If your solver can solve a set of representative problems that either have analytical solutions or can be worked out using some other tool, you can be more confident that it will work on your specific problem. Moreover, writing integration tests pushes you to develop more general components. Instead of writing a routine that only solves the differential equations you need, you write a solver that can solve many different types of differential equations. This allows your components to be reused in other projects and by other people.

To many, this rigorous approach to testing software might seem like a waste of time. Our view is that testing software is crucial to the scientific process and we should strive to apply the same level of rigour to our software as we do to every other aspect of our work. On a more pragmatic level, you can either spend your time writing tests and make sure your components work, or you can spend your time debugging when something goes wrong and worry that your results are not valid. We definitely prefer, from own and other people's experience, the first approach.

### 8.7.2 Tracking Changes

If you're not using a tool to track the changes you make to your code, now is the time to start. There are several tools available, but the authors are using git (https://git-scm.com/), an open-source version-control system that can run on Linux, OSX, and Windows. By tracking changes, it is easier to correct a mistake when it inevitably creeps into the code. It is possible to go back to a previously validated version and by using branches, you can work on different versions of the code simultaneously. For example, you can create a production branch where everything is validated and ready to run, and you can create a development branch to implement new features. There are also code repositories where you can store a copy of your code for free, without worrying about things getting lost. The source codes discussed in this book are hosted on for example GitHub (https://github.com/), which uses git to track all changes to the code. By using a service like this, it is easier to synchronize code between multiple machines. Multiple developers can work on the same code at the same time and share changes without worrying about losing contributions. It can also become the official public repository of your software to enable your peers to verify your work. The software discussed in this chapter is available from our GitHub repository https://github.com/ManyBodyPhysics/LectureNotesPhysics/tree/master/Programs/Chapter8-programs/.

### 8.7.3 Profile-Guided Optimization

The aim of this subsection is to discuss in more detail how we can make the computations discussed in connection with Eqs. (8.52) and (8.53) more efficient using physical constraints, algorithm improvements, and parallel processing. For pedagogical reasons, we will use the MBPT parts of the program due to their simplicity while still containing the important elements of a larger, more complicated CCD calculation. The codes can be found at the github link https://github.com/ManyBodyPhysics/LectureNotesPhysics/tree/master/Programs/Chapter8-programs/cpp/MBPT/src. We will demonstrate the use of a simple profiler to help guide our development efforts. Our starting points are naive implementations of many-body perturbation theory to second (MBPT2) and third order (MBPT3) in the interaction. For reference, we calculate properties of nuclear matter and construct our Hamiltonian in a free-wave basis using the Minnesota [57] potential discussed in Sect. 8.2.3. As the model is not as important as the performance in this section, we postpone a discussion of the model to Sect. 8.7.4.

**Code Listing 8.1** Trivial implementation of a MBPT2 diagram

```
double energy = 0.0;
for(int i = 0; i < modelspace.indhol; ++i){
  for(int j = 0; j < modelspace.indhol; ++j){
    if(i == j){ continue; }
    for(int a = modelspace.indhol; a < modelspace.indtot; ++a){
      for(int b = modelspace.indhol; b < modelspace.indtot; ++b)
          {
        if(a == b){ continue; }
        energy0 = potential->get_element(modelspace.qnums, i, j,
            a, b);
        energy0 *= energy0;
        energy0 /= (modelspace.qnums[i].energy + modelspace.
            qnums[j].energy -
                    modelspace.qnums[a].energy - modelspace.
                        qnums[b].energy);
        energy += energy0;
      }
    }
  }
}
energy *= 0.25;
return energy;
}
```

Listing 8.1 shows a possible early implementation to solve Eq. (8.52) from MBPT2. This function has a loop over all single-particle indices and calls the V_Minnesota function via the get_element function to calculate the two-body interaction for each set of indices. The energy denominators are calculated from the single-particle energies stored in the modelspace structure and partial results are accumulated into the energy variable. This function represents a straightforward implementation of MBPT2. We normally recommend, when developing a code, to write the first implementation in a way which is as close as possible to the mathematical expressions, in this particular case Eq. (8.52).

Table 8.3 shows the total execution time for this application for different model spaces (defined by the number of single-particle states) and number of particles on a local workstation. Your runtimes will be different. Our goals are converged calculations of pure neutron matter as well as nuclear matter, where the number of states and the number of protons and neutrons goes to infinity. It suffices to say that we cannot reach our goals with this code.

We want to decrease the run time of this application, but it can be difficult to decide where we should spend our time improving this code. Our first approach is to observe what goes on inside the program. For that we will use one the simplest possible profiling tools called gprof (https://sourceware.org/binutils/docs/gprof/). Alternatively, software like Valgrind is also highly recommended http://valgrind.org. If you are using integrated development environments (IDEs) like Qt https://www.qt.io/, performance and debugging tools are integrated with the IDE.

**Table 8.3** Total runtime for the MBPT2 implementation in Listing 8.1 for different model spaces and particle numbers

| Number of states | Number of protons | Number of neutrons | Runtime (s) Listing 8.1 |
|---|---|---|---|
| 342 | 0 | 2 | < 0.01 |
| | 0 | 14 | 0.15 |
| | 0 | 38 | 1.00 |
| | 0 | 54 | 1.81 |
| 684 | 2 | 2 | 0.88 |
| | 14 | 14 | 2.43 |
| | 38 | 38 | 15.7 |
| | 54 | 54 | 28.2 |
| 1598 | 0 | 2 | 0.04 |
| | 0 | 14 | 3.32 |
| | 0 | 38 | 25.0 |
| | 0 | 54 | 58.9 |
| 3196 | 2 | 2 | 0.88 |
| | 14 | 14 | 54.3 |
| | 38 | 38 | 399 |
| | 54 | 54 | 797 |

**Table 8.4** Flat profile for the MBPT2 implementation in Listing 8.1 using 1598 states calculating pure neutron matter with 54 neutrons

```
Flat profile:

Each sample counts as 0.01 seconds.
  %   cumulative   self              self     total
 time   seconds   seconds    calls  ms/call  ms/call  name
 58.01     26.26    26.26 2523524846     0.00     0.00  V_Minnesota(...)
 39.64     44.21    17.95                              mbpt2V00::getEnergy()
  2.35     45.27     1.07                              spinExchangeTerm(...)
```

To use gprof the code must first be compiled and linked with the -pg flag. This flag enables the collection of runtime information so that a call graph and a profile can be constructed when your program is run.

Table 8.4 shows the top few lines of the flat profile generated for MBPT2 version in Listing 8.1. The leftmost column shows the percentage of run time spent in the different functions and it shows that about 58% of the time is spent calculating the potential while about 40% is spent in the loops in the actual MBPT2 function. The remaining part is spent in the spinExchangeTerm function which is called from the potential function. Even though the application spends most of its time generating the potential, we don't want to spend too much time on improving this code. We use the Minnesota potential for testing and benchmark purposes only. For more realistic calculations, one should employ the chiral interaction models discussed earlier. It is, however, possible to reduce the number of times this function is called. The 4th column in Table 8.4 shows that for this particular instance, the potential function was called 2.5 billion times. However, due to known symmetries of the nuclear

interaction we know that most of these calls result in matrix elements that are zero. If we can exploit this structure to reduce the number of calls to the potential function we will greatly reduce the total run time of this program. The details of how this is done is presented in Sect. 8.7.4.

**Code Listing 8.2** Block-sparse implementation of a MBPT2 diagram

```
double mbpt2V02::getEnergy() {
  double energy = 0.0;
  double energy0;
  int nhh, npp, i, j, a, b;
  for(int chan = 0; chan < channels.size; ++chan){
    nhh = channels.nhh[chan];
    npp = channels.npp[chan];
    if(nhh*npp == 0){ continue; }

    for(int hh = 0; hh < nhh; ++hh){
      i = channels.hhvec[chan][2*hh];
      j = channels.hhvec[chan][2*hh + 1];
      for(int pp = 0; pp < npp; ++pp){
        a = channels.ppvec[chan][2*pp];
        b = channels.ppvec[chan][2*pp + 1];
        energy0 = V_Minnesota(modelspace, i, j, a, b, L);
        energy0 *= energy0;
        energy0 /= (modelspace.qnums[i].energy + modelspace.qnums[
            j].energy -
                modelspace.qnums[a].energy - modelspace.qnums[b
                    ].energy);
        energy += energy0;
      }
    }
  }
  energy *= 0.25;
  return energy;

}
```

Listing 8.2 shows a version of this code where the potential function is not called when we know that the matrix element is zero. This code loops over channels, which are the dense blocks of the full interaction. We have pre-computed the two-body configurations allowed in each channel and store them in the channels structure. The potential is computed in the same way as before, but for fewer combinations of indices.

The profile in Table 8.5 shows that the potential function is now only called 2.5 million times, a reduction of three orders of magnitude. Table 8.6 summarizes the execution times of these two versions of MBPT2.

**Code Listing 8.3** Block-sparse implementation of a MBPT3 diagram

```
double mbpt3V02::getEnergy() {
  double energy = 0.0;
```

**Table 8.5** Flat profile for the MBPT2 implementation in Listing 8.2 using 1598 states calculating pure neutron matter with 54 neutrons

```
Flat profile:

Each sample counts as 0.01 seconds.
  %   cumulative   self              self     total
 time   seconds   seconds    calls  ms/call  ms/call  name
 66.69      0.08     0.08  2520526     0.00     0.00  V_Minnesota(...)
 16.67      0.10     0.02  4770508     0.00     0.00  Chan_2bInd(...)
  8.34      0.11     0.01        1    10.00    10.00  Build_Model_Space(...)
  8.34      0.12     0.01        1    10.00    30.01  Setup_Channels_MBPT(...)
```

**Table 8.6** Total runtime for different MBPT2 implementations for different model spaces

| Number of states | Number of protons | Number of neutrons | Runtime (s) | |
|---|---|---|---|---|
| | | | Listing 8.1 | Listing 8.2 |
| 342 | 0 | 2 | < 0.01 | < 0.01 |
| | 0 | 14 | 0.15 | < 0.01 |
| | 0 | 38 | 1.00 | 0.03 |
| | 0 | 54 | 1.81 | 0.05 |
| 684 | 2 | 2 | 0.88 | < 0.01 |
| | 14 | 14 | 2.43 | 0.04 |
| | 38 | 38 | 15.7 | 0.19 |
| | 54 | 54 | 28.2 | 0.31 |
| 1598 | 0 | 2 | 0.04 | < 0.01 |
| | 0 | 14 | 3.32 | 0.03 |
| | 0 | 38 | 25.0 | 0.23 |
| | 0 | 54 | 58.9 | 0.44 |
| 3196 | 2 | 2 | 0.88 | < 0.01 |
| | 14 | 14 | 54.3 | 0.21 |
| | 38 | 38 | 399 | 1.40 |
| | 54 | 54 | 797 | 2.67 |

```
3   double energy0, energy1;
4   int nhh, npp, i, j, a, b, c, d;
5   for(int chan = 0; chan < channels.size; ++chan){
6     nhh = channels.nhh[chan];
7     npp = channels.npp[chan];
8     if(nhh*npp == 0){ continue; }
9
10    for(int hh = 0; hh < nhh; ++hh){
11      i = channels.hhvec[chan][2*hh];
12      j = channels.hhvec[chan][2*hh + 1];
13      for(int ab = 0; ab < npp; ++ab){
14        a = channels.ppvec[chan][2*ab];
15        b = channels.ppvec[chan][2*ab + 1];
16        energy0 = V_Minnesota(modelspace, i, j, a, b, L);
```

```
17        energy0 /= (modelspace.qnums[i].energy + modelspace.qnums[
              j].energy -
18                    modelspace.qnums[a].energy - modelspace.qnums[b
                          ].energy);
19        for(int cd = 0; cd < npp; ++cd){
20          c = channels.ppvec[chan][2*cd];
21          d = channels.ppvec[chan][2*cd + 1];
22          energy1 = V_Minnesota(modelspace, a, b, c, d, L);
23          energy1 *= V_Minnesota(modelspace, c, d, i, j, L);
24          energy1 /= (modelspace.qnums[i].energy + modelspace.
                qnums[j].energy -
25                    modelspace.qnums[c].energy - modelspace.qnums[
                          d].energy);
26          energy += energy0*energy1;
27        }
28      }
29    }
30  }
31  energy *= 0.125;
32  return energy;
33 }
```

**Table 8.7** Flat profile for the MBPT3 implementation in Listing 8.3 using 3196 states calculating nuclear matter with 14 protons and 14 neutrons

```
Flat profile:

Each sample counts as 0.01 seconds.
  %   cumulative   self              self     total
 time   seconds   seconds    calls  ms/call  ms/call  name
 90.76    177.21   177.21 6068445596     0.00     0.00  V_Minnesota(...)
  8.76    194.31    17.11                              mbpt3V02::getEnergy()
```

Listing 8.3 shows an implementation of MBPT3 that uses a block-sparse representation of the interaction. Compared to MBPT2 it loops over two additional particle indices which increases the computational complexity by several orders of magnitude. However, we are now calculating the interaction many more times than what is necessary. The profile in Table 8.7 shows that we calculated over six billion

matrix elements. By moving the construction of the interaction out of the main loops and storing the elements, we can eliminate these redundant calls to the potential function at the expense of using memory to store the elements.

**Code Listing 8.4** Block-sparse implementation of a MBPT3 diagram with interaction stored in memory

```
double mbpt3V05::getEnergy() {
  double energy = 0.0;
  double *V1, *S1, *V2, *S2;
  char N = 'N';
  char T = 'T';
  double fac0 = 0.0;
  double fac1 = 1.0;
  int nhh, npp, i, j, a, b, c, d, idx;
  double energy0;
  for(int chan = 0; chan < channels.size; ++chan){
    nhh = channels.nhh[chan];
    npp = channels.npp[chan];
    if(nhh*npp == 0){ continue; }

    V1 = new double[nhh * npp];
    S1 = new double[nhh * npp];
    V2 = new double[npp * npp];
    S2 = new double[nhh * nhh];
    for(int ab = 0; ab < npp; ++ab){
      a = channels.ppvec[chan][2*ab];
      b = channels.ppvec[chan][2*ab + 1];
      for(int hh = 0; hh < nhh; ++hh){
        i = channels.hhvec[chan][2*hh];
        j = channels.hhvec[chan][2*hh + 1];
        idx = hh * npp + ab;
        energy0 = V_Minnesota(modelspace, i, j, a, b, L);
        energy0 /= (modelspace.qnums[i].energy + modelspace.qnums[j].
            energy -
                 modelspace.qnums[a].energy - modelspace.qnums[b].
                     energy);
        V1[idx] = energy0;
      }
      for(int cd = 0; cd < npp; ++cd){
        c = channels.ppvec[chan][2*cd];
        d = channels.ppvec[chan][2*cd + 1];
        idx = ab * npp + cd;
        V2[idx] = V_Minnesota(modelspace, a, b, c, d, L);
      }
    }

    RM_dgemm(V1, V2, S1, &nhh, &npp, &npp, &fac1, &fac0, &N, &N);
    RMT_dgemm(S1, V1, S2, &nhh, &nhh, &npp, &fac1, &fac0, &N, &T);
    delete V1; delete V2; delete S1;
    for(int hh = 0; hh < nhh; ++hh){
      energy += S2[nhh*hh + hh];
    }
```

```
45      delete S2;
46    }
47    energy *= 0.125;
48
49    return energy;
50  }
```

Listing 8.4 shows the new version of the code that stores matrix elements of the interaction. The explicit summation to calculate the energy can now be done by using matrix products by calling the BLAS (Basic Linear Algebra Subprograms) [76] dgemm wrappers `RM_dgemm` and `RMT_dgemm`. Note that the code has grown more complicated for every new optimization we have introduced. This increases the possibility of introducing errors significantly. It is a good thing we have tests to make sure that the results haven't changed between versions. Table 8.8 shows the profile for this version and we have reduced considerably the number of calls to the function which sets up the interaction.

Table 8.9 summarizes the execution times so far.

Table 8.8 shows that the potential function is still the most expensive function in our program, but we would like to get a more detailed profile of this function. The code to calculate the potential is filled with calls to the exponential function which is part of the standard library. Since we have linked to the standard library dynamically, gprof is not able to show time spent in these functions. We can get a little bit more detail by linking statically. This is done by introducing the static flag to the compiler. Table 8.10 shows the new profile.

The profile is now a lot more busy and it shows a longer runtime than the previous profile. This is because gprof doesn't sample time spent in dynamically linked libraries. The total runtime in this profile corresponds better with Table 8.9, but it is also more difficult to read. What is clear is that the call to the function labelled `__ieee754_exp_avx` takes up almost 70% of the total run time. This function represents the calls to the exponential function in the potential code. If we can reduce the number of evaluations of the exponential function, we can further reduce the run time of this application. We leave that as an exercise to the reader.

The next level of optimization that we will discuss here is the introduction of parallelism. Most modern computers have more than one cpu core available for

**Table 8.8** Flat profile for the MBPT3 implementation in Listing 8.4 using 3196 states calculating nuclear matter with 14 protons and 14 neutrons

```
Flat profile:

Each sample counts as 0.01 seconds.
  %   cumulative   self              self     total
 time   seconds   seconds    calls  ms/call  ms/call  name
 91.16     14.59    14.59 484191644     0.00     0.00  V_Minnesota(...)
  7.68     15.82     1.23                              mbpt3V05::getEnergy()
```

**Table 8.9** Total runtime for the MBPT3 implementation in Listing 8.3 for different model spaces

| Number of states | Number of protons | Number of neutrons | Runtime (s) | |
|---|---|---|---|---|
| | | | Listing 8.3 | Listing 8.4 |
| 342 | 0 | 2 | 0.08 | 0.02 |
| | 0 | 14 | 2.38 | 0.31 |
| | 0 | 38 | 9.20 | 0.49 |
| 684 | 2 | 2 | 1.05 | 0.18 |
| | 14 | 14 | 27.8 | 2.00 |
| | 38 | 38 | 107 | 3.18 |
| 1598 | 0 | 2 | 1.81 | 0.46 |
| | 0 | 14 | 80.0 | 10.5 |
| | 0 | 38 | 456 | 29.8 |
| 3196 | 2 | 2 | 23.1 | 4.00 |
| | 14 | 14 | 884 | 69.8 |
| | 38 | 38 | $> 10^3$ | 190 |

**Table 8.10** Flat profile for the MBPT3 implementation in Listing 8.4 compiled with the static flag enabled using 3196 states calculating nuclear matter with 14 protons and 14 neutrons

```
Flat profile:

Each sample counts as 0.01 seconds.
  %   cumulative   self              self     total
 time   seconds   seconds    calls  ms/call  ms/call  name
 68.06     44.68    44.68                             __ieee754_exp_avx
 21.26     58.64    13.96 484191644     0.00     0.00  V_Minnesota(...)
  5.37     62.17     3.53                             exp
  2.18     63.60     1.43                             mbpt3V05::getEnergy()
  0.94     64.22     0.62                             dgemm_otcopy
  0.55     64.58     0.36                             dgemm_kernel
  0.53     64.93     0.35                             __mpexp_fma4
  0.25     65.09     0.17                             __floor_sse41
```

computation, but the codes we have presented so far will only run on one of these cores. The simplest way to make this code run in parallel is to introduce OpenMP (http://www.openmp.org/) directives. This will split the work between multiple execution streams that all share the same view of memory. Listing 8.5 shows a new version of the MBPT3 function where we have introduced OpenMP directives in lines 19 and 21. The first line marks the start of a parallel region and defines which variables the cores can share and which must be duplicated. The second line defines a parallel loop, where each core is responsible for only a section of the loop. As long as we have enough work in the outermost loop, this strategy will work quite well as shown in Fig. 8.3. Here we show the total run time of this code using different number of cores compared to the best run times we could have gotten with this approach if our parallel regions scaled perfectly with the number of cores. In reality this never happens. In this particular case, we could have made

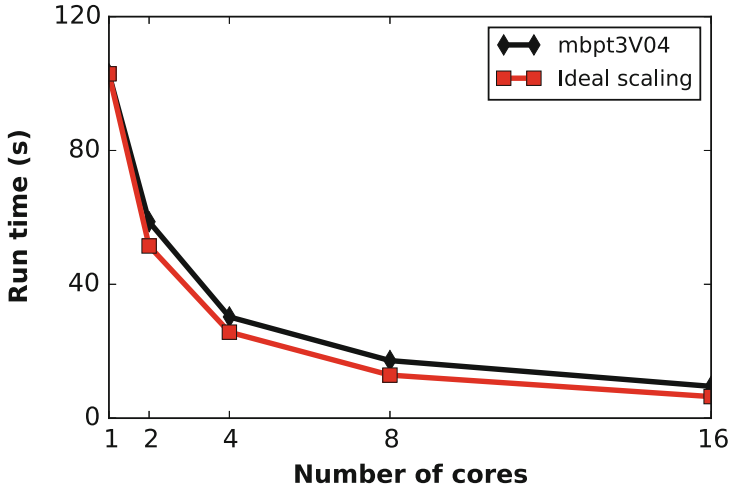


**Fig. 8.3** Total runtime for the mbpt3 code in Listing 8.5 using different number of OpenMP threads on a 16 code node of a Cray XK7

the potential function more cache friendly. With this version the different cores are fighting each other for access to memory and cache. This reduces performance somewhat.

**Code Listing 8.5** Block-sparse implementation of a MBPT3 diagram with interaction stored in memory and openmp directives

```
double mbpt3V04::getEnergy() {
  double energy = 0.0;
  double *V1, *S1, *V2, *S2;
  char N = 'N';
  char T = 'T';
  double fac0 = 0.0;
  double fac1 = 1.0;
  int nhh, npp, i, j, a, b, c, d, idx;
  double energy0;
  for(int chan = 0; chan < channels.size; ++chan){
    nhh = channels.nhh[chan];
    npp = channels.npp[chan];
    if(nhh*npp == 0){ continue; }

    V1 = new double[nhh * npp];
    S1 = new double[nhh * npp];
    V2 = new double[npp * npp];
    S2 = new double[nhh * nhh];
    #pragma omp parallel shared(V1, V2) private(i, j, a, b, c, d,
         idx, energy0)
    {
      #pragma omp for schedule(static)
      for(int ab = 0; ab < npp; ++ab){
        a = channels.ppvec[chan][2*ab];
        b = channels.ppvec[chan][2*ab + 1];
        for(int hh = 0; hh < nhh; ++hh){
          i = channels.hhvec[chan][2*hh];
          j = channels.hhvec[chan][2*hh + 1];
          idx = hh * npp + ab;
```

```
29          energy0 = V_Minnesota(modelspace, i, j, a, b, L);
30          energy0 /= (modelspace.qnums[i].energy + modelspace.
                qnums[j].energy -
31                      modelspace.qnums[a].energy - modelspace.qnums[
                            b].energy);
32          V1[idx] = energy0;
33        }
34        for(int cd = 0; cd < npp; ++cd){
35          c = channels.ppvec[chan][2*cd];
36          d = channels.ppvec[chan][2*cd + 1];
37          idx = ab * npp + cd;
38          V2[idx] = V_Minnesota(modelspace, a, b, c, d, L);
39        }
40      }
41    }
42
43    RM_dgemm(V1, V2, S1, &nhh, &npp, &npp, &fac1, &fac0, &N, &N);
44    RMT_dgemm(S1, V1, S2, &nhh, &nhh, &npp, &fac1, &fac0, &N, &T)
          ;
45    delete V1; delete V2; delete S1;
46    for(int hh = 0; hh < nhh; ++hh){
47      energy += S2[nhh*hh + hh];
48    }
49    delete S2;
50  }
51  energy *= 0.125;
52
53  return energy;
54 }
```

In this function we have used the matrix-matrix multiplication function *dgemm* of BLAS [76]. Finally, the above codes can easily be extended upon by including MPI [77, 78] and/or a mix of OpenMP and MPI commands for distributed memory architectures. We leave this as a challenge to the reader. The coding practices and examples developed in this section, are reused in our development of the coupled cluster code discussed in the next section. There we discuss however in more detail how to develop an efficient coupled cluster code for infinite matter, with a focus on validation and verification and simplifications of the equations.

### *8.7.4 Developing a CCD Code for Infinite Matter*

This section focuses on writing a working CCD code from scratch. Based on the previous discussion, what follows serves also the scope of outlining how to start a larger numerical project. We will in particular pay attention to possible benchmarks that can be used to validate our codes.

We will assume that you have opted for a specific mathematical method for solving Schrödinger's equation. Here the mathematics is given by the CCD equations. Our basic steps can then be split up as follows

- Write a first version of the CCD code which is as close as possible to the mathematics of your equations. In this stage we will not focus on high-performance computing aspects and code efficiency. This will mimick our discussion of many-body perturbation theory, in particular the calculation of the correlation energy to second order discussed above.
- Try to find possible benchmarks you can test your code against. In our case, the pairing model serves as an excellent testcase.
- With a functioning code that reproduces possible analytical and/or numerical results, we can start to analyze our code. In particular, if there are mathematical operations which can be simplified and/or can be represented in simpler ways etc. The modified code can hopefully reduce memory needs and time spent on computations. The usage of specific symmetries of the interaction will turn out particularly useful.

In this specific section, we will try to follow the above three steps, with less attention on speed and numerical efficiency. Our aim is to have a code which passes central tests and can be properly validated and verified. If you are familiar with high-performance computing topics, you are obviously not limited to follow the basic steps outlined here. However, when developing a numerical project we have often found it easier and less error-prone to start with the basic mathematical expressions. With a first functioning code, we will delve into high-performance computing topics. A good read on developing numerical projects and clear code is Martin's recent text [79]. We recommend it highly and have borrowed many ideas and coding philosophies therefrom.

We start with implementing the CCD equations as they stand here

$$\begin{aligned}\left(\epsilon_i+\epsilon_j-\epsilon_a-\epsilon_b\right)t_{ij}^{ab} &= \langle ab|\hat{v}|ij\rangle+\frac{1}{2}\sum_{cd}\langle ab|\hat{v}|cd\rangle t_{ij}^{cd}+\frac{1}{2}\sum_{kl}\langle kl|\hat{v}|ij\rangle t_{kl}^{ab}\\ &+\hat{P}(ij|ab)\sum_{kc}\langle kb|\hat{v}|cj\rangle t_{ik}^{ac}+\frac{1}{4}\sum_{klcd}\langle kl|\hat{v}|cd\rangle t_{ij}^{cd}t_{kl}^{ab}\\ &+\hat{P}(ij)\sum_{klcd}\langle kl|\hat{v}|cd\rangle t_{ik}^{ac}t_{jl}^{bd}-\frac{1}{2}\hat{P}(ij)\sum_{klcd}\langle kl|\hat{v}|cd\rangle t_{ik}^{dc}t_{lj}^{ab}\\ &-\frac{1}{2}\hat{P}(ab)\sum_{klcd}\langle kl|\hat{v}|cd\rangle t_{lk}^{ac}t_{ij}^{db},\end{aligned}\tag{8.34}$$

for all $i<j$ and all $a<b$, using the standard notation that $a,b,\ldots$ are particle states and $i,j,\ldots$ are hole states. The CCD correlation energy is given by

$$\Delta E_{CCD}=\frac{1}{4}\sum_{ijab}\langle ij|\hat{v}|ab\rangle\, t_{ij}^{ab}.\tag{8.35}$$

One way to solve these equations, is to write Eq. (8.34) as a series of iterative nonlinear algebraic equations

$$
\begin{aligned}
t_{ij}^{ab\,(n+1)} = \frac{1}{\epsilon_{ij}^{ab}}\Big(&\langle ab|\hat{v}|ij\rangle + \frac{1}{2}\sum_{cd}\langle ab|\hat{v}|cd\rangle t_{ij}^{cd\,(n)} + \frac{1}{2}\sum_{kl}\langle kl|\hat{v}|ij\rangle t_{kl}^{ab\,(n)} \\
&+ \hat{P}(ij|ab)\sum_{kc}\langle kb|\hat{v}|cj\rangle t_{ik}^{ac\,(n)} \\
&+ \frac{1}{4}\sum_{klcd}\langle kl|\hat{v}|cd\rangle t_{ij}^{cd\,(n)} t_{kl}^{ab\,(n)} + \hat{P}(ij)\sum_{klcd}\langle kl|\hat{v}|cd\rangle t_{ik}^{ac\,(n)} t_{jl}^{bd\,(n)} \\
&- \frac{1}{2}\hat{P}(ij)\sum_{klcd}\langle kl|\hat{v}|cd\rangle t_{ik}^{dc\,(n)} t_{lj}^{ab\,(n)} - \frac{1}{2}\hat{P}(ab)\sum_{klcd}\langle kl|\hat{v}|cd\rangle t_{lk}^{ac\,(n)} t_{ij}^{db\,(n)}\Big),
\end{aligned}
\tag{8.36}
$$

for all $i < j$ and all $a < b$, where $\epsilon_{ij}^{ab} = \left(\epsilon_i + \epsilon_j - \epsilon_a - \epsilon_b\right)$, and $t_{ij}^{ab\,(n)}$ is the $t$ amplitude for the nth iteration of the series. This way, given some starting guess $t_{ij}^{ab\,(0)}$, we can generate subsequent $t$ amplitudes that converge to some value. Discussions of the mathematical details regarding convergence will be presented below; for now we will mainly focus on implementing these equations into a computer program and assume convergence. In pseudocode, the function that updates the $t$ amplitudes looks like

```
CCD_Update()
for i ∈ {0, N_Fermi − 1} do
    for j ∈ {0, N_Fermi − 1} do
        for a ∈ {N_Fermi, N_sp − 1} do
            for b ∈ {N_Fermi, N_sp − 1} do
                sum ← TBME[index(a, b, i, j)]
                for c ∈ {N_Fermi, N_sp − 1} do
                    for d ∈ {N_Fermi, N_sp − 1} do
                        sum ← sum + 0.5 × TBME[index(a, b, c, d)] ×
t_amplitudes_old[index(c, d, i, j)]
                    end for
                end for
                ...
                sum ← sum + (all other terms)
                ...
                energy_denom = SP_energy[i]+SP_energy[j]-
SP_energy[a]-SP_energy[b]
                t_amplitudes[index(a, b, i, j)] = sum/energy_denom
```

(continued)

```
            end for
        end for
    end for
end for
```

Here we have defined $N_{\text{Fermi}}$ to be the fermi level while $N_{sp}$ is the total number of single particle (s.p.) states, indexed from 0 to $N_{sp} - 1$. At the most basic level, the CCD equations are just the addition of many products containing $t_{ij}^{ab}$ amplitudes and two-body matrix elements (TBMEs) $\langle ij|\hat{v}|ab\rangle$. Care should thus be placed into how we store these objects. These are objects with four indices and a sensible first implementation of the CCD equations would be to create two four-dimensional arrays to store the objects. However, it is often more convenient to work with simple one-dimensional arrays instead. The function *index*() maps the four indices onto one index so that a one-dimensional array can be used. An example of a brute force implementation of such a function is

```
function INDEX(p, q, r, s)
    return p × N_sp^3 + q × N_sp^2 + r × N_sp + s
end function
```

Because elements with repeated indices vanish, $t_{ii}^{ab} = t_{ij}^{aa} = 0$ and $\langle pp|\hat{v}|rs\rangle = \langle pq|\hat{v}|rr\rangle = 0$, data structures using this index function will contain many elements that are automatically zero. This means that we need to discuss more efficient storage strategies later. Notice also that we are looping over all indices $i, j, a, b$, rather than the restricted indices. This means that we are doing redundant work. The reason for presenting the equations this way is merely pedagogical. When developing a program, we would recommend to write a code which is as close as possible to the mathematical expressions. The first version of our code will then often be slow, as discussed in Sect. 8.7.3. Below we will however unrestrict these indices in order to achieve a better speed up of our code.

The goal of our code is to calculate the correlation energy, $\Delta E_{CCD}$, meaning that after each iteration of our equations, we use our newest $t$ amplitudes to update the correlation energy

$$\Delta E_{CCD}^{(n)} = \frac{1}{4} \sum_{ijab} \langle ij|\hat{v}|ab\rangle \, t_{ij}^{ab\,(n)}. \tag{8.37}$$

We check that our result is converged by testing whether the most recent iteration has changed the correlation energy by less than some tolerance threshold $\eta$,

$$\eta > |\Delta E_{CCD}^{(n+1)} - \Delta E_{CCD}^{(n)}|. \tag{8.38}$$

The basic structure of the iterative process looks like

```
while (abs(energy_Diff) > tolerance) do
    CCD_Update()
    correlation_Energy ← CCD_Corr_Energy()
    energy_Diff ← correlation_Energy - correlation_Energy_old
    correlation_Energy_old ← correlation_Energy
    t_amplitudes_old ← t_amplitudes
end while
```

Prior to this algorithm, the $t$ amplitudes should be initialized, $t_{ij}^{ab\,(0)}$. A particularly convenient choice, as discussed above, is to use many-body perturbation theory for the wave operator with

$$t_{ij}^{ab\,(0)} = \frac{\langle ab|\hat{v}|ij\rangle}{\epsilon_{ij}^{ab}}, \tag{8.39}$$

which results in the correlation energy

$$\Delta E_{CCD}^{(1)} = \frac{1}{4}\sum_{ijab}\frac{\langle ij|\hat{v}|ab\rangle\langle ab|\hat{v}|ij\rangle}{\epsilon_{ij}^{ab}}. \tag{8.40}$$

This is the familiar result from many-body perturbation theory to second order (MBPT2). It is a very useful result, as one iteration of the CCD equations can be ran, and checked against MBPT2 to give some confidence that everything is working correctly. Additionally, running a program using a minimal test case is another useful way to make sure that a program is working correctly. For this purpose, we turn our attention to the simple pairing model Hamiltonian of Problem 8.10,

$$\hat{H}_0 = \delta\sum_{p\sigma}(p-1)a_{p\sigma}^{\dagger}a_{p\sigma} \tag{8.41}$$

$$\hat{V} = -\frac{1}{2}g\sum_{pq}a_{p+}^{\dagger}a_{p-}^{\dagger}a_{q-}a_{q+} \tag{8.42}$$

which represents a basic pairing model with $p$ levels, each having a spin degeneracy of 2. The form of the coupled cluster equations uses single-particle states that are

**Table 8.11** Single-particle states and their quantum numbers and their energies from Eq. (8.43)

| State label | $p$ | $2s_z$ | $E$ | Type |
|---|---|---|---|---|
| 0 | 1 | 1 | $-g/2$ | Hole |
| 1 | 1 | $-1$ | $-g/2$ | Hole |
| 2 | 2 | 1 | $1-g/2$ | Hole |
| 3 | 2 | $-1$ | $1-g/2$ | Hole |
| 4 | 3 | 1 | 2 | Particle |
| 5 | 3 | $-1$ | 2 | Particle |
| 6 | 4 | 1 | 3 | Particle |
| 7 | 4 | $-1$ | 3 | Particle |

The degeneracy for every quantum number $p$ is equal to 2 due to the two possible spin values

eigenstates of the Hartree-Fock operator, $(\hat{u}+\hat{u}_{\rm HF})\,|p\rangle = \epsilon_p|p\rangle$. In the pairing model, this condition is already fulfilled. All we have to do is define the lowest $N_{\rm Fermi}$ states as holes and redefine the single-particle energies,

$$\epsilon_q = h_{qq} + \sum_i \langle qi|\hat{v}|qi\rangle\,. \tag{8.43}$$

To be more specific, let us look at the pairing model with four particles and eight single-particle states. These states (with $\delta = 1.0$) could be labeled as shown in Table 8.11. The Hamiltonian matrix for this four-particle problem with no broken pairs is defined by six possible Slater determinants, one representing the ground state and zero-particle-zero-hole excitations $0p-0h$, four representing various $2p-2h$ excitations and finally one representing a $4p-4h$ excitation. Problem 8.10 gives us for this specific problem

$$H = \begin{bmatrix} 2\delta-g & -g/2 & -g/2 & -g/2 & -g/2 & 0 \\ -g/2 & 4\delta-g & -g/2 & -g/2 & -0 & -g/2 \\ -g/2 & -g/2 & 6\delta-g & 0 & -g/2 & -g/2 \\ -g/2 & -g/2 & 0 & 6\delta-g & -g/2 & -g/2 \\ -g/2 & 0 & -g/2 & -g/2 & 8\delta-g & -g/2 \\ 0 & -g/2 & -g/2 & -g/2 & -g/2 & 10\delta-g \end{bmatrix}$$

The python program (included for pedagogical purposes only) at https://github.com/ManyBodyPhysics/LectureNotesPhysics/tree/master/Programs/Chapter8-programs/python/mbpt.py diagonalizes the above Hamiltonian matrix for a given span of interaction strength values, performing a full configuration interaction calculation. It plots the correlation energy, that is the difference between the ground state energy and the reference energy. Furthermore, for the pairing model we have added results from perturbation theory to second order (MBPT2) and third order in the interaction MBPT3. Second order perturbation theory includes diagram (2) of Fig. 8.2 while MBPT3 includes diagrams (3), (4), (5), (8) and (9) as well. Note that diagram (3)

is zero for the pairing model and that diagrams (8) and (9) do not contribute either if we work with a canonical Hartree-Fock basis. In the case of the simple pairing model it is easy to calculate $\Delta E_{MBPT2}$ analytically. This is a very useful check of our codes since this analytical expression can also be used to check our first CCD iteration. We restate this expression here but restrict the sums over single-particle states

$$\Delta E_{MBPT2} = \frac{1}{4}\sum_{abij}\frac{\langle ij|\hat{v}|ab\rangle\,\langle ab|\hat{v}|ij\rangle}{\epsilon_{ij}^{ab}} = \sum_{a<b,i<j}\frac{\langle ij|\hat{v}|ab\rangle\,\langle ab|\hat{v}|ij\rangle}{\epsilon_{ij}^{ab}}$$

For our pairing example we obtain the following result

$$\Delta E_{MBPT2} = \frac{\langle 01|\hat{v}|45\rangle^2}{\epsilon_{01}^{45}} + \frac{\langle 01|\hat{v}|67\rangle^2}{\epsilon_{01}^{67}} + \frac{\langle 23|\hat{v}|45\rangle^2}{\epsilon_{23}^{45}} + \frac{\langle 23|\hat{v}|67\rangle^2}{\epsilon_{23}^{67}},$$

which translates into

$$\Delta E_{MBPT2} = -\frac{g^2}{4}\left(\frac{1}{4+g} + \frac{1}{6+g} + \frac{1}{2+g} + \frac{1}{4+g}\right).$$

This expression can be used to check the results for any value of $g$ and provides thereby an important test of our codes. Figure 8.4 shows the resulting correlation energies for the exact case, MBPT2 and MBPT3. We note from the above program

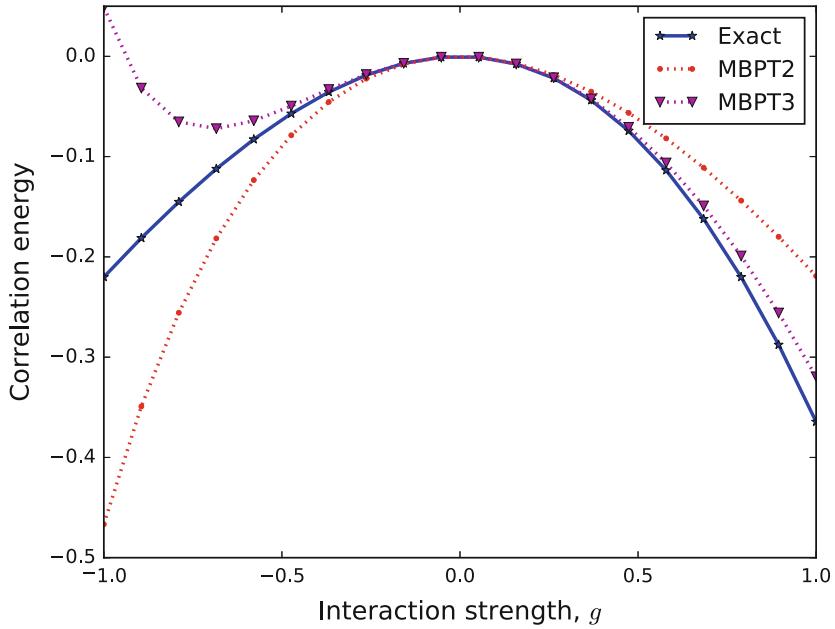


**Fig. 8.4** Correlation energy for the pairing model with exact diagonalization, MBPT2 and perturbation theory to third order MBPT3 for a range of interaction values. A canonical Hartree-Fock basis has been employed in all MBPT calculations

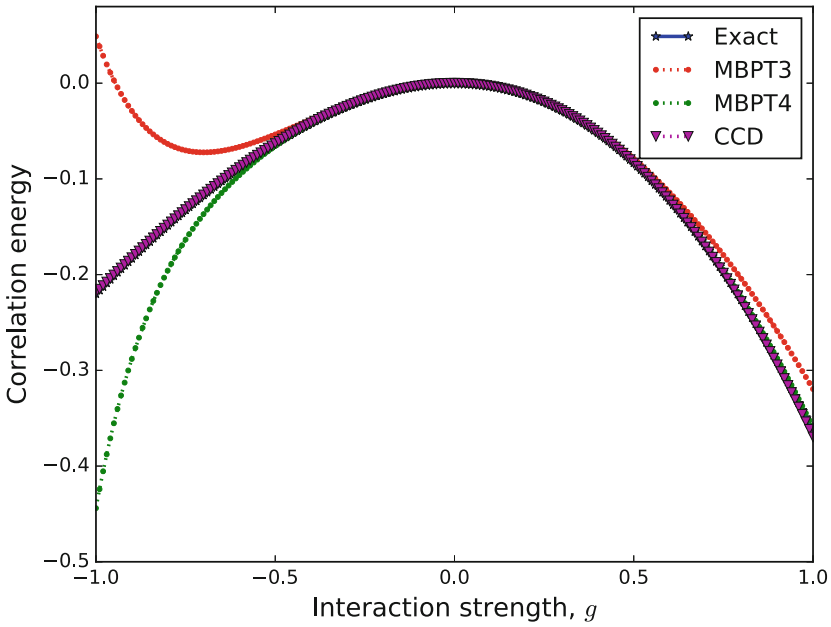


**Fig. 8.5** Correlation energy for the pairing model with exact diagonalization, CCD and perturbation theory to third (MBPT3) and fourth order (MBPT4) for a range of interaction values

that we have coded the expressions for the various diagrams following strictly the mathematical expressions of for example Eqs. (8.24)–(8.26). This means that for every diagram we loop explicitly over every single-particle state. The python program linked to above is included mainly for pedagogical reasons. As we have already seen, this approach is extremely inefficient from a computational point of view. In our discussions of MBPT, as well as for CCD code, we rewrite the computations of most diagrams in terms of efficient matrix-matrix multiplications or matrix-vector multiplications. Figure 8.4 shows us that the approximation to both second and third order are very good when the interaction strength is small and contained in the interval $g \in [-0.5, 0.5]$, but as the interaction gets stronger in absolute value the agreement with the exact reference energy for MBPT2 and MBPT3 worsens. We also note that the third-order result is actually worse than the second order result for larger values of the interaction strength, indicating that there is no guarantee that higher orders in many-body perturbation theory may reduce the relative error in a systematic way. Adding fourth order contributions as shown in Fig. 8.5 for negative interaction strengths gives a better result than second and third order. The fourth order contributions include also four-particle-four-hole correlations. However, the disagreement for stronger interaction values hints at the possibility that many-body perturbation theory may not converge order by order. Perturbative studies of nuclear systems may thus be questionable, unless selected contributions that soften the interactions are properly softened. We note also the non-variational character of many-body perturbation theory, with results at different levels of many-body perturbation theory either overshooting or undershooting the true ground state correlation energy. The coupled cluster results are included in

**Table 8.12** Coupled cluster and MBPT2 results for the simple pairing model with eight single-particle levels and four spin $1/2$ fermions for different values of the interaction strength $g$

| g | $E_{ref}$ | $\Delta E_{MBPT2}$ | $\Delta E_{CCD}$ |
|---|---|---|---|
| $-1.0$ | 3 | $-0.46667$ | $-0.21895$ |
| $-0.5$ | 2.5 | $-0.08874$ | $-0.06306$ |
| 0.0 | 2 | 0 | 0 |
| 0.5 | 1.5 | $-0.06239$ | $-0.08336$ |
| 1.0 | 1 | $-0.21905$ | $-0.36956$ |

Fig. 8.5 where we display the difference between the exact correlation energy and the correlation energy obtained with many-body perturbation theory to third order. Coupled cluster theory with doubles only shows a very good agreement with the exact results. For larger values of $g$ one will however observe larger discrepancies. In Table 8.12 we list for the sake of completeness also our coupled cluster results at the CCD level for the same system. The $g = -1.0$ case diverges without implementing iterative mixing. Sometimes iterative solvers run into oscillating solutions, and mixing can help the iterations break this cycle.

$$t^{(i)} = \alpha t^{(i)}_{no\_mixing} + (1-\alpha)t^{(i-1)} \tag{8.44}$$

Once a working pairing model has been implemented, improvements can start to be made, all the while using the pairing model to make sure that the code is still working and giving correct answers. Realistic systems will be much larger than this small pairing example.

One limitation that will be ran into while trying to do realistic CCD calculations is that of memory. The four-indexed two-body matrix elements (TBMEs) and $t$-amplitudes have to store a lot of elements, and the size of these arrays can quickly exceed the available memory on a machine. If a calculation wants to use 500 single-particle basis states, then a structure like $\langle pq|v|rs\rangle$ will need a length of 500 for each of its four indices, which means it will have $500^4 = 625 \times 10^8$ elements. To get a handle on how much memory is used, consider the elements as double-precision floating point type. One double takes up 8 bytes of memory. This specific array would take up $8 \times 625 \times 10^8$ bytes = $5000 \times 10^8$ bytes = 500 GB of memory. Most personal computers in 2016 have 4–8 GB of RAM, meaning that this calculation would be way out of reach. There are supercomputers that can handle applications using 500 GB of memory, but we can quickly reduce the total memory required by applying some physical arguments. In addition to vanishing elements with repeated indices, mentioned above, elements that do not obey certain symmetries are also zero. Almost all realistic two-body forces preserve some quantities due to symmetries in the interaction. For example, an interaction with rotational symmetry will conserve angular momentum. This means that a two-body ket state $|rs\rangle$, which has some set of quantum numbers, will retain quantum numbers corresponding to the interaction symmetries after being acted on by $\hat{v}$. This state is then projected onto $|pq\rangle$ with its own set of quantum numbers. Thus $\langle pq|v|rs\rangle$ is only non-zero if

$|pq\rangle$ and $|rs\rangle$ share the same quantum numbers that are preserved by $\hat{v}$. In addition, because the cluster operators represent excitations due to the interaction, $t_{ij}^{ab}$ is only non-zero if $|ij\rangle$ has the same relevant quantum numbers as $|ab\rangle$.

To take advantage of this, these two-body ket states can be organized into symmetry "channels" of shared quantum numbers. In the case of the pairing model, the interaction preserves the total spin projection of a two-body state, $S_z = s_{z1} + s_{z2}$. The single particle states can have spin of $+1/2$ or $-1/2$, so there can be three two-body channels with $S_z = -1, 0, +1$. These channels can then be indexed with a unique label in a similar way to the single particle index scheme. In more complicated systems, there will be many more channels involving multiple symmetries, so it is useful to create a data structure that stores the relevant two-body quantum numbers to keep track of the labeling scheme.

It is more efficient to use two-dimensional array data structures, where the first index refers to the channel number and the second refers to the element within that channel. So to access matrix elements or $t$ amplitudes, you can loop over the channels first, then the indices within that channel. To get an idea of the savings using this block diagonal structure, let's look at a case with a plane wave basis, with three momentum and one spin quantum numbers, with an interaction that conserves linear momentum in all three dimensions, as well as the total spin projection. Using 502 basis states, the TBME's require about 0.23 Gb of memory in block diagonal form, which is an enormous saving from the 500 Gb mentioned earlier in the naïve storage scheme.

Since the calculation of all zeros can now be avoided, improvements in speed and memory will now follow. To get a handle on how these CCD calculations are implemented we need only to look at the most expensive sum in Eq. (8.34). This corresponds to the sum over $klcd$. Since this sum is repeated for all $i < j$ and $a < b$, it means that these equations will scale as $\mathcal{O}(n_p^4 n_h^4)$. However, they can be rewritten using intermediates as

$$\begin{aligned} 0 = {} & \langle ab|\hat{v}|ij\rangle + \hat{P}(ab)\sum_c \langle b|\chi|c\rangle \langle ac|t|ij\rangle - \hat{P}(ij)\sum_k \langle k|\chi|j\rangle \langle ab|t|ik\rangle \\ & + \frac{1}{2}\sum_{cd} \langle ab|\chi|cd\rangle \langle cd|t|ij\rangle + \frac{1}{2}\sum_{kl} \langle ab|t|kl\rangle \langle kl|\chi|ij\rangle \\ & + \hat{P}(ij)\hat{P}(ab)\sum_{kc} \langle ac|t|ik\rangle \langle kb|\chi|cj\rangle \,, \end{aligned} \tag{8.45}$$

for all $i, j, a, b$, the reason why these indices are now unrestricted will be explained later. The intermediates $\chi$ are defined as

$$\langle b|\chi|c\rangle = \langle b|f|c\rangle - \frac{1}{2}\sum_{kld} \langle bd|t|kl\rangle \langle kl|v|cd\rangle \,, \tag{8.46}$$

$$\langle k|\chi|j\rangle = \langle k|f|j\rangle + \frac{1}{2}\sum_{cdl} \langle kl|v|cd\rangle \langle cd|t|jl\rangle \,, \tag{8.47}$$

$$\langle kl|\chi|ij\rangle = \langle kl|v|ij\rangle + \frac{1}{2}\sum_{cd}\langle kl|v|cd\rangle\,\langle cd|t|ij\rangle\,, \tag{8.48}$$

$$\langle kb|\chi|cj\rangle = \langle kb|v|cj\rangle + \frac{1}{2}\sum_{dl}\langle kl|v|cd\rangle\,\langle db|t|lj\rangle\,, \tag{8.49}$$

$$\langle ab|\chi|cd\rangle = \langle ab|v|cd\rangle\,. \tag{8.50}$$

With the introduction of the above intermediates, the CCD equations scale now as $\mathcal{O}(n_h^2 n_p^4)$, which is an important improvement. This is of course at the cost of computing the intermediates at the beginning of each iteration, where the most expensive one, $\langle kb|\chi|cj\rangle$ scales as $\mathcal{O}(n_h^3 n_p^3)$. To further speed up these computations, we see that these sums can be written in terms of matrix-matrix multiplications. It is not obvious how to write all of these sums in such a way, but it is useful to first recall that the expression for the multiplication of two matrices $\hat{C} = \hat{A} \times \hat{B}$ can be written as

$$C_{ij} = \sum_k A_{ik} \times B_{kj}. \tag{8.51}$$

We see then that Eq. (8.48) can be written as

$$\langle K|\chi|I\rangle = \langle K|v|I\rangle + \frac{1}{2}\sum_C \langle K|v|C\rangle\,\langle C|t|I\rangle$$

by mapping the two index pairs $kl \rightarrow K, ij \rightarrow I, cd \rightarrow C$. The sum looks now like a matrix-matrix multiplication. This is useful because there are packages like BLAS (Basic Linear Algebra Subprograms) [76] which have extremely fast implementations of matrix-matrix multiplication, as discussed in connection with the listing 8.5. The simplest example to consider is the expression for the correlation energy from MBPT2. We rewrite

$$\Delta E_{MBPT2} = \frac{1}{4}\sum_{abij}\frac{\langle ij|\hat{v}|ab\rangle\,\langle ab|\hat{v}|ij\rangle}{\epsilon_{ij}^{ab}}, \tag{8.52}$$

by defining the matrices $\hat{A}$ and $\hat{B}$ with new indices $I = (ij)$ and $A = (ab)$. The individual matrix elements of these matrices are

$$A_{IA} = \langle I|\hat{v}|A\rangle,$$

and

$$B_{AI} = \frac{\langle A|\hat{v}|I\rangle}{\epsilon_I^A}.$$

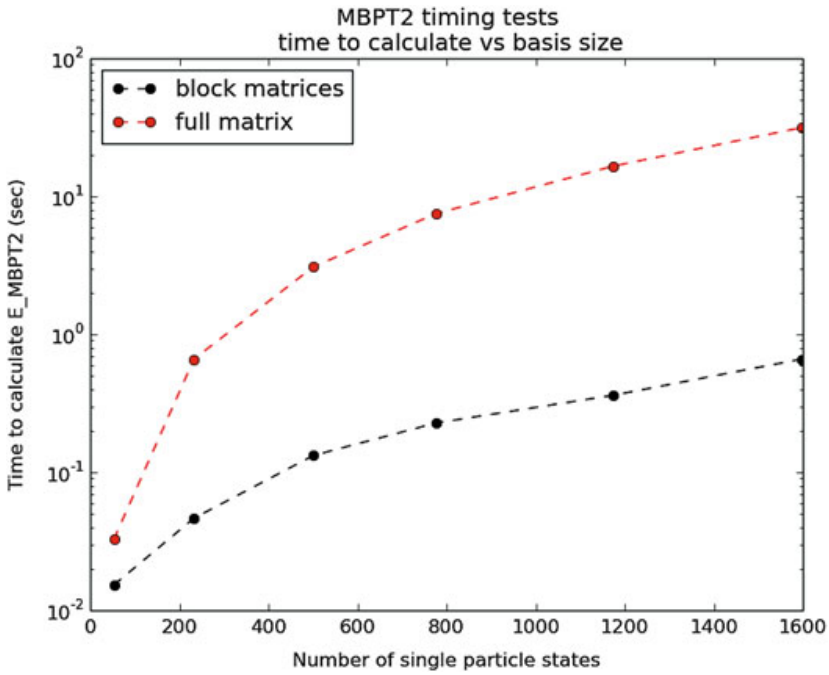


**Fig. 8.6** MBPT2 contribution to the correlation for pure neutron matter with $N = 14$ neutrons and periodic boundary conditions. Up to approximately 1600 single-particle states have been included in the sums over intermediate states in Eqs. (8.52) and (8.53)

We can then rewrite the correlation energy from MBPT2 as

$$\Delta E_{MBPT2} = \frac{1}{4}\hat{A} \times \hat{B}. \tag{8.53}$$

Figure 8.6 shows the difference between the brute force summation over single-particle states of Eq. (8.52) and the smarter set up in terms of indices including two-body configurations only, that is Eq. (8.53). In these calculations we have only considered pure neutron matter with $N = 14$ neutrons and a density $n = 0.08\,\text{fm}^{-3}$ and plane wave single-particle states with periodic boundary conditions, allowing for up to 1600 single-particle basis states. The Minnesota interaction model [57] has been used in these calculations. With 40 single-particle shells, see Table 8.1 for example, we have in total 2713 single-particle states. Using the smarter algorithm the final calculation time is 2.4 s (this is the average time from ten numerical experiments). The total time using the brute force summation over single-particle indices is 100.6 s (again the average of ten numerical experiments), resulting in a considerable speed up. It is useful to dissect the final time in terms of different operations. For the smarter algorithm most of the time is spent setting up the matrix elements for the two-body channels and to load the matrix elements. The final matrix-matrix multiplication takes only 1% of the total time. For the brute force algorithm, the multiplication and summation over the various single-particle states takes almost half of the total time. Here we have deliberately only focused on the difference between the two ways of computing Eqs. (8.52) and (8.53). We have, on

purpose, not performed a proper timing analysis since this was done in the previous subsection. In this section we have chosen to focus on the development of a program which produces the correct results. As mentioned above, the true elephant in the room, in terms of computational time, is our computation of the matrix elements of the nucleon-nucleon potential. We have deliberately omitted the time spent on setting up the interactions here. For the rest of this section we will focus on various physics applications of our newly developed CCD code.

With the definition of the intermediates and appropriate matrix-matrix multiplications and a working CCD program, we can move on to more realistic cases. One such case is infinite nuclear matter using a plane-wave basis. These states are solutions to the free-particle Hamiltonian,

$$\frac{-\hbar^2}{2m}\nabla^2\phi(\mathbf{x}) = \epsilon\,\phi(\mathbf{x})\,. \tag{8.54}$$

For a finite basis, as discussed earlier, we approximate the problem by constructing a box with sides of length $L$, which quantizes the momentum, and impose periodic boundary conditions in each direction by requiring $\phi(x_i) = \phi(x_i + L)$.

The first step in calculating infinite matter is to construct a model space by finding every single-particle state relevant to a given problem. In our case, this amounts to looping over the quantum numbers for spin, isospin, and the three momentum directions. To control the model space size, the momentum can be truncated to give a cubic space, where $n_i \leq n_{\max}$, or a spherical space, where $n_x^2 + n_y^2 + n_z^2 \leq N_{\max}$. The number of single-particle states in a cubic space increases rapidly with $n_{\max}$ compared to the spherical case with $N_{\max}$. For example, in pure neutron matter a cubic space with $n_{\max} = 3$ has 668 states while the spherical space with $N_{\max} = 17$ has 610 states. Therefore, the spherical case will be used for the rest of the calculations here. The loop increases in energy by counting the number of shells, so states can be 'filled' by labeling the first $P$ proton and $N$ neutron states as holes. The following loop is for pure neutron matter and requires the number of neutrons, $N$ and density, $\rho = N/L^3$, as input. Symmetric nuclear matter requires an extra loop over isospin.

```
n = 0
for shell ∈ {0, ..., N_max} do
    for −√N_max ≤ n_x ≤ √N_max do
        for −√N_max ≤ n_y ≤ √N_max do
            for −√N_max ≤ n_z ≤ √N_max do
                for s_z ∈ {−1/2, 1/2} do
                    if n_x^2 + n_y^2 + n_z^2 = shell then
                        Energy = 4π^2ħ^2/2m × shell
                        if n < N then
```

(continued)

```
                        type = "hole"
                    else
                        type = "particle"
                    end if
                    STATES ← (n, n_x, n_y, n_z, s_z, Energy, type)
                    n ← n + 1
                end if
            end for
        end for
    end for
end for
```

The next step is to build every two-body state in the model space and separate them by their particle/hole character and combined quantum numbers. While each single-particle state is unique, two-body states can share quantum numbers with other members of a particular two-body channel. These channels allow us to remove matrix elements and cluster amplitudes that violate the symmetries of the interaction. This reduces greatly the size and speed of the calculation. Our structures will depend on direct two-body channels, $T$, where the quantum numbers are added, and cross two-body channels, $X$, where the quantum numbers are subtracted. Before filling the channels, it is helpful to order them with an index function which returns a unique index for a given set of two-body quantum numbers. Without an index function, one has to loop over all the channels for each two-body state, adding a substantial amount of time to this algorithm. An example of an index function for the direct channels in symmetric nuclear matter is, for $N_x = n_{x,1} + n_{x,2}$, $N_y = n_{y,1} + n_{y,2}$, $N_z = n_{z,1} + n_{z,2}$, $S_z = s_{z,1} + s_{z,2}$, $T_z = t_{z,1} + t_{z,2}$, $m = 2\lfloor\sqrt{N_{\max}}\rfloor$, and $M = 2m + 1$,

$$\begin{aligned}\mathrm{Ind}\left(N_x, N_y, N_z, S_z, T_z\right) = {} & 2\left(N_x + m\right) M^3 + 2\left(N_y + m\right) M^2 + 2\left(N_z + m\right) M \\ & + 2\left(S_z + 1\right) + \left(T_z + 1\right). \end{aligned} \tag{8.55}$$

This function, which can also be used for the cross-channel index function, is well suited for a cubic model space but can be applied in either case. An additional restriction for two-body states is that they must be composed of two different states to satisfy the Pauli-exclusion principle.

```
for sp1 ∈ STATES do
    for sp2 ∈ STATES do
        if sp1 ≠ sp2 then
            N_i ← n_{i,1} + n_{i,2}
            S_z ← s_{z,1} + s_{z,2}
            T_z ← t_{z,1} + t_{z,2}
            i_dir ← Ind(N_x, N_y, N_z, S_z, T_z)
            T ← (sp1, sp2, i_dir)
            N'_i ← n_{i,1} − n_{i,2}
            S'_z ← s_{z,1} − s_{z,2}
            T'_z ← t_{z,1} − t_{z,2}
            i_cross ← Ind(N'_x, N'_y, N'_z, S'_z, T'_z)
            X ← (sp1, sp2, i_cross)
        end if
    end for
end for
```

From the cross channels, one can construct the cross channel complements, $X'$, where $X\,(pq) \equiv X'\,(qp)$. Also from the direct channels, one can construct one-body, and corresponding three-body, channels for each single-particle state, $K$ by finding every combination of two two-body states within a direct channel that contains that single particle state, $T\,(pq) = T\,(rs) \Rightarrow K_p \leftarrow (qrs)$.

```
for Chan ∈ T do
    for tb1 ∈ Chan do
        for tb2 ∈ Chan do
            K ← tb1_1
            K_{tb1_1} ← tb1_2, tb2_1, tb2_2
        end for
    end for
end for
```

These different structures can be further categorized by a two-body state's particle-hole character, $\langle pp|t|hh\rangle$ , $\langle hh|v|hh\rangle$ , $\langle pp|v|pp\rangle$ , $\langle hh|v|pp\rangle$, and $\langle hp|v|hp\rangle$, which greatly simplifies the matrix-matrix multiplications of the CCD iterations by indexing the summed variables in a systematic way. Summations are constructed by placing two structures next to each other in such a way that the inner summed indices are of the same channel. The resulting structure is indexed by the outer channels as

shown here for several of the intermediates defined above

$$\begin{aligned}
\langle b|\chi|c\rangle &= \langle b|f|c\rangle - \frac{1}{2}\sum_{kld}\langle bd|t|kl\rangle\langle kl|v|cd\rangle \rightarrow f_c^b\left(K\left(b\right),K\left(c\right)\right)\\
&\quad -\frac{1}{2}t_{kl}^{bd}\left(K\left(b\right),K_b\left(kld\right)\right)v_{cd}^{kl}\left(K_c\left(kld\right),K\left(c\right)\right),\\
\langle kl|\chi|ij\rangle &= \langle kl|v|ij\rangle + \frac{1}{2}\sum_{cd}\langle kl|v|cd\rangle\langle cd|t|ij\rangle \rightarrow v_{ij}^{kl}\left(T\left(kl\right),T\left(ij\right)\right)\\
&\quad +\frac{1}{2}v_{cd}^{kl}\left(T\left(kl\right),T\left(cd\right)\right)t_{ij}^{cd}\left(T\left(cd\right),T\left(ij\right)\right),\\
\langle kb|\chi|cj\rangle &= \langle kb|v|cj\rangle + \frac{1}{2}\sum_{dl}\langle kl|v|cd\rangle\langle db|t|lj\rangle \rightarrow v_{cj}^{kb}\left(X\left(kc\right),X\left(jb\right)\right)\\
&\quad +\frac{1}{2}v_{cd}^{kl}\left(X\left(kc\right),X\left(dl\right)\right)t_{lj}^{db}\left(X\left(dl\right),X\left(jb\right)\right),\\
\langle ab|\chi|cd\rangle &= \langle ab|v|cd\rangle \rightarrow v_{cd}^{ab}\left(T\left(ab\right),T\left(cd\right)\right),\\
\sum_c\langle b|\chi|c\rangle\langle ac|t|ij\rangle &\rightarrow \chi_c^b\left(K\left(b\right),K\left(c\right)\right)\cdot t_{ij}^{ac}\left(K\left(c\right),K_c\left(ija\right)\right),\\
\sum_k\langle k|\chi|j\rangle\langle ab|t|ik\rangle &\rightarrow \chi_j^k\left(K\left(j\right),K\left(k\right)\right)\cdot t_{ik}^{ab}\left(K\left(c\right),K_c\left(ija\right)\right),\\
\sum_{cd}\langle ab|\chi|cd\rangle\langle cd|t|ij\rangle &\rightarrow \chi_{cd}^{ab}\left(T\left(ab\right),T\left(cd\right)\right)\cdot t_{ij}^{cd}\left(T\left(cd\right),T\left(ij\right)\right),\\
\sum_{kl}\langle ab|t|kl\rangle\langle kl|\chi|ij\rangle &\rightarrow t_{kl}^{ab}\left(T\left(ab\right),T\left(kl\right)\right)\cdot \chi_{ij}^{kl}\left(T\left(kl\right),T\left(ij\right)\right),
\end{aligned}$$

and finally

$$\begin{aligned}
\sum_{kc}\langle ac|t|ik\rangle\langle kb|\chi|cj\rangle &= \sum_{kc}\langle ai^{-1}|t|kc^{-1}\rangle\langle kc^{-1}|\chi|jb^{-1}\rangle\\
&\rightarrow t_{ik}^{ac}\left(X\left(ia\right),X\left(kc\right)\right)\cdot\chi_{cj}^{kb}\left(X\left(kc\right),X\left(jb\right)\right).
\end{aligned}$$

Figure 8.7 displays the convergence of the energy per particle for pure neutron matter as function of number particles for the CCD approximation with the Minnesota interaction model [57] for different with $\mathrm{N_{max}} = 20$. Similarly, Fig. 8.8 shows the convergence in terms of different model space sizes $\mathrm{N_{max}} = 20$ with a fixed number of neutrons $N = 114$. We see from Fig. 8.8 that at the CCD level and neutron matter only there is a good convergence with $\mathrm{N_{max}} = 25$. These results depends however on the type of interaction and many-body approximation.

In these calculations we approximated our problem with periodic boundary conditions, $\phi(x_i) = \phi(x_i + L)$, but we could have chosen anti-periodic boundary

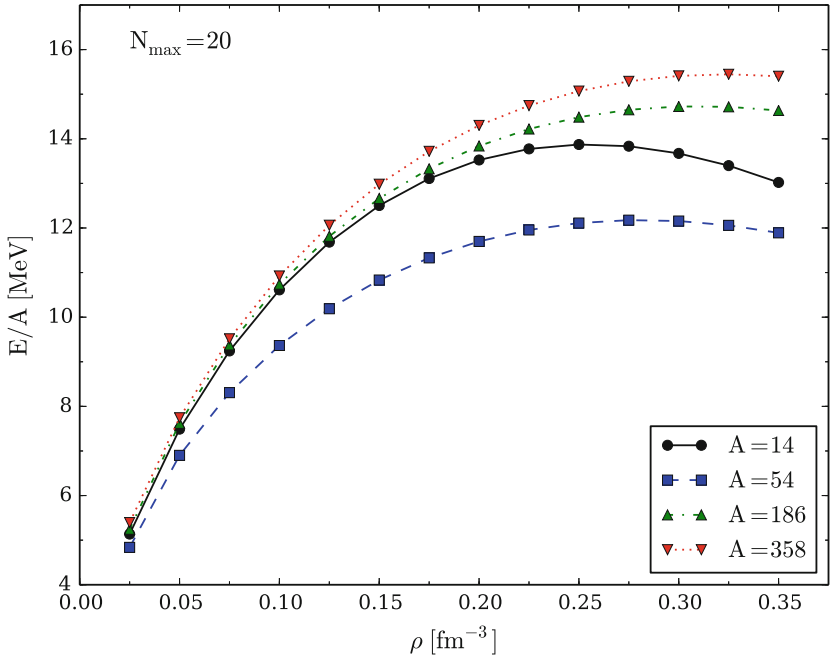


**Fig. 8.7** Energy per particle of pure neutron matter computed in the CCD approximation with the Minnesota interaction model [57] for different numbers of particles with $N_{max} = 20$

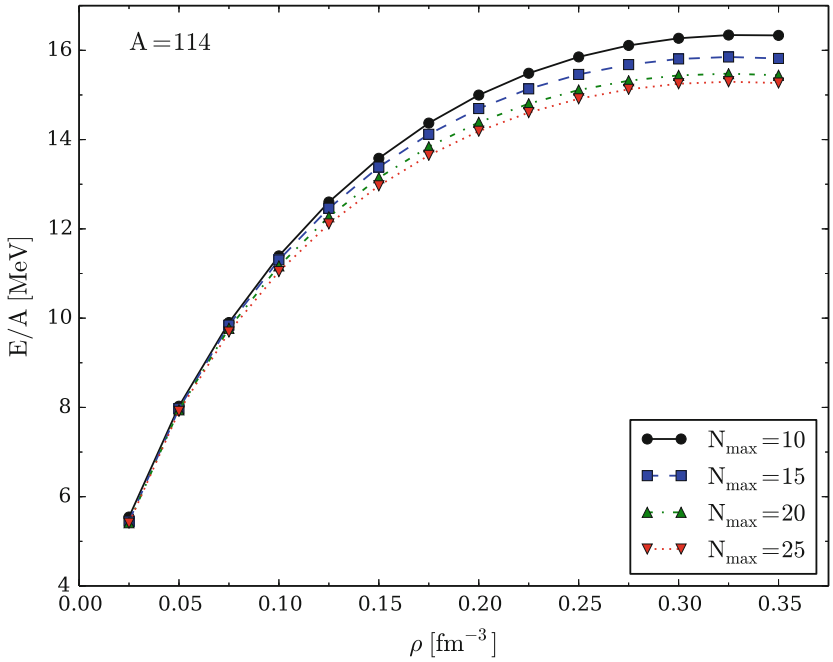


**Fig. 8.8** Energy per particle of pure neutron matter computed in the CCD approximation with the Minnesota interaction model [57] for different model space sizes with $A = 114$

conditions, $\phi(x_i) = -\phi(x_i + L)$. The difference between these two shows how the correlation energy contains finite-size effects [80–83]. One solution to this problem is by integrating over solutions between periodic and anti-periodic conditions, known as twist-averaging [84]. First, we multiply the single-particle states by a phase for each direction, characterized by a twist-angle, $\theta_i$.

$$\phi_{\mathbf{k}}(\mathbf{x} + \mathbf{L}) \rightarrow e^{i\boldsymbol{\theta}} \phi_{\mathbf{k}}(\mathbf{x}) \tag{8.56}$$

$\theta_i = 0$ for PBC and $\theta_i = \pi$ for APBC

$$\mathbf{k} \rightarrow \mathbf{k} + \frac{\boldsymbol{\theta}}{L} \tag{8.57}$$

$$\epsilon_{\mathbf{k}} \rightarrow \epsilon_{\mathbf{k}} + \frac{\pi}{L}\mathbf{k} \cdot \boldsymbol{\theta} + \frac{\pi^2}{L^2} \tag{8.58}$$

Adding these phases changes the single-particle energies, the correction of which disappear as $L \rightarrow \infty$, depending on $\boldsymbol{\theta}$ and thus changes the shell structure so that hole states can jump up to particle states and *vice versa*. It is thence necessary to fill hole states separately for each $\boldsymbol{\theta}$. Integration over a quantity is approximated by a weighted sum, such as Gauss-Legendre quadrature, over the quantity for each set of twist angles. The algorithm becomes then

```
Build mesh points and weights for each direction i: {θ_i, w_i}
E_twist = 0
for (θ_x, w_x) ∈ {θ_x, w_x} do
    for (θ_y, w_y) ∈ {θ_y, w_y} do
        for (θ_z, w_z) ∈ {θ_z, w_z} do
            Build Basis States with k_i → k_i + θ_i/L
            Order States by Energy and Fill Holes
            Get Result E (T,HF,CCD)
            E_twist = E_twist + 1/π^3 w_x w_y w_z E
        end for
    end for
end for
```

This technique gives results which depend much less on the particle number, but requires a full calculation for each set of twist angles, which can grow very quickly. For example, using 10 twist angles in each direction requires 1000 calculations. To see the effects of twist averaging, it is easy to calculate the kinetic energy per particle and the Hartree-Fock energy per particle, which avoids the full CCD calculation. These calculations can be compared to the exact values for infinite matter, which are calculated by integrating the relevant values up to the fermi surface. The kinetic

energy is given by

$$\mathrm{T_{inf}} = \frac{3\hbar^2 k_f^2}{10m},$$

while the potential energy to first order (corresponding to the Hartree-Fock contribution) reads

$$\mathrm{HF_{inf}} = \frac{1}{(2\pi)^6}\frac{L^3}{2\rho}\int_0^{k_f} d\mathbf{k}_1 \int_0^{k_f} d\mathbf{k}_2 \, \langle \mathbf{k}_1\mathbf{k}_2|\hat{v}|\mathbf{k}_1\mathbf{k}_2\rangle \, .$$

Figure 8.9 shows the CCD kinetic energy of pure neutron matter computed with the Minnesota interaction model [57] as a function of the number of particles for both periodic boundary conditions (PBC) and twist-averaged boundary conditions (TABC5). We see clearly that the twist-averaged boundary conditions soften the dependence on finite size effects. Similarly, Fig. 8.10 displays the corresponding Hartree-Fock energy (the reference energy) obtained with Minnesota interaction using both periodic and twist-average boundary conditions.

The results show again a weaker dependence on finite size effects.

With all these ingredients, we can now compute the final CCD energy and thereby the equation of state for infinite neutron matter. Figure 8.11 displays the total CCD energy (including the reference energy) as well as the reference energy obtained with the Minnesota interaction model. The computations have been performed with

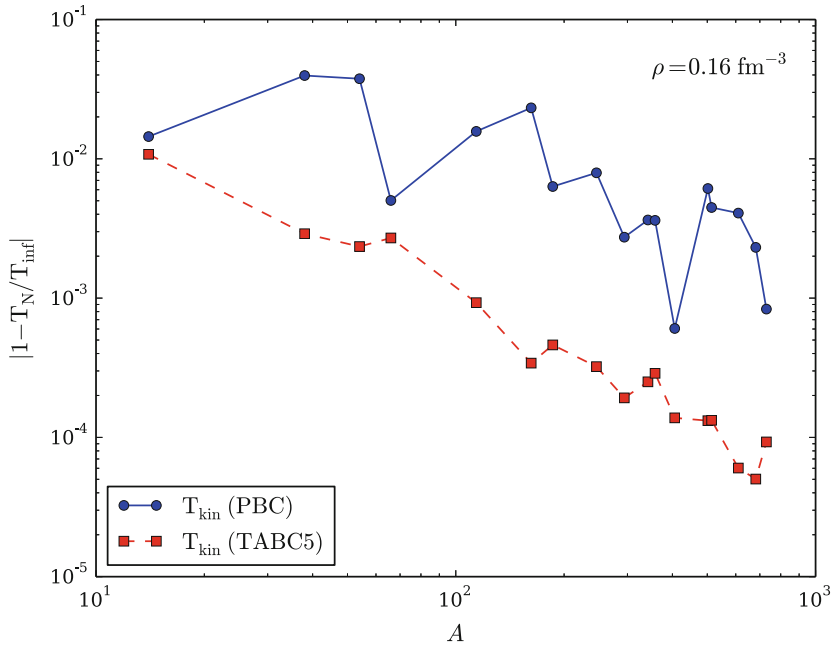


**Fig. 8.9** Finite-size effects in the kinetic energy of pure neutron matter computed with the Minnesota interaction model [57] as a function of the number of particles for both periodic boundary conditions (PBC) and twist-averaged boundary conditions (TABC5)

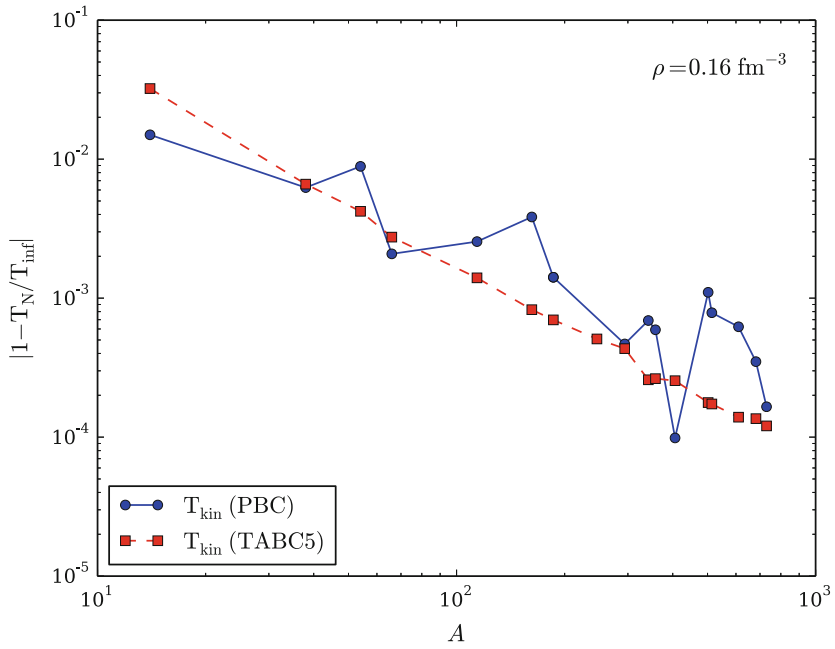


**Fig. 8.10** Finite-size effects in the Hartree-Fock energy of pure neutron matter computed with the Minnesota interaction model [57] as a function of the number of particles for both periodic boundary (PBC) conditions and twist-averaged boundary conditions (TABC5)

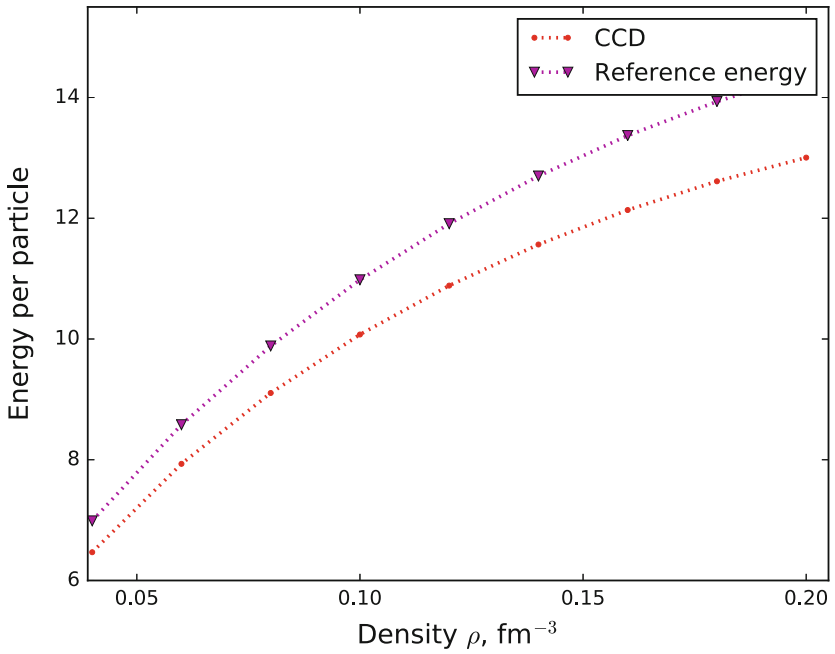


**Fig. 8.11** Energy per particle for pure neutron matter as function of density from coupled cluster calculations with doubles correlations only. The reference energy is included for comparison. The results have been obtained with Minnesota interaction model using periodic boundary conditions and $N = 66$ neutrons and single-particle states up to $N_{max} = 36$, resulting in a total of 2377 single-particle states

**Table 8.13** CCD and MBPT2 results for infinite neutron matter with $N = 66$ neutrons and a maximum number of single-particle states constrained by $N_{max} = 36$

| Density $\rho$ fm$^{-3}$ | $E_{MBPT2}$ | $E_{CCD}$ |
|---|---|---|
| 0.04 | 6.472 | 6.468 |
| 0.06 | 7.919 | 7.932 |
| 0.08 | 9.075 | 9.136 |
| 1.0 | 9.577 | 10.074 |
| 1.2 | 10.430 | 10.885 |
| 1.4 | 11.212 | 11.565 |
| 1.6 | 11.853 | 12.136 |
| 1.8 | 12.377 | 12.612 |
| 2.0 | 12.799 | 13.004 |

$N = 66$ neutrons and a maximum number of single-particle states constrained by $N_{max} = 36$. This corresponds to 2377 single-particle states.

We see from this figure that the correlations brought by coupled cluster theory are at the order of 10% roughly of the reference energy. It means that for this system (neutrons only) with the Minnesota potential, higher-order correlations can most likely be treated in a perturbative way. Many-body perturbation theory to second order gives results which are very close to our CCD results, as seen in Table 8.13. For low densities we observe a good agreement while higher densities bring in particle-particle correlations that become more important as the density increases. Coupled cluster theory sums to infinite order for example particle-particle correlations and with increasing densities this is reflected in differences between the two many-body approximations. The above results agree well with the recent coupled cluster calculations of [36, 37], obtained with interaction models from effective field theory. With the inclusion of proton correlations as well as other potential models we may expect larger differences between different methods and interactions. In Chaps. 9, 10 and 11 we compare the above results with those obtained with Monte Carlo methods, the in-medium renormalization group approach and Green's function theory.

The discussions hitherto have focused on the development of an efficient and flexible many-body code. The codes have been structured to allow users and developers to study and add different physical systems, spanning from the simple pairing model to quantum dots and infinite nuclear matter. Structuring the codes in for example an abstract system class and a solver class allows an eventual user to study different physical systems and add new many-body solvers without having to write a totally new program. As demonstrated in Chap. 10, with few additions one can add the widely popular similarity renormalization group method.

Till now we have limited our discussion to the construction of a many-body code following the underlying mathematical expressions, including elements like how to structure a code in terms of functions, how to modularize the code, how to develop classes and how to verify and validate our computations (our checks provided by the simple pairing model and many-body perturbation theory to second order) against known results. With the rewriting of our equations in terms of efficient

matrix and vector operations we have also shown how to make our code more efficient. Matrix and vector operations can easily be parallelized, as demonstrated in our discussion of many-body perturbation theory to second and third order. Such algorithmic improvements are necessary in order to be able to study complicated physical systems. Our codes can also be easily parallelized in order to run on shared memory architectures using either OpenMP [85] and/or MPI/OpenMPI [77, 78].

We conclude this section by summarizing and emphasizing some topics we feel can help in structuring a large computational project. Amongst these, the validation and verification of the correctness of the employed algorithms and programs are central issues which can save you a lot of time when developing a numerical project. In the discussions above we used repeatedly the simple pairing model of Problem 8.10. This model allows for benchmarks against exact results. In addition, it provides analytical answers to several approximations, from perturbation theory to specific terms in the solution of the coupled cluster equations, the in-medium similarity renormalization group approach of Chap. 10 and the Green's function approach of Chap. 11.

It is also important to develop an understanding of how our algorithms can go wrong and how they can be implemented in order to run as efficiently as possible. When working on a numerical project it is important to keep in mind that computing covers numerical as well as symbolic computing and paper and pencil solutions. Furthermore, version control is something we strongly recommend. It does not only save you time in case you struggle with odd errors in a new version of your code. It allows you also to make science reproducible. Making your codes available to a larger audience and providing proper benchmarks allows fellow scientists to test what you have developed, and perhaps come with considerable improvements and/or find flaws or errors you were not aware of. Sharing your codes using for example modern version control software makes thus your science reproducible and adds in a natural way a sound ethical scientific element to what you develop. In this chapter we have thus provided several code examples, hoping they can serve as good examples.

## 8.8 Conclusions

In this chapter we have presented many of the basic ingredients that enter theoretical studies of infinite nuclear matter, with possible extensions to the homogeneous electron gas in two and three dimensions or other quantum mechanical systems. We have focused on the construction of a single-particle and many-body basis appropriate for such systems, as well as introducing post Hartree-Fock many-body methods like full configuration interaction theory, many-body perturbation theory and coupled cluster theory. The results here, albeit being obtained with a simpler model for the nuclear forces, can easily be extended to more complicated and realistic models for nuclear interactions and to include other many-body methods. We have however, for pedagogical reasons, tried to keep the theoretical inputs to the

various many-body methods as simple as possible. The reader should however, with the inputs from Chaps. 2–6, be able to have a better understanding of nuclear forces and how these can be derived from the underlying theory for the strong force and effective field theory. The last exercise in this chapter replaces the simple Minnesota potential with realistic interactions from effective field theory.

The subsequent Chaps. 9, 10 and 11 show how many of the theoretical concepts and code elements discussed in this chapter can be used to add other many-body methods, without having to develop a new numerical project. With a proper modularization and flexible classes, we can add new physical systems as well as new many-body methods. The codes which have been developed in this chapter can be reused in the development and analysis of the in-medium similarity renormalization group approach of Chap. 10 or the Green's function approach in Chap. 11. Similarly, the theoretical concepts we have developed in this chapter, such as the definition of a single-particle basis using plane wave functions and correlations from many-body perturbation theory or coupled cluster theory, can be used in Chaps. 9, 10 and 11 as well. Chapter 9 for example, uses results from coupled cluster theory in order to provide better ways to constrain the Jastrow factor, which accounts for correlations beyond a mean-field picture, in Monte Carlo calculations.

## 8.9 Exercises

**8.1** Show that the one-body part of the Hamiltonian

$$\hat{H}_0 = \sum_{pq} \langle p| \hat{h}_0 |q\rangle \, a_p^\dagger a_q$$

can be written, using standard annihilation and creation operators, in normal-ordered form as

$$\hat{H}_0 = \sum_{pq} \langle p| \hat{h}_0 |q\rangle \, \{a_p^\dagger a_q\} + \sum_i \langle i| \hat{h}_0 |i\rangle$$

Explain the meaning of the various symbols. Which reference vacuum has been used?

**8.2** Show that the two-body part of the Hamiltonian

$$\hat{H}_I = \frac{1}{4} \sum_{pqrs} \langle pq| \hat{v} |rs\rangle \, a_p^\dagger a_q^\dagger a_s a_r$$

can be written, using standard annihilation and creation operators, in normal-ordered form as

$$\hat{H}_I = \frac{1}{4}\sum_{pqrs} \langle pq|\,\hat{v}\,|rs\rangle\, a_p^\dagger a_q^\dagger a_s a_r$$
$$= \frac{1}{4}\sum_{pqrs} \langle pq|\,\hat{v}\,|rs\rangle\, \left\{a_p^\dagger a_q^\dagger a_s a_r\right\} + \sum_{pqi} \langle pi|\,\hat{v}\,|qi\rangle\, \left\{a_p^\dagger a_q\right\} + \frac{1}{2}\sum_{ij} \langle ij|\,\hat{v}\,|ij\rangle$$

Explain again the meaning of the various symbols.

**8.3** Derive the normal-ordered form of the threebody part of the Hamiltonian.

$$\hat{H}_3 = \frac{1}{36}\sum_{\substack{pqr\\stu}} \langle pqr|\,\hat{v}_3\,|stu\rangle\, a_p^\dagger a_q^\dagger a_r^\dagger a_u a_t a_s,$$

and specify the contributions to the two-body, one-body and the constant part.

**8.4** Develop a program which sets up a single-particle basis for nuclear matter calculations with input a given number of nucleons and a user specified density or Fermi momentum. Follow the setup discussed in Table 8.1. You need to define the number of particles $A$ and the density of the system using

$$\rho = g\frac{k_F^3}{6\pi^2}.$$

Here you can either define the density itself or the Fermi momentum $k_F$. With the density/Fermi momentum and a fixed number of nucleons $A$, we can define the length $L$ of the box used with our periodic boundary contributions via the relation

$$V = L^3 = \frac{A}{\rho}.$$

We can then can use $L$ to define the spacing between various $k$-values, that is

$$\Delta k = \frac{2\pi}{L}.$$

**8.5** The interaction we will use for these calculations is a semirealistic nucleon-nucleon potential known as the Minnesota potential [57] which has the form, $V_\alpha(r) = V_\alpha \exp -(\alpha r^2)$. The spin and isospin dependence of the Minnesota potential is given by,

$$V(r) = \frac{1}{2}\left(V_R + \frac{1}{2}\left(1 + P_{12}^\sigma\right)V_T + \frac{1}{2}\left(1 - P_{12}^\sigma\right)V_S\right)\left(1 - P_{12}^\sigma P_{12}^\tau\right),$$

where $P_{12}^{\sigma} = \frac{1}{2}(1+\sigma_1\cdot\sigma_2)$ and $P_{12}^{\tau} = \frac{1}{2}(1+\tau_1\cdot\tau_2)$ are the spin and isospin exchange operators, respectively. Show that a Fourier transform to momentum space results in

$$\langle \mathbf{k}_p\mathbf{k}_q|V_\alpha|\mathbf{k}_r\mathbf{k}_s\rangle = \frac{V_\alpha}{L^3}\left(\frac{\pi}{\alpha}\right)^{3/2}\exp\frac{-q^2}{4\alpha}\delta_{\mathbf{k}_p+\mathbf{k}_q,\mathbf{k}_r+\mathbf{k}_s}.$$

Write thereafter a function which sets up the full anti-symmetrized matrix elements for the Minnesota potential using the parameters listed in Table 8.2.

**8.6** Consider a Slater determinant built up of orthogonal single-particle orbitals $\psi_\lambda$, with $\lambda = 1, 2, \ldots, A$.

The unitary transformation

$$\psi_a = \sum_\lambda C_{a\lambda}\phi_\lambda,$$

brings us into the new basis. The new basis has quantum numbers $a = 1, 2, \ldots, A$. Show that the new basis is orthogonal.

(a) Show that the new Slater determinant constructed from the new single-particle wave functions can be written as the determinant based on the previous basis and the determinant of the matrix $C$.
(b) Show that the old and the new Slater determinants are equal up to a complex constant with absolute value unity. Hint: $C$ is a unitary matrix.

**8.7** Use the ansatz for the ground state in second quantization

$$|\Phi_0\rangle = \left(\prod_{i\le F}\hat{a}_i^\dagger\right)|0\rangle,$$

where the index $i$ defines different single-particle states up to the Fermi level, to calculate using Wick's theorem (see the appendix) the expectation value

$$E[\Phi_0] = E_{\mathrm{Ref}} = \sum_{i\le F}^{A}\langle i|\hat{h}_0|i\rangle + \frac{1}{2}\sum_{ij\le F}^{A}\langle ij|\hat{v}|ij\rangle.$$

Insert thereafter the plane wave function basis for the various single-particle states and show that the above energy can be written as

$$E[\Phi_0] = \sum_{i\le F}^{A}\langle k_i|\hat{t}|k_i\rangle + \frac{1}{2}\sum_{ij\le F}^{A}\langle k_ik_j|\hat{v}|k_ik_j\rangle,$$

where we use the shorthand $|k_i\rangle = |\mathbf{k}_i, \sigma_i, \tau_{z_i}\rangle$ for the single-particle states in three dimensions.

Replace then the discrete sums with integrals, that is

$$\sum_i \rightarrow \sum_{\sigma_i} \sum_{\tau_{z_i}} \frac{L^3}{(2\pi)^3} \int_0^{\mathbf{k}_F} d\mathbf{k},$$

and show that the energy per particle $A$ can be written as (for symmetric nuclear matter)

$$\frac{E_{\mathrm{Ref}}}{A} = \frac{3\hbar^2 k_F^2}{10 M_N} + \frac{1}{2n} \frac{L^3}{(2\pi)^6} \sum_{\sigma_i \sigma_j} \sum_{\tau_{z_i} \tau_{z_j}} \int_0^{\mathbf{k}_F} d\mathbf{k}_i \int_0^{\mathbf{k}_F} d\mathbf{k}_j \langle k_i k_j | \hat{v} | k_i k_j \rangle,$$

with the density $n = V/A = L^3/A$.

Find the following expression for pure neutron matter. Use the Minnesota interaction and try to simplify the above six-dimensional integral for pure neutron matter (Hint: the interaction depends only the momentum transfer squared and fix one of the momentum integrations along the $z$-axis. Integrate out the dependence on the various angles).

Finally, write a program which computes the above energy for pure neutron matter using the Minnesota potential.

**8.8** We will assume that we can build various Slater determinants using an orthogonal single-particle basis $\psi_\lambda$, with $\lambda = 1, 2, \ldots, A$.

The aim of this exercise is to set up specific matrix elements that will turn useful when we start our discussions of different many-body methods. In particular you will notice, depending on the character of the operator, that many matrix elements will actually be zero.

Consider three $A$-particle Slater determinants $|\Phi_0\rangle$, $|\Phi_i^a\rangle$ and $|\Phi_{ij}^{ab}\rangle$, where the notation means that Slater determinant $|\Phi_i^a\rangle$ differs from $|\Phi_0\rangle$ by one single-particle state, that is a single-particle state $\psi_i$ is replaced by a single-particle state $\psi_a$. It will later be interpreted as a so-called one-particle-one-hole excitation. Similarly, the Slater determinant $|\Phi_{ij}^{ab}\rangle$ differs by two single-particle states from $|\Phi_0\rangle$ and is normally thought of as a two-particle-two-hole excitation.

Define a general one-body operator $\hat{F} = \sum_i^A \hat{f}(x_i)$ and a general two-body operator $\hat{G} = \sum_{i>j}^A \hat{g}(x_i, x_j)$ with $g$ being invariant under the interchange of the coordinates of particles $i$ and $j$.

(a)

$$\langle \Phi_0 | \hat{F} | \Phi_0 \rangle,$$

and

$$\langle \Phi_0 | \hat{G} | \Phi_0 \rangle.$$

(b) Find thereafter

$$\langle \Phi_0 | \hat{F} | \Phi_i^a \rangle,$$

and

$$\langle \Phi_0 | \hat{G} | \Phi_i^a \rangle,$$

(c) Finally, find

$$\langle \Phi_0 | \hat{F} | \Phi_{ij}^{ab} \rangle,$$

and

$$\langle \Phi_0 | \hat{G} | \Phi_{ij}^{ab} \rangle.$$

(d) What happens with the two-body operator if we have a transition probability of the type

$$\langle \Phi_0 | \hat{G} | \Phi_{ijk}^{abc} \rangle,$$

where the Slater determinant to the right of the operator differs by more than two single-particle states?

(e) With an orthogonal basis of Slater determinants $\Phi_\lambda$, we can now construct an exact many-body state as a linear expansion of Slater determinants, that is, a given exact state

$$\Psi_i = \sum_{\lambda=0}^{\infty} C_{i\lambda} \Phi_\lambda.$$

In all practical calculations the infinity is replaced by a given truncation in the sum.

If you are to compute the expectation value of (at most) a two-body Hamiltonian for the above exact state

$$\langle \Psi_i | \hat{H} | \Psi_i \rangle,$$

based on the calculations above, which are the only elements which will contribute? [there is no need to perform any calculation here, use your results from exercises (a), (b), and (c)].

These results simplify to a large extent shell-model calculations.

**8.9** Write down the analytical expressions for diagrams (8) and (9) in Fig. 8.2 and discuss whether these diagrams should be accounted for or not in the calculation of the energy per particle of infinite matter. If a Hartree-Fock basis is used, should these diagrams be included? Show also that diagrams (2), (6)–(7) and (10)–(16) are zero in infinite matter due to the lack of momentum conservation.

**8.10** We present a simplified Hamiltonian consisting of an unperturbed Hamiltonian and a so-called pairing interaction term. It is a model which to a large extent mimicks some central features of atomic nuclei, certain atoms and systems which exhibit superfluidity or superconductivity. To study this system, we will use a mix of many-body perturbation theory (MBPT), Hartree-Fock (HF) theory and full configuration interaction (FCI) theory. The latter will also provide us with the exact answer. When setting up the Hamiltonian matrix you will need to solve an eigenvalue problem.

We define first the Hamiltonian, with a definition of the model space and the single-particle basis. Thereafter, we present the various exercises (some of them are solved).

The Hamiltonian acting in the complete Hilbert space (usually infinite dimensional) consists of an unperturbed one-body part, $\hat{H}_0$, and a perturbation $\hat{V}$.

We limit ourselves to at most two-body interactions and our Hamiltonian is represented by the following operators

$$\hat{H} = \sum_{\alpha\beta} \langle \alpha | h_0 | \beta \rangle a_\alpha^\dagger a_\beta + \frac{1}{4} \sum_{\alpha\beta\gamma\delta} \langle \alpha\beta | V | \gamma\delta \rangle a_\alpha^\dagger a_\beta^\dagger a_\delta a_\gamma,$$

where $a_\alpha^\dagger$ and $a_\alpha$ etc. are standard fermion creation and annihilation operators, respectively, and $\alpha\beta\gamma\delta$ represent all possible single-particle quantum numbers. The full single-particle space is defined by the completeness relation

$$\hat{\mathbf{1}} = \sum_{\alpha=1}^{\infty} |\alpha\rangle\langle\alpha|.$$

In our calculations we will let the single-particle states $|\alpha\rangle$ be eigenfunctions of the one-particle operator $\hat{h}_0$. Note that the two-body part of the Hamiltonian contains anti-symmetrized matrix elements.

The above Hamiltonian acts in turn on various many-body Slater determinants constructed from the single-basis defined by the one-body operator $\hat{h}_0$. As an example, the two-particle model space $\mathscr{P}$ is defined by an operator

$$\hat{P} = \sum_{\alpha\beta=1}^{m} |\alpha\beta\rangle\langle\alpha\beta|,$$

where we assume that $m = \dim(\mathscr{P})$ and the full space is defined by

$$\hat{P} + \hat{Q} = \hat{\mathbf{1}},$$

with the projection operator

$$\hat{Q} = \sum_{\alpha\beta=m+1}^{\infty} |\alpha\beta\rangle\langle\alpha\beta|,$$

being the complement of $\hat{P}$.

Our specific model consists of $N$ doubly-degenerate and equally spaced single-particle levels labelled by $p = 1, 2, \ldots$ and spin $\sigma = \pm 1$. We write the Hamiltonian as

$$\hat{H} = \hat{H}_0 + \hat{V},$$

where

$$\hat{H}_0 = \delta \sum_{p\sigma} (p-1) a^\dagger_{p\sigma} a_{p\sigma}$$

and

$$\hat{V} = -\frac{1}{2} g \sum_{pq} a^\dagger_{p+} a^\dagger_{p-} a_{q-} a_{q+}.$$

Here, $H_0$ is the unperturbed Hamiltonian with a spacing between successive single-particle states given by $\delta$, which we will set to a constant value $\delta = 1$ without loss of generality. The two-body operator $\hat{V}$ has one term only. It represents the pairing contribution and carries a constant strength $g$.

The indices $\sigma = \pm$ represent the two possible spin values. The interaction can only couple pairs and excites therefore only two particles at the time.

(a) Show that the unperturbed Hamiltonian $\hat{H}_0$ and $\hat{V}$ commute with both the spin projection $\hat{S}_z$ and the total spin $\hat{S}^2$, given by

$$\hat{S}_z := \frac{1}{2} \sum_{p\sigma} \sigma a^\dagger_{p\sigma} a_{p\sigma}$$

and

$$\hat{S}^2 := \hat{S}_z^2 + \frac{1}{2}(\hat{S}_+ \hat{S}_- + \hat{S}_- \hat{S}_+),$$

where

$$\hat{S}_{\pm} := \sum_{p} a^{\dagger}_{p\pm} a_{p\mp}.$$

This is an important feature of our system that allows us to block-diagonalize the full Hamiltonian. We will focus on total spin $S = 0$. In this case, it is convenient to define the so-called pair creation and pair annihilation operators

$$\hat{P}^{+}_{p} = a^{\dagger}_{p+} a^{\dagger}_{p-},$$

and

$$\hat{P}^{-}_{p} = a_{p-} a_{p+},$$

respectively.

(b) Show that you can rewrite the Hamiltonian (with $\delta = 1$) as

$$\hat{H} = \sum_{p\sigma} (p-1) a^{\dagger}_{p\sigma} a_{p\sigma} - \frac{1}{2} g \sum_{pq} \hat{P}^{+}_{p} \hat{P}^{-}_{q}.$$

(c) Show also that Hamiltonian commutes with the product of the pair creation and annihilation operators. This model corresponds to a system with no broken pairs. This means that the Hamiltonian can only link two-particle states in so-called spin-reversed states.

(d) Construct thereafter the Hamiltonian matrix for a system with no broken pairs and total spin $S = 0$ for the case of the four lowest single-particle levels. Our system consists of four particles only that can occupy four doubly degenerate single-particle states. Our single-particle space consists of only the four lowest levels $p = 1, 2, 3, 4$. You need to set up all possible Slater determinants. Find all eigenvalues by diagonalizing the Hamiltonian matrix. Vary your results for values of $g \in [-1, 1]$. We refer to this as the exact calculation. Comment the behavior of the ground state as function of $g$.

**8.11** (a) We will now set up the Hartree-Fock equations by varying the coefficients of the single-particle functions. The single-particle basis functions are defined as

$$\psi_p = \sum_{\lambda} C_{p\lambda} \psi_{\lambda}.$$

where in our case $p = 1, 2, 3, 4$ and $\lambda = 1, 2, 3, 4$, that is the first four lowest single-particle orbits. Set up the Hartree-Fock equations for this system by varying the coefficients $C_{p\lambda}$ and solve them for values of $g \in [-1, 1]$. Comment your results and compare with the exact solution. Discuss also which diagrams

in Fig. 8.2 that can be affected by a Hartree-Fock basis. Compute the total binding energy using a Hartree-Fock basis and comment your results.

(b) We will now study the system using non-degenerate Rayleigh-Schrödinger perturbation theory to third order in the interaction. If we exclude the first order contribution, all possible diagrams (so-called anti-symmetric Goldstone diagrams) are shown in Fig. 8.2.

Based on the form of the interaction, which diagrams contribute to the binding energy of the ground state? Write down the expressions for the diagrams that contribute and find the contribution to the ground state energy as function $g \in [-1, 1]$. Comment your results. Compare these results with those you obtained from the exact diagonalization with and without the $4p - 4h$ state. Discuss your results for a canonical Hartree-Fock basis and a non-canonical Hartree-Fock basis.

Diagram 1 in Fig. 8.2 represents a second-order contribution to the energy and a so-called $2p - 2h$ contribution to the intermediate states. Write down the expression for the wave operator in this case and compare the possible contributions with the configuration interaction calculations without the $4p-4h$ Slater determinant. Comment your results for various values of $g \in [-1, 1]$.

We limit now the discussion to the canonical Hartree-Fock case only. To third order in perturbation theory we can produce diagrams with $1p-1h$, $2p-2h$ and $3p - 3h$ intermediate excitations as shown in

Define first linked and unlinked diagrams and explain briefly Goldstone's linked diagram theorem. Based on the linked diagram theorem and the form of the pairing Hamiltonian, which diagrams will contribute to third order?

Calculate the energy to third order with a canonical Hartree-Fock basis for $g \in [-1, 1]$ and compare with the full diagonalization case in exercise (b). Discuss the results.

**8.12** This project serves as a continuation of the pairing model with the aim being to solve the same problem but now by developing a program that implements the coupled cluster method with double excitations only. In doing so you will find it convenient to write classes which define the single-particle basis and the Hamiltonian. Your functions that solve the coupled cluster equations will then just need to set up variables which point to interaction elements and single-particle states with their pertinent quantum numbers.

(a) Explain why no single excitations are involved in this model.

(b) Set up the coupled cluster equations for doubles excitations and convince yourself about their meaning and correctness.

(c) Write a class which holds single-particle data like specific quantum numbers, single-particle Hamiltonian etc. Write also a class which sets up and stores two-body matrix elements defined by the single-particle states. Write thereafter functions/classes which implement the coupled cluster method with doubles only.

(d) Compare your results with those from the exact diagonalization with and without the $4p4h$ excitation. Compare also your results to perturbation theory at different orders, in particular to second order. Discuss your results.

**8.13** Derive the amplitude equations of Eq. (8.31) starting with

$$0 = \langle \Phi^{a_1 \dots a_n}_{i_1 \dots i_n} | \overline{H} | \Phi_0 \rangle.$$

**8.14** Replace the Minnesota interaction model with realistic models for nuclear forces based on effective field theory. In particular replace the Minnesota interaction with the low-order (LO) contribution which includes a contact term and a one-pion exchange term only. The expressions are discussed in Sect. 8.2.4 and Eq. (8.4). Reference [62] contains a detailed compilation of all terms up to order NNLO, with tabulated values for all constants. When adding realistic interaction models we recommend that you use the many-body perturbation theory codes to second order in the interaction, see the code link at https://github.com/ManyBodyPhysics/LectureNotesPhysics/tree/master/Programs/Chapter8-programs/cpp/MBPT2/src/.

## 8.10 Solutions to Selected Exercises

**8.1** To solve this problem, we start by introducing the shorthand label for single-particle states below the Fermi level $F$ as $i, j, \dots \leq F$. For single-particle states above the Fermi level we reserve the labels $a, b, \dots > F$, while the labels $p, q, \dots$ represent any possible single particle state. Using the ansatz for the ground state $|\Phi_0$ as new reference vacuum state, the anticommutation relations are

$$\{a_p^\dagger, a_q\} = \delta_{pq}, p, q \leq F,$$

and

$$\{a_p, a_q^\dagger\} = \delta_{pq}, \ p, q > F.$$

It is easy to see then that

$$a_i|\Phi_0\rangle = |\Phi_i\rangle \neq 0, \qquad a_a^\dagger|\Phi_0\rangle = |\Phi^a\rangle \neq 0,$$

and

$$a_i^\dagger|\Phi_0\rangle = 0 \qquad a_a|\Phi_0\rangle = 0.$$

We can then rewrite the one-body Hamiltonian as

$$\begin{aligned}\hat{H}_0 &= \sum_{pq} \langle p|\, \hat{h}_0\, |q\rangle\, a_p^\dagger a_q \\ &= \sum_{pq} \langle p|\, \hat{h}_0\, |q\rangle\, \{a_p^\dagger a_q\} + \delta_{pq\in i} \sum_{pq} \langle p|\, \hat{h}_0\, |q\rangle \\ &= \sum_{pq} \langle p|\, \hat{h}_0\, |q\rangle\, \{a_p^\dagger a_q\} + \sum_{i} \langle i|\, \hat{h}_0\, |i\rangle\,,\end{aligned}$$

where the curly brackets represent normal-ordering with respect to the new vacuum state. Withe respect to the new vacuum reference state, the

**8.2** Using our anti-commutation rules, Wick's theorem discussed in the appendix and the definition of the creation and annihilation operators from the previous problem, we can rewrite the set of creation and annihilation operators of

$$\hat{H}_I = \frac{1}{4} \sum_{pqrs} \langle pq|\, \hat{v}\, |rs\rangle\, a_p^\dagger a_q^\dagger a_s a_r$$

as

$$\begin{aligned}a_p^\dagger a_q^\dagger a_s a_r &= \{a_p^\dagger a_q^\dagger a_s a_r\} \\ &\quad + \{a_p^\dagger \overbrace{a_q^\dagger a_s} a_r\} + \{a_p^\dagger \overbrace{a_q^\dagger a_s a_r}\} + \{\overbrace{a_p^\dagger a_q^\dagger} a_s a_r\} \\ &\quad + \{\overbrace{a_p^\dagger a_q^\dagger a_s} a_r\} + \{\overbrace{a_p^\dagger \overbrace{a_q^\dagger a_s} a_r}\} + \{\overbrace{a_p^\dagger \overbrace{a_q^\dagger a_s a_r}}\} \\ &= \{a_p^\dagger a_q^\dagger a_s a_r\} + \delta_{qs\in i} \{a_p^\dagger a_r\} - \delta_{qr\in i} \{a_p^\dagger a_s\} - \delta_{ps\in i} \{a_q^\dagger a_r\} \\ &\quad + \delta_{pr\in i} \{a_q^\dagger a_s\} + \delta_{pr\in i}\delta_{qs\in i} - \delta_{ps\in i}\delta_{qr\in i}.\end{aligned}$$

Inserting the redefinition of the creation and annihilation operators with respect to the new vacuum state, we have

$$\begin{aligned}\hat{H}_I &= \frac{1}{4} \sum_{pqrs} \langle pq|\, \hat{v}\, |rs\rangle\, a_p^\dagger a_q^\dagger a_s a_r \\ &= \frac{1}{4} \sum_{pqrs} \langle pq|\, \hat{v}\, |rs\rangle\, \{a_p^\dagger a_q^\dagger a_s a_r\} + \frac{1}{4} \sum_{pqrs} \Big( \delta_{qs\in i} \langle pq|\, \hat{v}\, |rs\rangle\, \{a_p^\dagger a_r\} \\ &\quad - \delta_{qr\in i} \langle pq|\, \hat{v}\, |rs\rangle\, \{a_p^\dagger a_s\} - \delta_{ps\in i} \langle pq|\, \hat{v}\, |rs\rangle\, \{a_q^\dagger a_r\} \\ &\quad + \delta_{pr\in i} \langle pq|\, \hat{v}\, |rs\rangle\, \{a_q^\dagger a_s\} + \delta_{pr\in i}\delta_{qs\in i} - \delta_{ps\in i}\delta_{qr\in i} \Big)\end{aligned}$$

$$
\begin{aligned}
&= \frac{1}{4}\sum_{pqrs} \langle pq|\,\hat{v}\,|rs\rangle \left\{a_p^\dagger a_q^\dagger a_s a_r\right\} \\
&\quad + \frac{1}{4}\sum_{pqi} \Big( \langle pi|\,\hat{v}\,|qi\rangle - \langle pi|\,\hat{v}\,|iq\rangle - \langle ip|\,\hat{v}\,|qi\rangle + \langle ip|\,\hat{v}\,|iq\rangle \Big) \left\{a_p^\dagger a_q\right\} \\
&\quad + \frac{1}{4}\sum_{ij} \Big( \langle ij|\,\hat{v}\,|ij\rangle - \langle ij|\,\hat{v}\,|ji\rangle \Big) \\
&= \frac{1}{4}\sum_{pqrs} \langle pq|\,\hat{v}\,|rs\rangle \left\{a_p^\dagger a_q^\dagger a_s a_r\right\} + \sum_{pqi} \langle pi|\,\hat{v}\,|qi\rangle \left\{a_p^\dagger a_q\right\} + \frac{1}{2}\sum_{ij} \langle ij|\,\hat{v}\,|ij\rangle \,.
\end{aligned}
$$

Summing up, we obtain a two-body part defined as

$$
\hat{V}_N = \frac{1}{4}\sum_{pqrs} \langle pq|\,\hat{v}\,|rs\rangle \left\{a_p^\dagger a_q^\dagger a_s a_r\right\},
$$

a one-body part given by

$$
\hat{F}_N = \sum_{pqi} \langle pi|\,\hat{v}\,|qi\rangle \left\{a_p^\dagger a_q\right\},
$$

and finally the so-called reference energy

$$
E_{\text{ref}} = \frac{1}{2}\sum_{ij} \langle ij|\,\hat{v}\,|ij\rangle \,.
$$

which is the energy expectation value for the reference state. Thus, our normal-ordered Hamiltonian with at most a two-body nucleon-nucleon interaction is defined as

$$
\hat{H}_N = \frac{1}{4}\sum_{pqrs} \langle pq|\,\hat{v}\,|rs\rangle \left\{a_p^\dagger a_q^\dagger a_s a_r\right\} + \sum_{pq} f_q^p \left\{a_p^\dagger a_q\right\} = \hat{V}_N + \hat{F}_N,
$$

with

$$
\hat{F}_N = \sum_{pq} f_q^p \left\{a_p^\dagger a_q\right\},
$$

and

$$
\hat{V}_N = \frac{1}{4}\sum_{pqrs} \langle pq|\,\hat{v}\,|rs\rangle \left\{a_p^\dagger a_q^\dagger a_s a_r\right\},
$$

where

$$f_q^p = \langle p|\,\hat{h}_0\,|q\rangle + \sum_i \langle pi|\,\hat{v}\,|qi\rangle$$

**8.4** The following python code sets up the quantum numbers for both infinite nuclear matter and neutron matter employing a cutoff in the value of $n$. The full code can be found at https://github.com/ManyBodyPhysics/LectureNotesPhysics/tree/master/Programs/Chapter8-programs/python/spstatescc.py.

```
from numpy import *

nmax =2
nshell = 3*nmax*nmax
count = 1
tzmin = 1

print "Symmetric nuclear matter:"
print "a, nx, ny, nz, sz, tz, nx^2 + ny^2 + nz^2"
for n in range(nshell):
   for nx in range(-nmax,nmax+1):
       for ny in range(-nmax,nmax+1):
         for nz in range(-nmax, nmax+1):
            for sz in range(-1,1+1):
               tz = 1
               for tz in range(-tzmin,tzmin+1):
                  e = nx*nx + ny*ny + nz*nz
                  if e == n:
                     if sz != 0:
                        if tz != 0:
                           print count, " ",nx," ",ny, " ",nz,"
                               ",sz," ",tz," ",e
                           count += 1


nmax =1
nshell = 3*nmax*nmax
count = 1
tzmin = 1
print "-----------------------------------"
print "Neutron matter:"
print "a, nx, ny, nz, sz, nx^2 + ny^2 + nz^2"
for n in range(nshell):
   for nx in range(-nmax,nmax+1):
       for ny in range(-nmax,nmax+1):
         for nz in range(-nmax, nmax+1):
            for sz in range(-1,1+1):
               e = nx*nx + ny*ny + nz*nz
               if e == n:
                  if sz != 0:
                     print count, " ",nx," ",ny, " ",sz," ",tz,"
                          ",e
                     count += 1
```

**Acknowledgements** We are much indebted to Carlo Barbieri, Scott Bogner, Alex Brown, David Dean, Heiko Hergert, Dean Lee, Titus Morris, Thomas Papenbrock, Nathan Parzuchowski, Piotr Piecuch and Fei Yuan for many discussions on many-body theory. Computational resources were provided by Michigan State University and the Norwegian Notur project (Supercomputing grant NN2977K). This work was supported by NSF Grant No. PHY-1404159 (Michigan State University), by the Oce of Nuclear Physics, U.S. Department of Energy, under grants DE-FG02-96ER40963, DE-SC0008499 (NUCLEI SciDAC collaboration) and the Field Work Proposal ERKBP57 at Oak Ridge National Laboratory (ORNL).

This research used also resources of the Oak Ridge Leadership Computing Facility located at ORNL, which is supported by the Office of Science of the Department of Energy under Contract No. DE-AC05-00OR22725.

This manuscript has been authored by UT-Battelle, LLC under Contract No. DE-AC05-00OR22725 with the U.S. Department of Energy. The U.S. Government retains a nonexclusive, paid-up, irrevocable, world-wide license to publish or reproduce the published form of this manuscript, or allow others to do so, for U.S. Government purposes. The views and conclusions contained herein are those of the authors and should not be interpreted as necessarily representing the official policies or endorsements, either expressed or implied, of the U.S. Government or any U.S. Government agency. The Department of Energy will provide public access to these results of federally sponsored research in accordance with the DOE Public Access Plan.

## Appendix, Wick's Theorem

Wick's theorem is based on two fundamental concepts, namely *normal ordering* and *contraction*. The normal-ordered form of $\hat{A}\hat{B}..\hat{X}\hat{Y}$, where the individual terms are either a creation or annihilation operator, is defined as

$$\left\{\hat{A}\hat{B}..\hat{X}\hat{Y}\right\} \equiv (-1)^p \,[\text{creation operators}] \cdot [\text{annihilation operators}]\,. \tag{8.59}$$

The $p$ subscript denotes the number of permutations that is needed to transform the original string into the normal-ordered form. A contraction between to arbitrary operators $\hat{X}$ and $\hat{Y}$ is defined as

$$\hat{X}\hat{Y} \equiv \langle 0|\hat{X}\hat{Y}|0\rangle. \tag{8.60}$$

It is also possible to contract operators inside a normal ordered products. We define the original relative position between two operators in a normal ordered product as $p$, the so-called permutation number. This is the number of permutations needed to bring one of the two operators next to the other one. A contraction between two operators with $p \neq 0$ inside a normal ordered is defined as

$$\left\{\overbrace{\hat{A}\hat{B}..\hat{X}\hat{Y}}\right\} = (-1)^p \left\{\hat{A}\hat{B}..\hat{X}\hat{Y}\right\}. \tag{8.61}$$

In the general case with $m$ contractions, the procedure is similar, and the prefactor changes to

$$(-1)^{p_1+p_2+..+p_m}. \tag{8.62}$$

Wick's theorem states that every string of creation and annihilation operators can be written as a sum of normal ordered products with all possible ways of contractions,

$$\hat{A}\hat{B}\hat{C}\hat{D}..\hat{R}\hat{X}\hat{Y}\hat{Z} = \left\{\hat{A}\hat{B}\hat{C}\hat{D}..\hat{R}\hat{X}\hat{Y}\hat{Z}\right\} \tag{8.63}$$

$$+ \sum_{[1]} \left\{\hat{A}\hat{B}\hat{C}\hat{D}..\hat{R}\hat{X}\hat{Y}\hat{Z}\right\} \tag{8.64}$$

$$+ \sum_{[2]} \left\{\hat{A}\hat{B}\hat{C}\hat{D}..\hat{R}\hat{X}\hat{Y}\hat{Z}\right\} \tag{8.65}$$

$$+ \ldots \tag{8.66}$$

$$+ \sum_{[\frac{N}{2}]} \left\{\hat{A}\hat{B}\hat{C}\hat{D}..\hat{R}\hat{X}\hat{Y}\hat{Z}\right\}. \tag{8.67}$$

The $\sum_{[m]}$ means the sum over all terms with $m$ contractions, while $\left[\frac{N}{2}\right]$ means the largest integer that not do not exceeds $\frac{N}{2}$ where $N$ is the number of creation and annihilation operators. When $N$ is even,

$$\left[\frac{N}{2}\right] = \frac{N}{2}, \tag{8.68}$$

and the last sum in Eq. (8.63) is over fully contracted terms. When $N$ is odd,

$$\left[\frac{N}{2}\right] \neq \frac{N}{2}, \tag{8.69}$$

and none of the terms in Eq. (8.63) are fully contracted.

An important extension of Wick's theorem allow us to define contractions between normal-ordered strings of operators. This is the so-called generalized Wick's theorem,

$$\left\{\hat{A}\hat{B}\hat{C}\hat{D}..\right\}\left\{\hat{R}\hat{X}\hat{Y}\hat{Z}..\right\} = \left\{\hat{A}\hat{B}\hat{C}\hat{D}..\hat{R}\hat{X}\hat{Y}\hat{Z}\right\} \tag{8.70}$$

$$+ \sum_{[1]} \left\{\hat{A}\hat{B}\hat{C}\hat{D}..\hat{R}\hat{X}\hat{Y}\hat{Z}\right\} \tag{8.71}$$

$$+ \sum_{[2]} \left\{ \overbrace{\hat{A}\hat{B}\hat{C}\hat{D}..\hat{R}\hat{X}\hat{Y}\hat{Z}}^{} \right\} \tag{8.72}$$

$$+ \ldots \tag{8.73}$$

Turning back to the many-body problem, the vacuum expectation value of products of creation and annihilation operators can be written, according to Wick's theorem in Eq. (8.63), as a sum over normal ordered products with all possible numbers and combinations of contractions,

$$\langle 0|\hat{A}\hat{B}\hat{C}\hat{D}..\hat{R}\hat{X}\hat{Y}\hat{Z}|0\rangle = \langle 0| \left\{ \hat{A}\hat{B}\hat{C}\hat{D}..\hat{R}\hat{X}\hat{Y}\hat{Z} \right\} |0\rangle \tag{8.74}$$

$$+ \sum_{[1]} \langle 0| \left\{ \overbrace{\hat{A}\hat{B}}^{}\hat{C}\hat{D}..\hat{R}\hat{X}\hat{Y}\hat{Z} \right\} |0\rangle \tag{8.75}$$

$$+ \sum_{[2]} \langle 0| \left\{ \overbrace{\hat{A}\hat{B}\overbrace{\hat{C}\hat{D}}^{}}^{}..\hat{R}\hat{X}\hat{Y}\hat{Z} \right\} |0\rangle \tag{8.76}$$

$$+ \ldots \tag{8.77}$$

$$+ \sum_{[\frac{N}{2}]} \langle 0| \left\{ \overbrace{\hat{A}\hat{B}\overbrace{\hat{C}\hat{D}}^{}}^{}.. \overbrace{\hat{R}\hat{X}\hat{Y}\hat{Z}}^{} \right\} |0\rangle. \tag{8.78}$$

All vacuum expectation values of normal ordered products without fully contracted terms are zero. Hence, the only contributions to the expectation value are those terms that *is* fully contracted,

$$\langle 0|\hat{A}\hat{B}\hat{C}\hat{D}..\hat{R}\hat{X}\hat{Y}\hat{Z}|0\rangle = \sum_{[all]} \langle 0| \left\{ \overbrace{\hat{A}\hat{B}\overbrace{\hat{C}\hat{D}}^{}}^{}.. \overbrace{\hat{R}\hat{X}\hat{Y}\hat{Z}}^{} \right\} |0\rangle \tag{8.79}$$

$$= \sum_{[all]} \overbrace{\hat{A}\hat{B}\overbrace{\hat{C}\hat{D}}^{}}^{}.. \overbrace{\hat{R}\hat{X}\hat{Y}\hat{Z}}^{}. \tag{8.80}$$

To obtain fully contracted terms, Eq. (8.68) must hold. When the number of creation and annihilation operators is odd, the vacuum expectation value can be set to zero at once. When the number is even, the expectation value is simply the sum of terms with all possible combinations of fully contracted terms. Observing that the only contractions that give nonzero contributions are

$$\overbrace{a_\alpha a_\beta^\dagger}^{} = \delta_{\alpha\beta}, \tag{8.81}$$

the terms that contribute are reduced even more.

Wick's theorem provides us with an algebraic method for easy determination of the terms that contribute to the matrix element.

## References


1. S.L. Shapiro, S.A. Teukolsky, *Black Holes, White Dwarfs, and Neutron Stars: The Physics of Compact Objects* (Wiley, New York, 1983)
2. J.M. Lattimer, M. Prakash, Astrophys. J. **550**, 426 (2001)
3. J.M. Lattimer, M. Prakash, Phys. Rep. **442**, 109 (2007)
4. A.W. Steiner, J.M. Lattimer, E.F. Brown, Astrophys J. **722**, 33 (2010)
5. A.W. Steiner, S. Gandolfi, Phys. Rev. Lett. **108**, 081102 (2012)
6. J.M. Lattimer, Ann. Rev. Nucl. Part. Sci. **62**, 485 (2012)
7. F. Weber, *Pulsars as Astrophysical Laboratories for Nuclear and Particle Physics* (Institute of Physics Publishing, London, 1999)
8. H. Heiselberg, M. Hjorth-Jensen, Phys. Rep. **328**, 237 (2000)
9. S. Weinberg, Phys. Lett. B **251**, 288 (1990)
10. S. Weinberg, Nucl. Phys. B **363**, 3 (1991)
11. C. Ordonez, U. van Kolck, Phys. Lett. B **291**, 459 (1992)
12. C. Ordonez, L. Ray, U. van Kolck, Phys. Rev. Lett. **72**, 1982 (1994)
13. U. van Kolck, Phys. Rev. C **49**, 2932 (1994)
14. U. van Kolck, Prog. Part. Nucl. Phys. **43**, 337 (1999)
15. R. Machleidt, D. Entem, Phys. Rep. **503**, 1 (2011)
16. E. Epelbaum, H.W. Hammer, U.G. Meißner, Rev. Mod. Phys. **81**, 1773 (2009)
17. G. Hagen, T. Papenbrock, M. Hjorth-Jensen, D.J. Dean, Rep. Prog. Phys. **77**, 096302 (2014)
18. A. Ekström, G.R. Jansen, K.A. Wendt, G. Hagen, T. Papenbrock, B.D. Carlsson, C. Forssén, M. Hjorth-Jensen, P. Navrátil, W. Nazarewicz, Phys. Rev. C **91**, 051301 (2015)
19. G. Hagen, M. Hjorth-Jensen, G.R. Jansen, T. Papenbrock, Phys. Scr. **91**, 063006 (2016)
20. L. Coraggio, J.W. Holt, N. Itaco, R. Machleidt, L.E. Marcucci, F. Sammarruca, Phys. Rev. C **89**, 044321 (2014)
21. F. Sammarruca, L. Coraggio, J.W. Holt, N. Itaco, R. Machleidt, L.E. Marcucci, Phys. Rev. C **91**, 054311 (2015)
22. R. Roth, S. Binder, K. Vobig, A. Calci, J. Langhammer, P. Navrátil, Phys. Rev. Lett. **109**, 052501 (2012)
23. S. Binder, P. Piecuch, A. Calci, J. Langhammer, P. Navrátil, R. Roth, Phys. Rev. C **88**, 054319 (2013)
24. H. Hergert, S. Bogner, T. Morris, A. Schwenk, K. Tsukiyama, Phys. Rep. **621**, 165 (2016)
25. P. Navratil, S. Quaglioni, G. Hupin, C. Romero-Redondo, A. Calci, Phys. Scr. **91**, 053002 (2016)
26. A. Carbone, A. Polls, A. Rios, Phys. Rev. C **88**, 044302 (2013)
27. T. Inoue, S. Aoki, T. Doi, T. Hatsuda, Y. Ikeda, N. Ishii, K. Murano, H. Nemura, K. Sasaki, Phys. Rev. Lett. **111**, 112503 (2013)
28. B.D. Day, Rev. Mod. Phys. **39**, 719 (1967)
29. K.A. Brueckner, C.A. Levinson, H.M. Mahmoud, Phys. Rev. **95**, 217 (1954)
30. K.A. Brueckner, Phys. Rev. **100**, 36 (1955)
31. M. Baldo, G.F. Burgio, Rep. Prog. Phys. **75**, 026301 (2012)
32. M. Baldo, A. Polls, A. Rios, H.J. Schulze, I. Vidaña, Phys. Rev. C **86**, 064001 (2012)
33. L. Coraggio, J.W. Holt, N. Itaco, R. Machleidt, F. Sammarruca, Phys. Rev. C **87**, 014322 (2013)
34. R.J. Bartlett, M. Musiał, Rev. Mod. Phys. **79**, 291 (2007)
35. I. Shavitt, R.J. Bartlett, *Many-Body Methods in Chemistry and Physics* (Cambridge University Press, Cambridge, 2009)

36. G. Baardsen, A. Ekström, G. Hagen, M. Hjorth-Jensen, Phys. Rev. C **88**, 054312 (2013)
37. G. Hagen, T. Papenbrock, A. Ekström, K.A. Wendt, G. Baardsen, S. Gandolfi, M. Hjorth-Jensen, C.J. Horowitz, Phys. Rev. C **89**, 014319 (2014)
38. G. Hagen, G.R. Jansen, T. Papenbrock, Phys. Rev. Lett. **117**, 172501 (2016)
39. J. Carlson, J. Morales, V.R. Pandharipande, D.G. Ravenhall, Phys. Rev. C **68**, 025802 (2003)
40. S. Gandolfi, A.Y. Illarionov, K.E. Schmidt, F. Pederiva, S. Fantoni, Phys. Rev. C **79**, 054005 (2009)
41. S. Gandolfi, A.Y. Illarionov, F. Pederiva, K.E. Schmidt, S. Fantoni, Phys. Rev. C **80**, 045802 (2009)
42. A. Gezerlis, J. Carlson, Phys. Rev. C **81**, 025803 (2010)
43. S. Gandolfi, J. Carlson, S. Reddy, Phys. Rev. C **85**, 032801 (2012)
44. A. Lovato, O. Benhar, S. Fantoni, K.E. Schmidt, Phys. Rev. C **85**, 024003 (2012)
45. A. Gezerlis, I. Tews, E. Epelbaum, S. Gandolfi, K. Hebeler, A. Nogga, A. Schwenk, Phys. Rev. Lett. **111**, 032501 (2013)
46. J. Carlson, S. Gandolfi, F. Pederiva, S.C. Pieper, R. Schiavilla, K.E. Schmidt, R.B. Wiringa, Rev. Mod. Phys. **87**, 1067 (2015)
47. V. Somà, A. Cipollone, C. Barbieri, P. Navrátil, T. Duguet, Phys. Rev. C **89**, 061301 (2014)
48. W. Dickhoff, C. Barbieri, Prog. Part. Nucl. Phys. **52**, 377 (2004)
49. T.D. Morris, N.M. Parzuchowski, S.K. Bogner, Phys. Rev. C **92**, 034331 (2015)
50. M. Prakash, I. Bombaci, M. Prakash, P.J. Ellis, J.M. Lattimer, R. Knorren, Phys. Rep. **280**, 1 (1997)
51. C.J. Horowitz, E.F. Brown, Y. Kim, W.G. Lynch, R. Michaels, A. Ono, J. Piekarewicz, M.B. Tsang, H.H. Wolter, J. Phys. G **41**, 093001 (2014)
52. J.P. Blaizot, G. Ripka, *Quantum Theory of Finite Systems* (MIT press, Cambridge, 1986)
53. W. Dickhoff, D. Van Neck, *Many-Body Theory Exposed!: Propagator Description of Quantum Mechanics in Many-Body Systems*, 2nd edn. (World Scientific, New Jersey, 2008)
54. R.D. Mattuck, *A guide to Feynman Diagrams in the Many-Body Problem*, 2nd edn. (Dover, New York, 1992)
55. S. Binder, A. Ekström, G. Hagen, T. Papenbrock, K.A. Wendt, Phys. Rev. C **93**, 044332 (2016)
56. K.S. McElvain, W.C. Haxton, Nuclear Physics without High-Momentum Potentials: Direct Construction of the Effective Interaction from Scattering Observables (2016). ArXiv:1607.06863
57. D. Thompson, M. Lemere, Y. Tang, Nucl. Phys. A **286**, 53 (1977)
58. S. Weinberg, Phys. Lett. B **363**, 288 (1990)
59. C. Ordóñez, L. Ray, U. van Kolck, Phys. Rev. C **53**, 2086 (1996)
60. U. van Kolck, Phys. Rev. C **49**, 2932 (1994)
61. A. Ekström, G. Baardsen, C. Forssén, G. Hagen, M. Hjorth-Jensen, G.R. Jansen, R. Machleidt, W. Nazarewicz, T. Papenbrock, J. Sarich, S.M. Wild, Phys. Rev. Lett. **110**, 192502 (2013)
62. B.D. Carlsson, A. Ekström, C. Forssén, D.F. Strömberg, G.R. Jansen, O. Lilja, M. Lindby, B.A. Mattsson, K.A. Wendt, Phys. Rev. X **6**, 011019 (2016)
63. E. Epelbaum, A. Nogga, W. Glöckle, H. Kamada, U.G. Meißner, H. Witała, Phys. Rev. C **66**, 064001 (2002)
64. P. Navrátil, S. Quaglioni, I. Stetcu, B.R. Barrett, J. Phys. G **36**(8), 083101 (2009)
65. G. Golub, C. Van Loan, *Matrix Computations* (John Hopkins University Press, Baltimore, 1996)
66. C. Lanczos, J. Res. Natl. Bur. Stand. **45**, 255 (1950)
67. E.R. Davidson, Comput. Phys. Commun. **53**, 49 (1989)
68. E.R. Davidson, Comput. Phys. **5**, 519 (1993)
69. F. Coester, Nucl. Phys. **7**, 421 (1958)
70. F. Coester, H. Kümmel, Nucl. Phys. **17**, 477 (1960)
71. H. Kümmel, K.H. Lührmann, J.G. Zabolitzky, Phys. Rep. **36**, 1 (1978)
72. B.H. Brandow, Rev. Mod. Phys. **39**, 771 (1967)
73. R.J. Bartlett, Ann. Rev. Phys. Chem. **32**, 359 (1981)

74. G.R. Jansen, M.D. Schuster, A. Signoracci, G. Hagen, P. Navrátil, Phys. Rev. C **94**, 011301 (2016)
75. A. Baran, A. Bulgac, M.M. Forbes, G. Hagen, W. Nazarewicz, N. Schunck, M.V. Stoitsov, Phys. Rev. C **78**, 014318 (2008)
76. L.S. Blackford, J. Demmel, I. Du, G. Henry, M. Heroux, L. Kaufman, A. Lumsdaine, A. Petitet, R.C. Whaley, ACM Trans. Math. Softw. **28**, 135 (2002)
77. W. Gropp, E. Lusk, A. Skjellum, *Using MPI* (MIT Press, Cambridge, 1999)
78. E. Gabriel, G.E. Fagg, G. Bosilca, T. Angskun, J.J. Dongarra, J.M. Squyres, V. Sahay, P. Kambadur, B. Barrett, A. Lumsdaine, R.H. Castain, D.J. Daniel, R.L. Graham, T.S. Woodall, in *Proceedings, 11th European PVM/MPI Users' Group Meeting*, Budapest (2004), p. 97
79. R.C. Martin, *Clean Code: A Handbook of Agile Software Craftsmanship* (Prentice Hall, Upper Saddle River, 2015)
80. C. Gros, Zeit. Phys. B **86**, 359 (1992)
81. C. Gros, Phys. Rev. B **53**, 6865 (1996)
82. J.J. Shepherd, A. Grüneis, G.H. Booth, G. Kresse, A. Alavi, Phys. Rev. B **86**, 035111 (2012)
83. J.J. Shepherd, J. Chem. Phys. **145**, 031104 (2016)
84. C. Lin, F.H. Zong, D.M. Ceperley, Phys. Rev. E **64**, 016702 (2001)
85. B. Chapman, G. Jost, R. van der Pas, *Using OpenMP. Portable Shared Memory Parallel Programming* (MIT Press, Cambridge, 2008)